GRI-94/0457
UCRL-CR-119242

Final Report

CONVERSION OF METHANE TO HIGHER HYDROCARBONS

(Biomimetic Catalysis of the Conversion of Methane to Methanol)

Prepared by:
Lawrence Livermore National Laboratory
University of California
7000 East Ave.
Livermore, CA 94550

Funded by:
Lawrence Livermore National Laboratory
United States Department of Energy
Gas Research Institute

Gas Research Institute
Gas Process Research Department
September 1993

DISCLAIMER

Work performed under the auspices of the U.S. Department of Energy by Lawrence Livermore National Laboratory under Contract W-7405-Eng-48.

Lawrence Livermore National Laboratory
Authors:

Bruce E. Watkins, Robert T. Taylor, Joe H. Satcher, M. Leslie Hanna,
Mary Ann Himmelsbach, Sunghoon Park, Robert A. Reibold, Robert Sanner,
Michael W. Droege, Clarance W. Morris, J.R. Weakley, Leroy Charffe, and Alan L. Balch

GRI-94/0457
UCRL-CR-119242

Final Report

CONVERSION OF METHANE TO HIGHER HYDROCARBONS

(Biomimetic Catalysis of the Conversion of Methane to Methanol)

Prepared by:
Lawrence Livermore National Laboratory
University of California
7000 East Ave.
Livermore, CA 94550

Funded by:
Lawrence Livermore National Laboratory
United States Department of Energy
Gas Research Institute

Gas Research Institute
Gas Process Research Department
September 1993

Table of Contents

Introduction

Transportation fuels are a critical energy commodity and they impact nearly every sector of this country. Currently, they account for 27% of the total U.S. energy consumption. Since nearly all transportation fuels are derived from crude oil, they also account for 63% of all U.S. oil needs (imported plus domestic oil).[1] The transportation sector alone has and will continue to use more oil than the nation produces. The need for transportation fuels is projected well into the next century. Consequently, there is a strong emphasis on the economical conversion of other domestic fossil energy resources (other than crude oil) to liquid hydrocarbons that can be used as transportation fuels.

Natural gas is currently a readily available resource that has a positive future outlook considering its known and anticipated reserves. The U.S. has large reserves of "remote" gas on the Alaskan North Slope, the Outer Continental Shelf, and offshore in the Gulf of Mexico. In addition, the Gas Research Institute is projecting large new gas supplies from deep drilling operations. Worldwide, natural gas is a very large resource with about 3900 trillion cubic feet (TCF) of proven reserves.[2] British Petroleum estimates that if these reserves could be processed to a liquid hydrocarbon, a 100 year worldwide supply of transportation fuels would result.[3] Thus, there is intense government and industrial interest in developing economic technologies to convert natural gas to liquid fuels.

Methane, CH_4, is the primary hydrocarbon (85-95%) in natural gas. But there are currently no experimental or established technologies that can economically process natural gas directly to liquid fuels. There are known indirect routes that first reform methane to synthesis gas ($CO + H_2$) and then catalytically (Fischer-Tropsch) convert the synthesis gas to hydrocarbons, waxes, and alcohols. However, these routes are capital intensive, are presently economically unattractive, and are not commercially practiced (New Zealand has a State-supported facility).

The future for methane conversion and natural gas chemical processing depends on the development of catalyzed routes that directly convert methane to liquid hydrocarbons. The thermodynamically allowed, general reaction that transforms methane to higher hydrocarbons (using oxygen), summarized here,

$$nCH_4 + (y/2)O_2 \longrightarrow C_nH_{4n-2y} + yH_2O$$

is an oxidative process that requires the use of a catalyst to facilitate the reaction. Even the most promising of the currently known catalysts require very high operating temperatures (700-800° C).[4,5] As a result, the desired product yield is unacceptably low, in large part due to the uncontrolled over-oxidation of methane to CO and CO_2. A key to upgrading methane to liquid fuels is the controlled

catalytic activation of the C–H bond at a lower temperature preventing over-oxidation to CO and CO_2.

In addition to inorganic catalysts that react with methane, it is well-known that a select group of aerobic soil/water bacteria called methanotrophs can efficiently and selectively utilize methane as the sole source of their energy and carbon for cellular growth.[6] The first reaction in this metabolic pathway is catalyzed by the enzyme methane monooxygenase (MMO) forming methanol:

$$CH_4 + O_2 + NADH + H^+ \xrightarrow[25\text{-}50\,^\circ C]{MMO} CH_3OH + H_2O + NAD^+$$

Methanol is a technologically important product from this partial oxidation of methane since it can be easily converted to liquid hydrocarbon transportation fuels (gasoline), used directly as a liquid fuel or fuel additive itself, or serve as a feedstock for chemicals production. This naturally occurring biocatalyst (MMO) is accomplishing a technologically important transformation (methane directly to methanol) for which there is currently no analogous chemical (non-biological) process.

Our approach has been to use the biocatalyst, MMO, as the initial focus in the development of discrete chemical catalysts (biomimetic complexes) for methane conversion. The advantage of this approach is that it exploits a biocatalytic system already performing a desired transformation of methane. In addition, this approach generates needed new experimental information on catalyst structure and function in order to develop new catalysts rationally and systematically. The first task is a comparative mechanistic, biochemical, and spectroscopic investigation of MMO enzyme systems. This work was directed at developing a description of the structure and function of the catalytically active sites in sufficient detail to generate a biomimetic material. The second task involve the synthesis, characterization, and chemical reactions of discrete complexes that mimic the enzymatic active site. These complexes were synthesized based on our best current understanding of the MMO active site structure.

References

1. DOE Office of Policy, Planning, and Analysis (1988). Assessment of Costs and Benefits of Flexible and Alternative Fuel Use in the U.S. Transportation Sector. Progress Report One: Context and Analytical Framework, January.
2. Kalisch, R.B. *Gas Energy Review* **1989**, *17*, 8.
3. Smith, D.J.H. *Petrole et Techniques* **1987**, *332*, 10.

4. Pitchai, P.; Klier, K. *Catal. Rev.-Sci. Eng.* **1986**, *28*, 13.
5. Lee, J.S.; Oyama, S.T. *Catal. Rev.-Sci. Eng.* **1988**, *30*, 249.
6. Dalton, H. *Adv. Appl. Microbiol.* **1980**, *26*, 71-87.

Part I: Production Soluble Methane Monooxygenase

Introduction

Methanotrophs are microorganisms which have the ability to derive both carbon and energy from the metabolism of methane. They are potentially useful in the bioremediation of polluted environments, since they can effectively degrade a number of chlorinated hydrocarbons.[9,17,25,33] Another potentially important application of methanotrophs is the production of methanol[21] and various alkene epoxides.[11,14] Methanol has attractive possible large-scale uses as an alternative cleaner-burning fuel and as a feedstock for the synthesis of the gasoline octane booster, methyl tertiarybutyl ether.[2,24,29] Among the alkene epoxides, propene oxide has an important commercial value and, furthermore, the biocatalyzed conversion of propene to propene oxide is of interest to study as a model gas-solid bioreactor system.[12]

The foregoing potential applications of methanotrophs are attributed to the presence of their rather non-specific enzymes called methane monooxygenases (MMOs). In some methanotrophs such as *Methylosinus trichosporium* OB3b and *Methylococcus capsulatus* (Bath), the MMO enzyme is known to be associated with either a membrane-bound (particulate) fraction or as a cytoplasmic (soluble) protein complex, depending on the growth conditions.[8,30,31] While the soluble MMO (sMMO) enzyme system has been purified and studied in some detail during the past five years,[10,19,26] the growth characteristics of microorganisms producing this enzyme have not been investigated and discussed in much detail. Harwood and Pirt examined the growth of M. *capsulatus* (Bath) and provided some basic information which is helpful in assessing the economic feasibility of producing microbial protein from natural gas.[13] They studied the effects of nutrient composition and several operational conditions, but did not address the production of MMO. The effect of oxygen tension on methylotrophic bacteria was examined by Dalton's group[22,23] and Maclennan et al.[20] In M. *capsulatus* (Bath), Dalton *et al.* noted that a high oxygen tension above a pO_2 of 0.1 atm inhibited nitrogen assimilation and reduced the growth rate under nitrate- or ammonium-limiting conditions. Maclennan et al. observed that increasing the oxygen tension decreased the cell yield, but it increased CO_2 production during the continuous culturing of *Pseudomonas* AM1 on methanol.

Establishment of the precise culture conditions governing the intracellular location or form of the MMO enzyme has been a conflicting, but important issue. Scott et al.[30] reported that M. *trichosporium* OB3b generated the particulate form of MMO (pMMO) during oxygen-limited, nitrate-excess chemostat culturing. However, Dalton's group reported that the enzyme location in *M. capsulatus* (Bath) and *M. trichosporium* OB3b was determined by copper availability in the culture medium: MMO activity was found in the membrane fraction when adequate copper was

added, and in the soluble fraction when copper availability became limited.[31] They also suggested that the conditions described by Scott et al.[30] masked the underlying copper effect. More recently, Higgin's group also demonstrated the role of copper in regulating the intracellular location of MMO in M *trichosporium* OB3b, but they did not clarify the effects of the nutrients that they previously proposed to be responsible for determining its location and form.[5,8]

This article deals with optimizing the culture conditions for the growth of M. *trichosporium* OB3b and the simultaneous production of sMMO activity. The parameters considered include pH, temperature, and the concentrations of some key culture medium components such as copper, phosphate, nitrate, and iron. The intracellular location of the MMO enzymes was monitored carefully, since defining the culture conditions which would lead to the exclusive formation of sMMO was desired. Experiments were also performed in an attempt to increase the final biomass density.

Materials and Methods

Microorganism and Culture Conditions

Methylosinus trichosporium OB3b obtained from Professor R. S. Hanson (Gray Freshwater Biological Institute, University of Minnesota) was used in all experiments. It was maintained on 1.7% agar plates of Higgins nitrate minimal salt medium[6] at 30°C (see Table I). The agar plates were cultured and stored several weeks in a gas-tight jar under a 1:1 (v/v) methane/air gas mixture. For long term storage, glycerol was added at 20% (w/v) to the fully grown shake-flask cultures and the mixture was maintained at—60°C.

The basal culture medium used for both the shakeflask nd the bioreactor experiments was the same nitrate minimal salt medium cited above, but it lacked $CuSO_4$. It was prepared from four separate concentrated stock solutions as described in Table I, except that $CuS0_4$ was deleted from solution 3. Cellulose acetate (0.22 μm) membranes, 50-mm-diameter disposable filter unit from Corning Glass Works (Corning NY) or a 142-mm-diameter 316 stainless-steel filter apparatus from Millipore Corp., were used for sterilizing all of the liquid solutions. For the bioreactor experiments which involved the continuous supply of an air/CO_2 gas mixture (see below), the fully constituted culture medium was sparged and saturated with this gas mixture for at least 6 h (along with automatic pH adjustment to 7.0) prior to the inoculations.

Flask experiments were performed at 30°C (unless stated otherwise) in a gyratory incubator (model G24, New Brunswick Scientific Co., New Brunswick, NJ) at a shaking speed of 300 rpm. Shake flasks (300 mL) having a 19-mm (o.d.) sidearm tube

(Wheaton Instruments) were employed to read the absorbance directly without removing samples during the cultivation. The liquid working volume was 20 mL. The small screw cap opening on the flask was used for introducing the methane/ air mixture. It was sealed with an open-top-closure screw cap and a PTFE-faced red rubber septum (Kimble Glass Inc.). The large opening on the flask was used for adding culture medium and the inoculum. It was plugged with a sponge stopper during autoclaving, but was subsequently sealed tightly during the cultivation with the rubber-lined plastic screw cap that was supplied with the flask. Before starting a new flask incubation, a 1:1 (v/v) methane/air gas mixture was bubbled into the inoculated culture medium for 5 min at a flow rate of 270 mL/min. It was added through a sterile intraveneous placement unit consisting of a needle and a long catheter (Delmed, Inc., New Brunswick, NJ). The methane and air were measured and mixed with a Matheson gas proportioner (model 7300, Matheson Gas Products, Syracuse, NJ) and sterilized through a 0.22-μm disposable filter unit (Corning Glass Works) before the gas mixture passed into the flasks. Generally, during flask culturing the gas phase was either not replenished or else it was replaced one time after 48 h. Whena longer growth period was desired, it was replenished every 24 h.

Fermentor-scale experiments were performed in a 5-L bioreactor (Bioflo II, New Brunswick Scientific Co.) with a continuous flow of gases. The incubation temperature was 30°C and the pH was maintained at 6.8-7.2 through the automatic addition of 2N NaOH. Dissolved oxygen (DO) levels were kept above 10% saturation in most cases by controlling the agitation speed (350-700 rpm) and the gas flow rates: 150-500 mL/h for methane and 450-1500 mL/h for air or 10% $C0_2^-$ containing air. They were regulated with Matheson mass flowmeters (model 8111) and high accuracy valves (Series 4170).

Table 1. Composition and concentration of stock solutions for Higgins nitrate minimal salt medium.

	Substance	Amount (g/L)
(1)	100x salt solution[b]	
	$NaNO_3$	85
	K_2SO_4	17
	$MgSO_4 \cdot 7H_2O$	3.7
	$CaCl_2 \cdot 2H_2O$	0.7
(2)	100x phosphate buffer solution[b]	
	KH_2PO_4	53
	Na_2HPO_4	86
	Adjust solution to pH 7.0	
(3)	500x trace metals solution[b]	
	$ZnSO_4 \cdot 7H_2O$	0.287
	$MnSO_4 \cdot 7H_2O$	0.223
	H_3BO_3	0.062
	$NaMoO_4 \cdot 2H_2O$	0.048
	$CoCl_2 \cdot 6H_2O$	0.048
	KI	0.083
	$CuSO_4 \cdot 5H_2O$	0.125
	1 mL of 1 m*M* H_2SO_4 per liter of trace metals	
(4)	1000x iron solution[b]	
	$FeSO_4 7H_2O$	11.2
	5 mL of 1 mM H_2SO_4 per 100 mL iron	

[a]Culture medium was made up as follows: Appropriate aliquots of concentrated solutions 1-3 were added to the desired volume of double distilled water and the combined diluted mixture was sterilized by passage through a 0.22 -μm membrane filter. Separate and freshly prepared sterile iron solution 4 was then added aseptically to this mixture. Higgins standard nitrate minimal medium contains Cu at a final concentration of 1.0 μM.

[b]Each stock solution was stored at 4°C after sterilization, except for the phosphate buffer which was stored at room temperature.

Analytical Methods

Cell Densities and Nitrate Concentration

Cell densities were determined by measuring the absorbance at 660 nm (A_{660}) in three spectrophotometers, two Spectronic model 21s (Milton-Roy Inc.) and a Gilford model 260 (Gilford Instrument Laboratory, Inc.). Sidearm shake-culture flasks were read in a Spectronic 21 that was equipped with a universal cuvette holder. The cell densities in the bioreactor were monitored continuously by pumping the culture broth into a flowthrough cell (glass tube, outside diameter of 10 mm) positioned in a separate Spectronic 21 which was connected to a chart recorder (BD 40, Kipp & Zonen, Holland). The conversion factors from the sidearm flask Spectronic 21 readings and the bioreactor flow-through cell Spectronic 21 readings to the Gilford 260 (10-mm cuvette) readings were 1.5 and 4.0, respectively. One unit of A_{660}, in the Spectronic 21 (sidearm flask) corresponded to 0.41 mg dry cell wt/mL; for the Gilford 260 (cuvette) it represented 0.27 mg dry cell wt/mL, based on a linear dry weight curve over an extended range of absorbances. Periodically, serial-dilution platings on 1.7% agar-Higgins medium were performed to validate that the shake-flask and bioreactor A_{660} readings were indeed representitive of cell densities.

Nitrate concentration was determined with an ionspecific nitrate electrode (Orion, model 93-07) and a doublejunction reference electrode (Orion, model 9002) connected to a pH/ion meter (model 701A, Orion Research Instruments). It was possible to measure nitrate concentrations as low as 0.01 m*M* without any pretreatment of the culture medium.

MMO Activity in Intact Washed Cell Suspensions

Microorganisms were harvested by centrifugation at room temperature in an Eppendorf microcentrifuge (model 5413, Brinkmann Instruments, Inc.) at $10^4 g$ for 2 min. The cell pellets were washed once with buffer [25 m*M* 3-N-morpholino)-propanesulfonic acid (MOPS), pH 7.0, plus 5 m*M* $MgCl_2$], resuspended in the same buffer to give a cell density of ca. 5.0 mg dry wt/mL, and placed on ice. Enzyme assays were performed immediately after sampling, usually within 30 min.

Total whole-cell MMO (soluble plus particulate) activity was determined routinely by measuring the epoxidation rate of propene.[15] The presence of sMMO in intact cells was assessed by measuring the disappearance rate of chloroform. Chloroform oxidation is a catalytic activity of the soluble, but not the particulate form of *M. trichosporium* OB3b MMO.[32] MMO assay incubations were carried out in 5-mL clear (for propene) or 5-mL amber (for chloroform which is light-sensitive) vials sealed with open-top-closure screw caps and PTFE-faced rubber septa; the PTFE facings of the septa were placed downward toward the gas phase within the vials. The reaction mixtures contained in a total liquid volume of 0.5 mL: 0.1-0.5 mg

equivalents of dry cell mass (0.3-1.5 mg of protein in the case of broken cell fractions); 12.5 μmol MOPS buffer, pH 7.0; 2.5 μmol $MgCl_2$; and 10 μmol sodium formate. Propene gas (44.6 μmol) was injected into the headspace of the vial. The alternate sMMO-specific substrate, chloroform (0.5-1.0 μmol), was incorporated into the 0.5 mL liquid volume. Reactions were initiated by placing the vials in a reciprocal water bath shaker (30°C, 180 rpm). Liquid samples of 3 μL (for propene activity) or gas samples of 30 μL (for chloroform activity) were analyzed at 3-5 min intervals over a total time period of 10-30 min with a gas chromatograph fitted with a flame ionization detector (Hach, Carle Chromatography Series 100, Hach Co.). A 6-ft stainless-steel column (outside diameter of 1/8 in.), packed with 0.1% SP1000 on Carbopack C, 80/100 mesh, was used for both the propene and the chloroform substrate assays. The column temperature was 85°C for propene and 130°C for chloroform. Helium was used as the carrier gas at a flow rate of 20 mL/min.

MMO Activity in the Cell-Free Systems

Cells from shake flasks were harvested by centrifugation (10^4g, 10 min, 4°C), washed once in ice-cold 25 m*M* MOPS buffer, pH 7.0, containing 5 mM MgCℽ2, and resuspended in the same buffer to give ca. 25 mg dry cell wt/mL. Bovine pancreas deoxyribonuclease I (Sigma Chemical Co.) was added to give a concentration of 10 μg/mL. Cells in suspension at 4°C were then broken by a single pass through a French pressure cell (SLM Instruments, Inc., IL) at 15,000 lb/in.^{2} and the unbroken cells were removed by centrifugation at 10^4g for 10 in, 4°C. The resulting cell-free extract was further centrifuged two successive times at 3.8 x 10^4g for 30 min, yielding a supernatant (S38) and an initial particulate (P38 combined sediment) fraction. In order to remove probable contamination from entrapped S38, the initial P38 fraction was washed, recentrifuged one additional time in the same cold buffer, and again resuspended to give the final P38 membrane material. MMO propene and chloroform oxidative activities in these cell-free systems were measured in the same way as for the intact cells, except that the buffer pH was 7.5 and 5 mM NADH was substituted for 20 mM sodium formate as the source of reducing equivalents. Protein content in S38 and P38 was determined by the method of Lowry et al.[18]

Results and Discussion

Flask Experiments

Effect of Copper

It has been known for almost 10 years that some methanotrophs produce soluble or particulate MMO, depending on the culture conditions,[8,30,31] and it is now becoming

accepted that Cu availability is the most important single factor governing the location or form of MMO in such microorganisms. In order to devise culture conditions for the production of exclusively soluble MMO, the effect of Cu concentration on both the enzyme location and specific cell growth rate (μ, net rate of cell mass growth per unit cell mass) was examined (Fig. 1). Two different inocula were tested, one grown and transferred several times in minus-Cu medium, and the other adapted by multiple transfers in 10, μ*M* Cu-containing medium. When cells from minus-Cu medium were used as inocula (Panel A), an optimal copper concentration was observed at 1-2 μM for cell growth and at 2-4, μM for total whole-cell MMO activity, respectively. (MMO activity refers to the conversion rate of propene to propene oxide, except where specified otherwise.) The maximum specific growth rate was about 0.085 h^{-1} and the maximum MMO activity was about 220 nmol/mg dry cell wt-min. When chloroform was used as a substrate, however, activity was observed only in the cells grown in Cu-free medium. Since chloroform is a highly specific and discriminative substrate for the sMMO,[32] it can be concluded from Figure 1 that a Cu concentration as low as 1 μM is sufficient to shift all of the cellular MMO activity from the soluble to the particulate form. When cells that had been repeatedly grown on 10 μ*M* Cu were employed as inocula (panel B), the same pattern was obtained for the chloroform activity. At copper concentrations above 4 μM, however, no inhibitory effects on cell growth and propene oxidative activity were observed. Figure 1 indicates that the adaptation of this microorganism to a Cu challenge is quite slow when it is first presented with a concentration above 4 μM. This is surprising since the conversion from active soluble enzyme to active particulate enzyme occurs relatively quickly.

The location of the MMO propene activity was also examined in broken cell fractions (Table II). When exogenous Cu was deleted from the culture medium, over 95% of the catalytic activity was observed in the soluble fraction (S38). When the cells were grown in the presence of 10 M Cu, most of the activity (about 70%) was found in the particulate fraction (P38). Inasmuch as intact cells grown on 10 μM Cu did not show any chloroform activity (Fig. 1), finding about 30% of the total MMO propene activity in S38 would appear to be inconsistent. A much more likely explanation is that during the cell rupture in the French pressure cell some membrane fractions are sheared to very small fragments that do not sediment during centrifugation at 3.8×10^4g.[27] This explanation is supported by the fact that the S38 fraction from cells grown on 10, μM Cu does not show any chloroform activity in spite of its appreciable propene activity.[32] All of the subsequent experiments described in this paper were carried out in minus-Cu medium.

Table II. Distribution of MMO activity and protein in broken cell homogenates of *Methylosinus Trichosporium* OB3b.[a]

Culture medium	MMO activity (nmol propene oxide/mg protein-min)		Protein (and dry wt) yields/mg dry cell wt	
	Particulate fraction (percent of total)	Soluble fraction (percent of total)	Particulate fraction (dry wt)	Soluble fraction (dry wt)
With 10 μM $CuSO_4$	61.6± 5.4 (72)	8.8 ± 2.3 (28)	0.13 ± 0.01 (0.27 ± 0.01)	0.41 ± 0.01 (0.52 ± 0.01)
Without $CuSO_4$	0.6 ± 0.3 (2)	36.0 ± 3.2 (98)	0.13 ± 0.02 (0.24 ± 0.04)	0.54 ± 0.04 (0.69 ± 0.07)

[a]Media contained 40 μM $FeSO_4$ and 10 m*M* phosphate buffer (pH 7.0); the cellular fractions were prepared from 48-h side-arm shake flask cultures, A 3-4 independent experiments; ± represent the standard deviations from the mean values.

Effect of Temperature and pH

The effect of temperature on cell growth and sMMO activity was examined (Fig. 2). The specific growth rate increased with increasing temperature up to 34°C and dropped above that. sMMO activity, however, was maximal at 30°C and rapidly decreased with a temperature change in either direction. Chloroform oxidative activities (not shown) were measured and found to be present at a constant ratio of 0.20-0.30 with respect to the propene activity, regardless of the culture temperature. The activation energy for cell growth was estimated to be 2×10^4 cal from a plot of Ln,μ vs. 1/T (Fig. 2, inset). This is slightly higher than the value reported for *Escherichia coli* [$(1.2\text{-}1.6) \times 10^4$ cal], but it falls within the broad range that has been determined for most other bacteria [$(1\text{-}3) \times 10^4$ cal].[28]

The effect of pH was examined in the pH range from 6.0 to 8.5 (Table III). The phosphate concentration was raised from 10 mM (standard level) to 40 mM and held constant to enhance the buffer capacity of the medium. In the pH 6.0-7.0 region, there was essentially no difference in growth rate. But above pH 7.5, an increased lag time was observed and the growth rate decreased with increasing pH. Also, it was found that the culture medium pH significantly shifted towards neutrality during the cultivation, despite buffering with an elevated phosphate concentration. One interesting feature is that the washed whole-cell sMMO activity remained rather constant regardless of significant variations in the culture media pH and the specific growth rates.

Effects of Phosphate Concentration

Figure 3 shows the effects of the culture medium phosphate concentration at pH 7.0 on cell growth and whole-cell MMO activity. Cell growth was inhibited progressively by phosphate concentrations above 40 mM. This is similar to previous results obtained by Harwood and Pirt[13] with M. *capsulatus* (Bath), although the phosphate concentration which is required to arrest cell growth completely is more than threefold higher for *M. trichosporium* OB3b. A high phosphate level is known to inhibit whole-cell methanol dehydrogenase (MDH) activity and to result in the accumulation of methanol in the culture medium.[21] But it is not clear why M. *trichosporium* OB3b can tolerate more highly elevated phosphate concentrations than M. *capsulatus* (Bath). Both the propene and the chloroform oxidative MMO activities in Figure 3 are seen to be constant up to 80 mM phosphate, irrespective of the decreasing trend in specific growth rate. At approximately 90-100 mM phosphate, however, a sharp increase in MMO propene activity was observed, yielding an absolute specific activity of 220 nmol/mg dry cell wt min. This higher propene oxidative activity is due to the production of pMMO, not an elevated production of sMMO, because cells grown on 100 mM or higher phosphate do not display any detectable activity with chloroform (Fig. 3).

Table III. Effect of pH on minus-copper cell growth and wholecell soluble MMO activity.[a]

pH		Specific growth rate	Lag time	MMO activity (nmol propene oxide/
Initial	Final	(h^{-1})	(h)	mg dry cell wt-min)
6.0	6.3	0.087	0	132
6.5	6.6	0.087	0	131
7.0	6.9	0.085	0	110
7.5	7.2	0.078	2	108
8.0	7.3	0.071	9	109
8.5	7.5	0.039	15	111

[a]The final pH and sMMO data were obtained with side-arm shake flask cultures (30°C, 300 rpm) at an absorbance of 0.5-0.7, Spectronic 21, and phosphate buffer concentrations of 40 mM in minus $CuSo_4$ media.

This observation raised an interesting question concerning the role of phosphate in regulating the form of MMO, namely whether the shift in enzyme location is due to a high phosphate concentration per se or due to Cu contaminants present in the Na/K salts that are used in preparing high phosphate culture medium. Another shake flask experiment combined with culture medium Cu analyses, therefore, was conducted to answer this question. With 100 mM phosphate, it was observed that propene oxidative activity was high (ca. 200 nmol/mg dry cell wt min) at a low cell density (A_{660} = 0.28), but it declined to 95 nmol/mg dry cell wt min when the A660 reached 0.6. Correspondingly, chloroform oxidative activity was not detected at the low cell density, but it appeared (22 nmol/mg dry cell wt min) at the higher cell density when the propene activity declined. Moreover, inductive coupled plasma-mass spectrometry (ICPS) analyses revealed that the Cu concentration was ca. 0.2 μM for 100 mM phosphate medium compared to only 0.02 M for 10 mM phosphate medium. Collectively, these results strongly suggest that the production of pMMO in Figure 3 at high phosphate concentrations is due to traces of carry-over Cu contamination in the Na/K salts.

Bioreactor Experiments

Much higher cell densities can be obtained in a bioreactor in which the gaseous substrates are continuously supplied. Our experiments in the bioreactor focussed on the batch culture conditions which yield a high *M trichosporium* OB3b cell density with an optimal whole-cell sMMO activity.

Effect of CO_2

Figure 4 shows the effect of CO_2 supplementation on cell growth. When CO_2 is either incorporated into the gas stream or supplied as bicarbonate in the culture medium, the initial lag period was greatly shortened. The maximum specific growth rates during the exponential growth phase, however, remained approximately the same (μ_{max} = 0.065-0.090 h-l). According to the serine pathway by which M. *trichosporium* OB3b is known to utilize formaldehyde for cell mass generation, one molecule of CO_2 is needed per two molecules of formaldehyde assimilated to convert phosphoenol pyruvate to oxaloacetate and to keep the cycle continuously operating.[1] Without an external supplementation, the initial CO_2 level in the culture medium must be too low to support immediate rapid cell growth. This is probably exacerbated in a bioreactor because the continuous sparging with an air/methane gas mixture initially strips off the small amounts of CO_2 produced from methane metabolism. As the cell density slowly increases, the medium CO_2 concentration apparently rises and finally becomes sufficient to support a maximal cell growth rate as indicated by the similar logarithmic slopes in Figure 4. Based on these results, all subsequent experiments in the bioreactor were conducted with 10% $C0_2$-containing air.

Effect of Nitrate and Diauxic Growth

Figure 5 shows batch profiles of cell growth, nitrate concentration, DO level, and sMMO activity. Exponential cell growth was associated with a large drop in the DO level. The initial specific growth rate (μ) was 0.08 h^{-1} and this fast rate continued until the cell density reached about 1.0 g dry cell wt/L. At 50-60 h, however, a rapid decrease of μ to 0.008 h^{-1} was observed and this slow rate continued for approximately a week before the cell growth completely stopped. The final cell density reached was about 2.5 g dry cell wt/L. The whole-cell sMMO activity was routinely assayed both with and without formate added as an oxidizable agent to regenerate intracellular NADH levels. The former assays of activity were always 4-6 times higher than the latter. In addition, whole-cell sMMO activity was almost constant throughout the cultivation, except for a decreasing trend near the end of the batch operation. It is worth noting that there was no appreciable change in sMMO activity at around 50-60 h, i.e., before and after the large shift in the growth rate. Under these culture conditions the level of sMMO catalysis and, presumably, the rate of methane assimilation are not proportional to the bacterial growth rate. A biphasic growth curve and the nonvarying sMMO activity have not been addressed in the past, but they may explain why the reported values for the methane consumption efficiency (defined as g dry cell wt produced/g methane consumed) of M. *trichosporium* OB3b and several other methanotrophs are not consistent and vary widely.[1,16] Figure 5 also shows that the decrease of the growth rate coincided with the depletion of culture medium nitrate at 50-60 h. This indicated that the

transition might be induced by a switch of the nitrogen source from nitrate to the gaseous nitrogen that is carried into the bioreactor as part of the 9:1 air/C02 mixture. It has been established that M. *trichosporium* OB3b can fix gaseous nitrogen through a nitrogenase which is inducible under either nitrate- or ammonium-limiting culture conditions.[3,4]

The effect of nitrate on the cell growth and the transition in the growth rate was investigated further: first, by varying its concentration in the bioreactor culture medium, and next, by transferring bioreactor cells growing in two different growth phases into fresh culture media. Figure 6 shows the cell densities both at the transitions (X_τ) and at the ends of the batch cultures as a function of the initial medium nitrate concentration. Parameter X_τ was determined by extrapolating the straight lines during both growth phases. When the nitrate concentration was varied over the range from 5 to 20 mM, X_τ increased with increasing nitrate although the final cell densities were practically constant. Cell yield on nitrate was determined from the slope in Figure 6 to be 100 g dry cell wt/mol nitrate or 7.14 g dry cell wt/g N. It is in close agreement with the theoretical value estimated from elemental analyses of various methanotrophs[1] At a much higher nitrate concentration (40 mM), however, the exponential fast growth rate began to decrease well before most of the nitrate was consumed and the proportionality shown in Figure 6 did not extent to this higher nitrate concentration (data not shown). Figure 7 shows the results of the culture transfer experiments. Microorganisms growing in the bioreactor were transferred at two separate times into shake flasks containing fresh media with either no added nitrate or 10 mM nitrate. When fast growing early stage bioreactor cells were transferred into the fresh nitrate-containing medium at 20 h, they exhibited the same rapid growth rate. Similarly, when slow growing late-stage bioreactor cells were transferred at 150 h, nitrate quickly restored most of their earlier fast growth rate. But when nitrate-free medium was used, the growth rate was slow regardless of the prior growth rate in the bioreactor. These results, along with those in Figures 5 and 6, demonstrate clearly that nitrate depletion is responsible for the diauxic growth pattern in the batch cultivation of M. trichosporium Ob3b in the bioreactor.

Effect of Iron

In most batch cultures, microorganisms stop growing at the end of cultivation due to either the depletion of essential nutrients or the accumulation of inhibitory metabolites in the culture medium. Since raising the medium nitrate concentration did not influence the final cell density (Fig. 6) and the metabolites present in the spent bioreactor medium did not inhibit cell growth (data not shown), the maximal cell density attainable with the medium in Table I (lacking $CuSO_4$) seems to be determined by some component(s) other than the C, O, and N sources. In an effort to identify one such limiting component, the effect of the culture medium Fe level

was investigated (Table IV). When about half of the usual Higgins medium Fe level (18 μmol/L) was employed, whole-cell propene oxidative sMMO activity decreased sharply from 105 nmol propene oxide formed/mg dry cell wt min to 47 nmol/mg dry cell wt min at around 70 h. The cell density at that time was 1.5 g dry wt/L, which was also about one-half of the final cell density achievable with the standard medium Fe level of 40 μmol/L (Table I). When an additional 50 μmol/L of Fe was supplemented at 90 h (total 68 μmol/L), a normal high level of the sMMO activity was restored within 24 h. Furthermore, cell growth (μ = 0.009 h^{-1}) continued up to 5.4 g dry cell wt/L without any appreciable decline in the whole cell enzymatic activity. This rapid and large Fe effect on the sMMO activity is not too suprising, considering that Fe is an essential cofactor for the sMMO enzyme complex which can represent more than 10% of the total soluble protein in some methanotrophs.[10,9,26] From the dependence of the final cell density on the initial medium Fe level, i.e., up to 40 μmol/L, it was possible to calculate the cell yield on Fe as approximately 1.3×10^3 g dry cell wt/g Fe. This is about five times lower than the value reported for *Klebsiella aerogenes*,[28] and it may be attributable to high Fe requirement for sMMO production by some methanotrophic bacteria. With an initial Fe level of either 40 or 80 μmol/L, no sudden decreases in whole-cell sMMO activity were observed during the bioreactor batch cultivations, although the higher Fe level raised the final cell density from 2.6 to 3.6 g dry wt/L (Table IV). We conclude that an Fe level of 40, μmol/L in the original Higgins nitrate minimal salts culture medium (Table I) is marginal.

Table IV. Effect of medium iron content on cell growth and soluble MMO activity

Initally added medium Fe	Bioreactor batch culture time						
	40-50 h		70-80 h		110-120 h		Final Cell density[a]
(μmol/L)	Cell density[a]	MMO[b]	Cell density[a]	MMO[b]	Cell density[a]	MMO[b]	(>180h)
18	0.40-0.78	105±5	1.50-1.64	47±3	—	—	
+Additional 50 Fe added at 90 h	—	—	—	—	2.55-3.57	126±4	5.4
40	0.31-0.64	150±10	1.15-1.25	119±3	1.58-1.66	120±10	2.6
80	0.33-0.64	149±7	1.17-1.38	139±5	1.94-2.10	160±5	3.6

[a]The unit of cell density is g dry cell wt/L culture broth.

[b]The unit of MMO activity is nmol of propene oxide formed/mg dry cell wt-min, determined with formate as a reducing agent.

Cultivation with Concentrated Medium

In spite of the somewhat increased final cell density with 80 μmol/L Fe (Table IV), it is still not certain that Fe at the standard level of 40, μmol/L is the key limiting medium component that determines the final cell density. Instead of further attempting to identify additional presumptive limiting component(s) in the standard medium, batch cultures were grown in twofold and fourfold concentrated minus-Cu medium in order to increase the final cell density. The results with the twofold concentrated medium are plotted in Figure 8. As anticipated, both the final cell density and $X\tau$ were about two times higher than those of the standard medium. The sMMO acitvity remained above 100 nmol of propene oxide formed/mg cell dry wt min until near the end of the cultivation. With fourfold concentrated medium (data not shown), however, there was a serious DO limitation. Initial cell growth was comparable to that of twofold medium, but the DO level decreased to zero when the cell density reached 2.5 g dry cell wt/L and it remained there in spite of our efforts to restore it to 10%. As a result, the growth rate then decreased and some cell lysis occurred causing massive foaming. Minus-Cu culture medium concentrated up to fourfold does not alter the early-stage cell growth and sMMO activity, but the advantages of using it are offset by the oxygen limitations, unless this can be overcome in a given bioreactor.

Conclusions

In the present article, we studied an obligatory methanotroph, *Methylosinus trichosporium* OB3b, in shake flasks and a 5-L bioreactor in order to optimize the culture conditions for cell growth and the production of sMMO enzyme. Our major findings can be summanzed as follows:

1. Exclusively sMMO activity was observed only in cells grown on minus-Cu medium.
2. Cell growth was found to be optimal at pH 6.0—7.0, a temperature of 30-34°C, and a phosphate concentration of 10-40 mM.
3. When M. *trichosporium* OB3b was cultivated in a bioreactor with continuous sparging of its gaseous substrates, external CO_2 addition was important to eliminate a long lag period in the cell growth.
4. In bioreactor experiments employing minus-Cu medium and the continuous supply of a methane/air/CO_2 gas mixture, a diauxic growth pattern was observed which was caused by a switch in the nitrogen source from nitrate to gaseous nitrogen. A twofold increase in the culture medium nitrate concentration is recommended to delay the nitrate depletion and hence to shorten the total cultivation time.
5. Sustaining a high whole-cell specific sMMO activity in the bioreactor was dependent on the Fe availability in Higgins culture medium lacking CuS04. It is recommended that the standard medium Fe level be increased to 80 μmol/L for bioreactor experiments.
6. The final bioreactor cell density was increased either by aising the culture medium Fe level or by using twofold concentrated complete medium. Therefore, the use of medium concentlated possibly up to fourfold is suggested, provided the greater oxygen demand can be satisfied in the bioreactor system to be used.

References

1. Anthony, C. 1982. The Biochemistry of Methylotrophs. Academic, New York.
2. Boutacoff, D. 1989. EPRI Journal, **Oct./Nov.**: 24.
3. Chen, Y.-P., Yoch, D. C. 1987. J. Bacteriol, **169**(10): 4778.
4. Chen, Y.-P., Yoch, D. C. 1988. J. Gen. Microbiol. **134**: 3123.
5. Cornish, A., McDonald, J., Burrows, K.J., King, T.S., Scott, D., Higgins, I. J. 1985. Biotechnol. Lett. 7(5): 319.
6. Cornish, A., Nicholls, K. M., Scott, D., Hunter, B. K., Aston, W. J., Higgins, 1. J., Sanders, J. K. M. 1984. J. Gen. Microbiol. **130**: 2565.
7. Dalton, H., Prior, S. D., Leak, D. J., Stanley, S. H. 1984. p. 7582. In: Crawford, R. L., Hanson, R. S. (ed.), Microbial Growth on C1 Compounds, American Society for Microbiology, Washington, D.C.
8. Davis, K. J., Cornish, A., Higgins, I. J. 1987. J. Gen. Microbiol. **133**: 291.

9. Fogel, M.M., Taddeo, A.R., Fogel, S. 1986. Appl. Environ. Microbiol. **51**: 720.
10. Fox, B. G., Froland, W. A., Dege, J. E., Lipscomb, J. D. 1989. J. Biol. Chem., **264**(17): 10023.
11. Habets-Crutzen, A. Q. H., de Bont, J. A. M. 1985. Appl. Microbiol. Biotechnol. **22**: 428.
12. Hamstra, R. S., Murris, M. R., Tramper, J. 1987. Biotechnol. Bioeng. **29**: 884.
13. Harwood, J. H., Pirt, S. J. 1972. J. Appl. Bacteriol. **35**: 597.
14. Hou, C.T. 1984. Appl. Microbial. Biotechnol. **19**: 1.
15. Hou, C.T., Patel, R., Laskin, A.I., Barnabe, N. 1979. Appl. Environ. Microbiol. **38**(1): 127.
16. Leak, D.J., Stanley, S.H., Dalton, H. 1985. Chap. 12. In: Poole, R. K., Dow, C. S. (ed.), Microbial Gas Metabolism, Academic, New York.
17. Little, C.D., Palumbo, A.V., Herbes, S.E., Lidstrom, M.E., Tyndall, R.L., Gilmer, P.J. 1988. Appl. Environ. Microbiol. **54**: 951.
18. Lowry, O.H., Rosebrough, N.J., Farr, A.L., Randall, R.J. 1951. J. Biol. Chem. **193**: 265.
19. Lund, J., Woodland, M. P., Dalton, H. 1985. Eur. J. Biochem. **147**: 297.
20. Maclennan, D.G., Ousby, J.C., Vasey, R.B., Cotton, N.T. 1971. J. Gen. Microbiol. **69**: 395.
21. Mehta, P.K., Mishra, S., Ghose, T.K. 1987. J. Gen. Appl. Microbiol. **33**: 221.
22. Murrell, J. C., Dalton, H. 1983. J. Gen. Microbiol. **129**: 3481.
23. Murrell, J. C., Dalton, H. 1983. J. Gen. Microbiol. **129**: 1197.
24. New Fuels Report, **10**(40): October (1989).
25. Oldenhuis, O., Vink, R.M.J.M., Jenssen, D.B., Witholt, B. 1989. Appl. Environ. Microbiol. **55**: 2819.
26. R. N. Patel, 1984. p. 83-90. In: Crawford, R. L., Hanson, R. S. (ed.) Microbial Growth on C1 Compounds, American Society for Microbiology, Washington, DC.
27. Patel, R. N., Hou, C.T., Laskin, A. l., Felix, A., Derelanko, P. 1979. J. Bacteriol. **139**(2): 675.
28. Pirt, S. J. 1975. Principles of Microbe and Cell Cultivation. Wiley, New York.
29. Russel, A.G., Pierre, D.St., Milford, J.B. 1990. Science, **247**: 201.
30. Scott, D., Best, D.J., Higgins, I.J. 1981. Biotechnol. Lett. **3**(11): 641.
31. Stanley, S. H., Prior, S. D., Leak, D. J., Dalton, H. 1983. Biotechnol. Lett. **5**(7): 487.
32. Taylor, R.T., Hanna, M. L., Park, S., Droege, M.W. 1990. Abstracts of the 90th Annual Meeting of the American Society for Microbiology, p. 221.
33. Tsien, H.-C., Brusseau, G. A., Hanson, R. S., Wackett, L. P. 1989. Appl. Environ. Microbiol. 55: 3155.

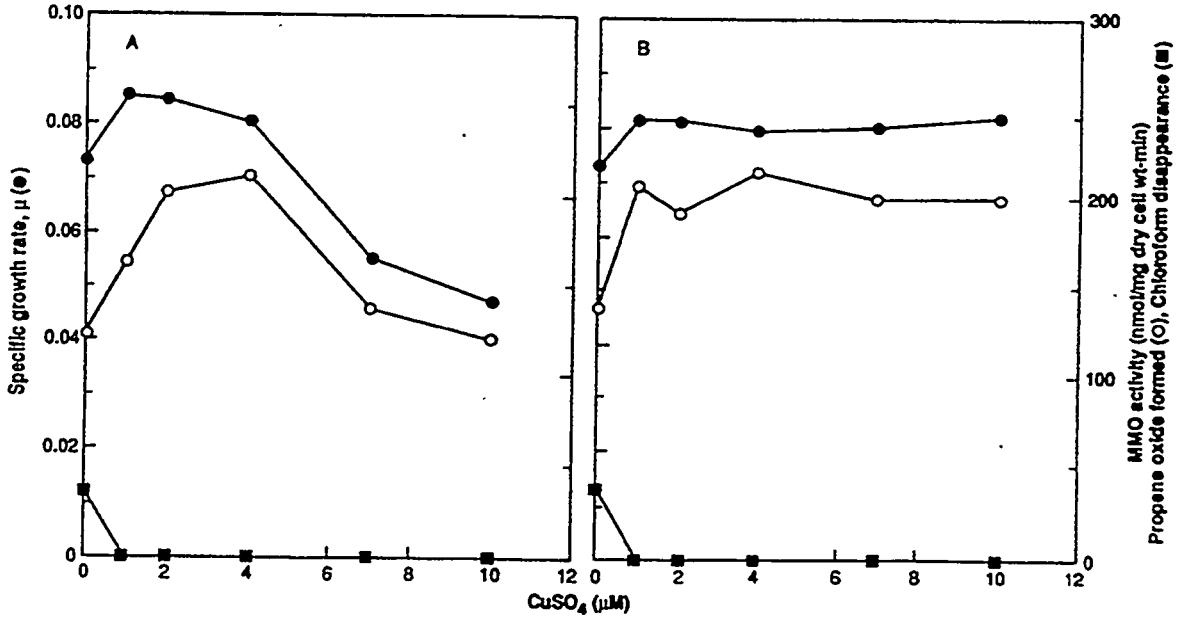

Figure 1. Effect of copper concentration on the specific growth rate and whole-cell MMO activity in sharke flask cultures. MMO activities were measured at an absorbance of 0.5-0.7 (19-mm sidearm, Spectronic 21) after a 48-96 h cultivation. Cells previously grown on minus-Cu (A) or 10 μ*M* Cu-supplemented (B) medium were used as inocula.

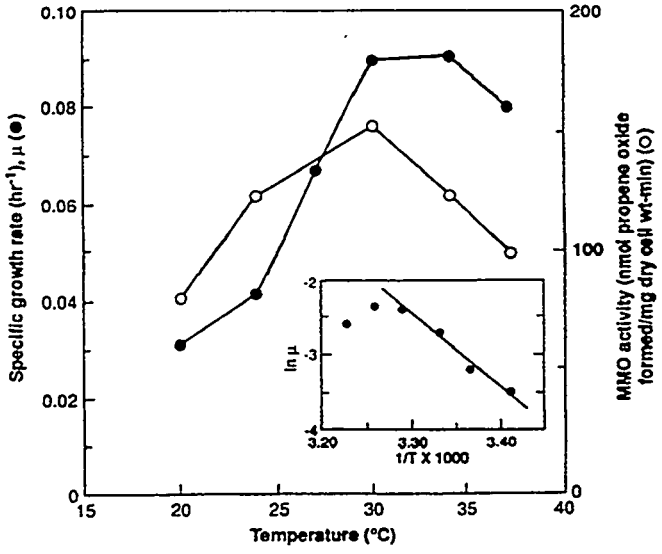

Figure 2. Effect of temperature on the specific growth rate and whole-cell sMMO activity in shake flask cultures (minus-Cu medium). MMO activities were measured at an absorbance of 0.50.7 (19-mm sidearm, Spectronic 21). Insert: Arrhenius plot for determination of the activation energy.

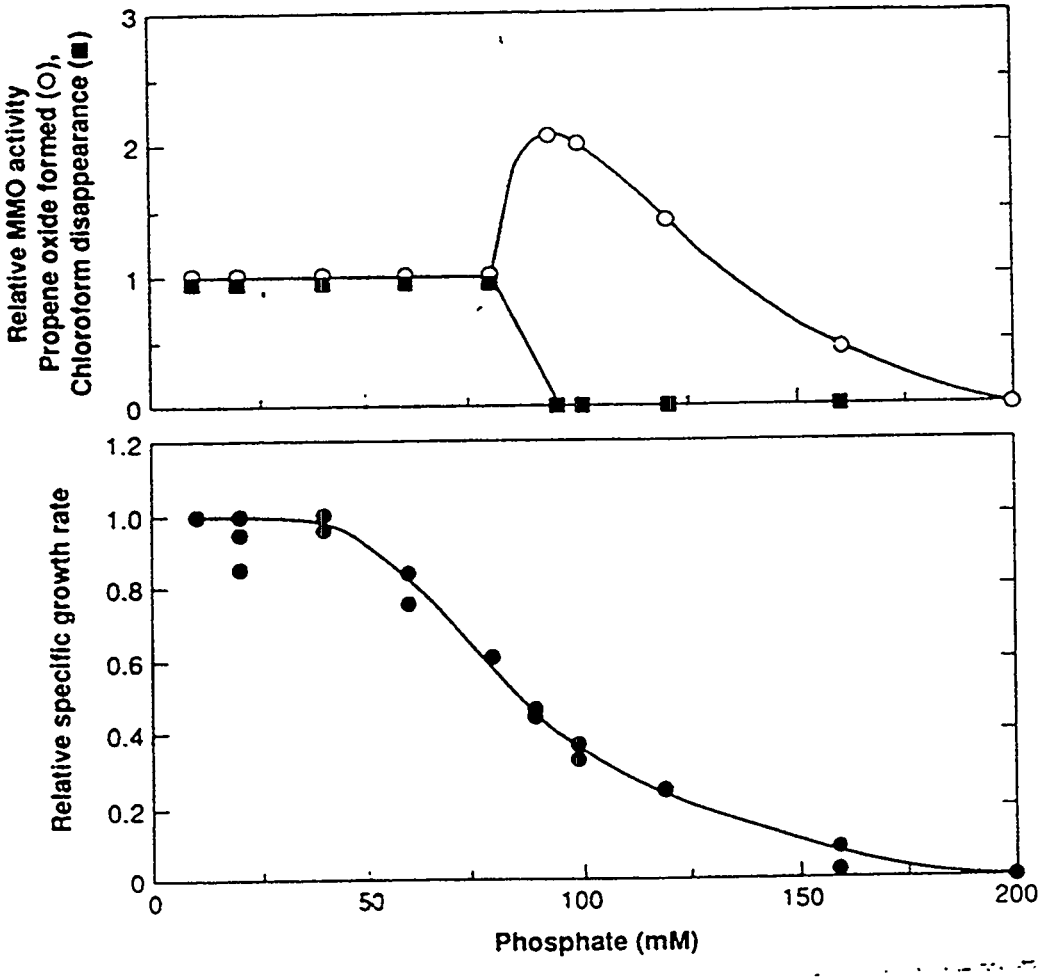

Figure 3. Effect of culture medium phosphate coocentration at pH 7.0 on the relative specific growth rate and relative whole-cell MMO activity (shake flask, minus-Cu medium). Relative growth rate and MMO activity were obtained by normalizing each against the corresponding value at 10 mM phosphate. MMO activities were measured when the cell cultures reached an absorbance of 0.5-0.7 (19-mm sidearm, Spectronic 21) up to a phosphate concentration of 80 mM, and at an absorbance of 0.1-0.3 above that phosphate concentration.

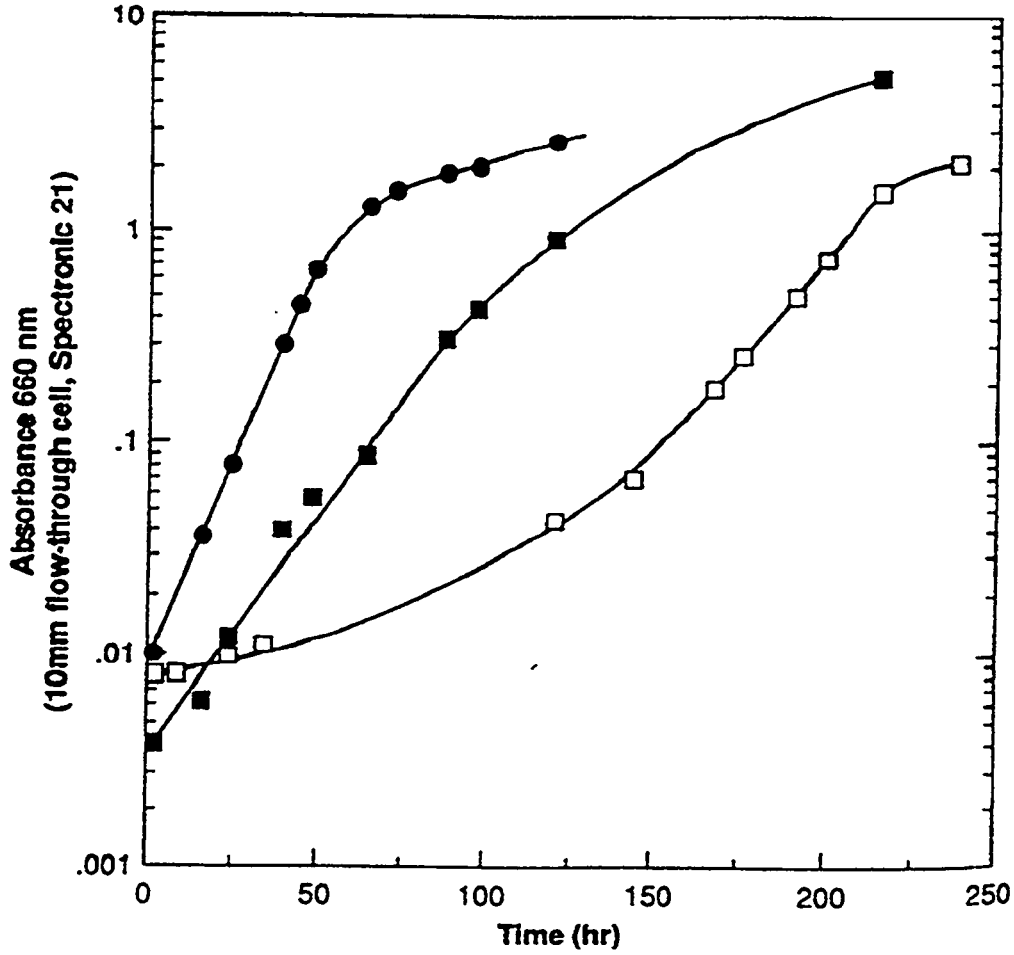

Figure 4. Effect of CO_2 or $NaHCO_3$ on cell growth in a 5-L bioreactor culture (minus-Cu medium). Symbols show (●) CO_2 was added in an air/CO_2 mixture (9:1 volume ratio); (■) $NaHCO_3$ was added to the culture medium at a concentration of 0.1% (w/v); (□) neither CO_2 nor $NaHCO_3$ was added.

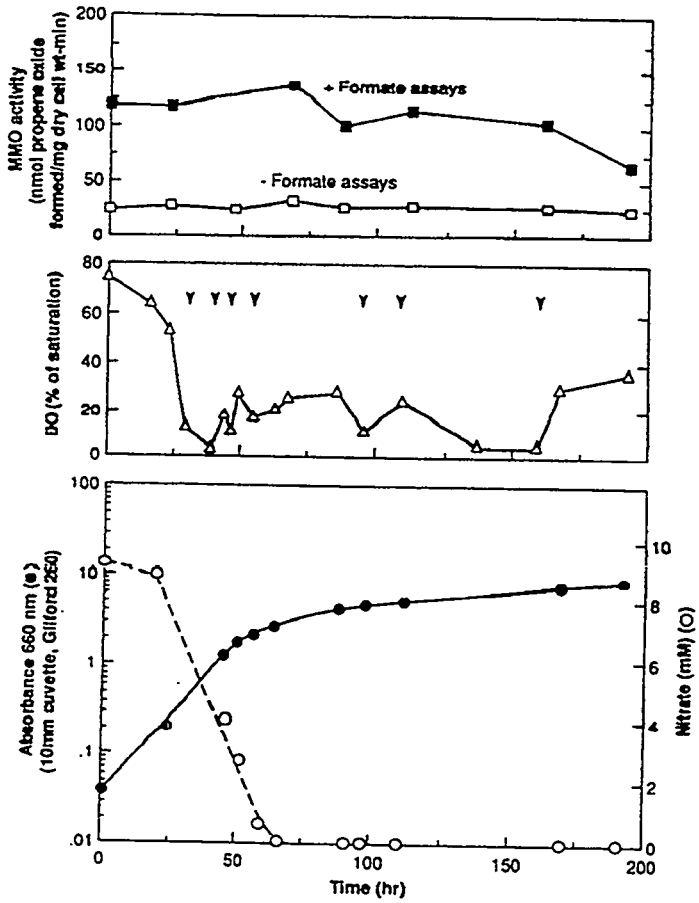

Figure 5. Batch culture profiles of cell growth, nitrate concentration, DO level, and whole-cell sMMO activity in the bioreactor. Cells were grown in Higgins nitrate minimal salts medium in the absence of added $CuSO_4$ and with a continuous supply of methane and 9:1 air/CO_2 gas mixtures (standard conditions for bioreactor culture). Vertical arrows indicate the times at which the agitation speed and gas flow rates were adjusted to maintain DO levels above 10%.

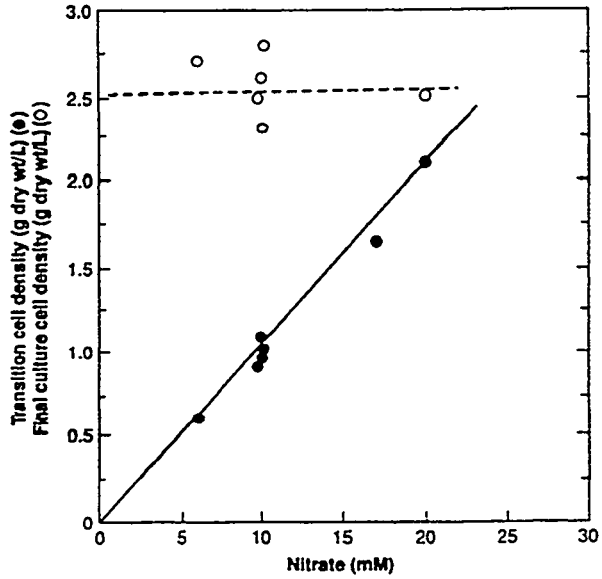

Figure 6. Effect of nitrate concentration on cell density at the transition time (X_t) and at the end of the total growth time in the bioreactor culture.

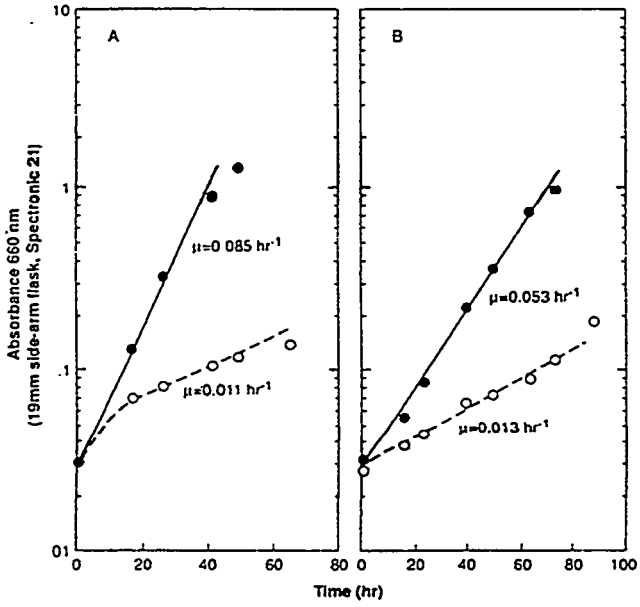

Figure 7. Effect of shake flask nitrate concentration on the growth of prior bioreactor-cultured cells. Inocula cells were transferred from the bioreactor (standard conditions as in Fig. 5) to side-arm shake flasks at 20 hr (A) and at 150 hr (B). They were centrifuged and washed once with nitrate-free medium before inoculation into the flasks. Nitrate concentration was (●) 10 m*M* and (○) 0 m*M*.

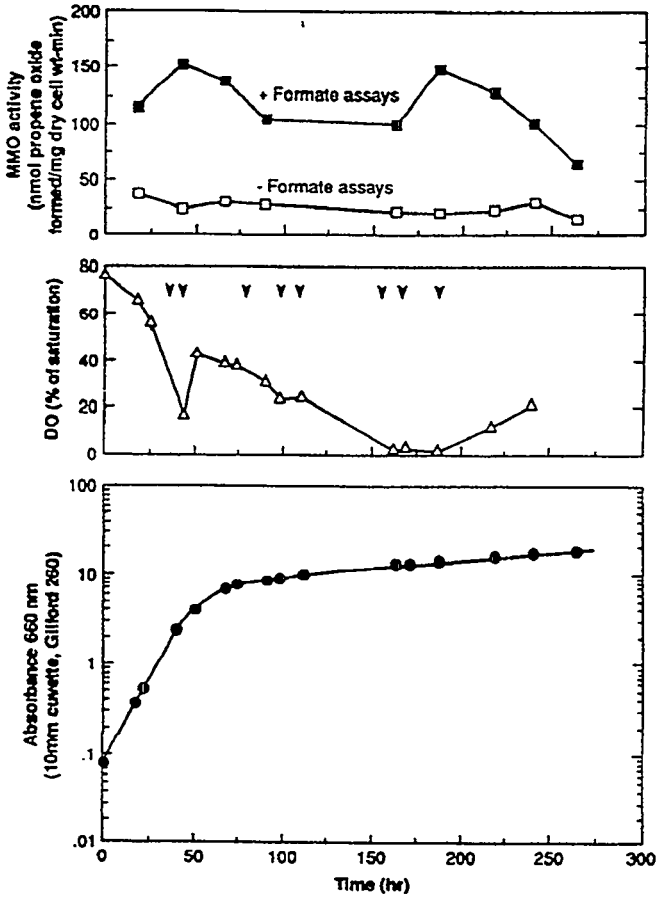

Figure 8. Bioreactor batch culture profiles of cell growth, DO level, and whole-cell sMMO activity with twofold concentrated medium lacking $CuSO_4$. Vertical arrows indicate the times at which the agitation speed and gas flow rates were adjusted in an effort to maintain DO levels above 10%.

Part II: Production of Particulate Methane Monooxygenase

Introduction

The methane monooxygenase (MMO) activity within the obligatory methanotroph *Methylosinus trichosporium* OB3b can exist in either a membrane-bound (particulate) or a cytoplasmic (soluble) form, depending on the growth conditions. When copper is sufficient in the culture medium particulate MMO (pMMO) is produced, while soluble MMO (sMMO) is produced when copper availability becomes acutely limiting.[4,16,18] These two intracellular forms of MMO are known to exhibit some remarkable differences in their specificities for various substrates and inhibitors.[3,18]

We have examined batch culture conditions for maximizing methanotrophic cellular MMO activity in order to better assess some practical applications of the intact cells in the biodegradation of certain chlorinated solvents,[7,13,15,20] in the production of the fuel-related chemicals, [2,8,12,14] and in the production of single-cell protein for animal feed supplementation.[10] In our previous study with *M. trichosporium* OB3b,[16] we reported that an extreme copper deficiency is essential for the batch production of exdusively sMMO. At low cell densities, a copper concentration as low as 1 μM is sufficient to switch all of the MMO activity from the soluble to the particulate form. In the absence of copper, we also observed a diauxic growth pattern caused by a change in nitrogen source from nitrate to gaseous nitrogen.[16] The sMMO activity was quite constant regardless of the grow rate or most changes in the culture conditions, unless Fe was depleted from the culture medium. The decreased sMMO activity due to thee Fe depletion could be restored by a further Fe supplementation.[16]

We have focused on the batch cultivation of M. *trichosporium* OB3b for the production of pMMO in the present work because very little correlative growth-activity data were available. The important medium components considered include copper, carbon dioxide, and nitrate. The effects of these components on the cell growth rate and whole-cell specific pMMO enzymatic zctivity are examined and optimal cultural conditions for maximally expressed pMMO are described.

The bioreactor cultivation of M. *trichosporium* OB3b cells containing pMMO, as opposed to sMMO, is of interest for several reasons. First is the otentially faster whole-cell methane, short-chain alkane, and alkene (eg. propene conversion to propene oxide[16]) partial oxidations for the generation of alcohols and epoxides. Second is the possible faster production of single cell protein from natural gas under ambient conditions. A third is the needed reproducible growth of cells containing maximal levels of expressed pMMO catalytic activity for comparative biochemical

structure-function studies of the pMMO versus the sMMO system within a single strain of methanotroph.

Materials and Methods

M. trichosporium OB3b was obtained from Professor R.S. Hanson (Gray Freshwater Biological Institute, University of Minnesota). The basal formulation employed for maintenance of the strain was Higgin's nitrate minimal salts medium.[5,16] For the various cell culturing experiments, the concentrations of several major components in this medium were modified as indicated in the text, but the incubation temperature was always 30°C.

Fermentor-scale experiments were performed in a 5L bioreactor (Bioflo II, New Brunswick, NJ) with continuous sparging of the gaseous subskates, methane and air or methane and 10% CO_2-containing air. Bioreactor inocula were cultivated under a 1:1 (vol/vol) air/methane gas mixture at 300 rpm in 2L shake-flasks with 200 mL of Higgin's medium containing 10 μM $CuSO_4$. For all inocula which were grown in shake-flasks, as well as several shakeflask experiments which are described, the initial medium content of iron was 40 μmol/L as in Higgin's medium.[5,16]

Cell densities and the growth rate were determined by measuring the absorbance at 660 nM with a Gilford (Model 260, Gilford Instrument Lab., Inc., OH) or a Spectronic 21 (Milton-Roy Inc.) spectrophotometer. Nitrate concentrations were determined with an ion-specific nitrate electrode (Orion, Model 93-07) and a double-junction reference electrode (Orion, Model 90-02) connected to a pH/ion meter (Model 701A, Orion Research Ins., MA). Total MMO activity (sMMO plus pMMO) for intact cells was determined by measuring the epoxidation rate of propene at 30°C in 25 mM 3-(*N*morpholino)-propanesulfonic acid (MOPS) buffer containing 5 mM $MgCl_2$. All MMO propene oxidative activities were measured routinely with and without added formate (20 mM) as an indirect reducing agent in the reaction mixture.[3,16] Since the MMO activity of intact cells was sensitive to the pH of the incubation culture (Fig. 1), all assays were conducted at pH 7. To exclude that the cells were producing any sMMO activity, the disappearance rate of chloroform was also measured. Chloroform is a substrate of the soluble enzyme only.[19] Moreover, bioreactor cultured cells were periodically disrupted and subfractionated by differential centrifugation to verify that the whole-cell MMO activity being measured was derived entirely from the membranous particulate fraction.[16] Analyses of propene oxide formation and chloroform disappearance were conducted with a gas chromatograph (Hach series 100 or Hewlett-Packard 5890A) equipped with a 6 ft stainless steel packed column (0.1% SP1000 on Carbopack C, Supelco, or 0.1% AT-1000 on Graphac-GC, Alltech) and a flame ionization detector. More detailed information on the shake flask and bioreactor culture conditions, as well as the MMO assay procedures, can be found elsewhere.[16]

Results and Discussion

Effect of the initial copper concentration

Preliminary shake-flask studies indicated that M. *trichosporium* OB3b is more copper tolerant than many other microorganisms.[1,9,17,21] Cells were adapted to copper by pre-growth at the same $CuSO_4$ concentration as the testflask culture up to the level of 40 μM. For higher copper concentrations, cells pre-grown on 40 μM $CuSO_4$ were used as inocula. As shown in Figure 2, the specific growth rate (μ) of M. *trichosporium* OB3b decreased about 50% with increasing copper concentrations up to 40 μM, but was further lowered only 25% between 40-120 μM. The whole-cell specific pMMO activity also decreased with increasing copper concentrations, but above 40 μM it remained essentially constant. The maximal specific growth rate and the maximal specific pMMO activity were observed at 10 μM, 0.11 hr^{-1} and 220 nmol of propene oxide formed/mg dry cell wt-min, respecdvely. Thus, M. *trichosporium* OB3b grows relatively well even at 100 μM copper (Fig. 2) and seems to be tolerant to high copper levels.

Typical bioreactor batch culture profile for copper-containing medium

Figure 3 shows the batch culture results in a 5L bioreactor with an inidal copper concentration of 10 μM. Profiles of the specific MMO activity and cell growth are plotted, along with the variations in nitrate concentration and volumetric MMO activity. The initial culture medium content of iron was increased from 40 to 80 μmol/L for all bioreactor experiments as recommended in our previous work.[16] The temperature and pH were maintained at 30°C and 6.7-7.4, respectively, while the gaseous substrates consisted of 25% methane and 75% air-CO_2 mixture. The gas flowrates and the agitation speed were varied as required to meet the cellular demand for methane and oxygen. The fast cell growth (μ = 0.12 hr^{-1}), which ensued without any appreciable lag upon inoculation, began to decline slowly at approximately 45 hr (Fig. 3, bottom panel). This decline always occured about 10 hr after the depletion of nitrate. The whole-cell specific pMMO activities with and without formate as an indirect reducing agent are shown in the middle panel of Figure 3. Oxidation of the added formate regenerates intracellular NADH,[3,16] and hence the activities with formate were 3 times higher than theose without added formate. The whole-cell specific pMMO activity was high during the early exponential growth period and the maximal value observed with formate was 220 nmol of propene oxide formed/mg dry cell wt-min. However, this high pMMO activity began to decrease at about 40 hr, before the fast exponential cell growth rate slowed. Chloroform degradation activity, a characteristic of the sMMO,[19] was not detected even after 70 hrs of culturing (6.0 g dry cell wt/L), indicating continual exclusive pMMO production in spite of the reduced whole-cell specific activity.

Comparison of Figure 3 with our previous data on the batch cultivation of M. *trichosporium* OB3b without added copper[16] reveals a 50% and 100% increase in 1l and whole-cell specific MMO activity, respectively, for the growth in the 10 μM copper containing medium. Since methane utilization is not the growth-rate limiting step and μM is not proportional to the whole cell MMO activity,[6,16] the increased specific growth rate in presence of copper may be due to an improved efficiency with which M. *trichosporium* OB3b produces energy (NADH and/or ATP) during methane oxidation to CO_2.

The effect of copper during a nitrate-limited state was investigated further by challenging the cells to grow in medium that was nitrate-deficient at the outset (Table 1). When copper was present at 10 μM, but nitrate was absent, the cells grew with a μ of 0.024 hr^{-1}, while in medium lacking both copper and nitrate, μ was only 0.012 hr^{-1}. These data further indicate that copper has a nitrate-sparing effect; although, the growth rate of 0.024 hr^{-1} in the flask culture is much lower than the rate (0.070 hr^{-1}) observed in the bioreactor batch culture during 20 hr after the onset of nitrate depletion (Fig. 3 and Table 1). The whole-cell specific MMO activity obtained with copper containing, nitrate-deficient medium was about the same as for the corresponding medium deficient in both copper and nitrate, but both were much lower compared to that for the meclium containing nitrate and copper (Table 1). However, when the bacteria were incubated and repeatedly transferred several times in mediurn containing copper without nitrate, the resulting whole-cell pMMO activity approximated the specific activity observed for cells grown in the presence of copper plus nitrate. Thus, by repeatedly growing these bacteria at slow growth rates and to low cell densities, they can eventually adapt their specific pMMO catalytic activity in nitrate deffcient medium. Such an adaptation does not occur during batch bioreactor culturing in which the cells are growing more rapidly and at much higher cell densities in the absence of nitrate (Fig. 3, 40-90 hr time period).

Effect of CO_2 and bioreactor-to-flask culture transfer experiments

Although, the specific pMMO activity drops rapidly upon nitrate depletion during the batch cultivation in 10 μM $CuSO_4$ containing medium, the volumetric pMMO activity remains high due to the increasing cell biomass (Fig. 3, top panel). In an attempt to determine the basis for this early whole-cell specific pMMO decrease, the effects of several medium components were studied by transferring culture broth samples from the bioreactor to shake-flasks. Unfortunately, the culture pH increased from pH 7.0 to approximately pH 7.8 as a result of these transfers, because the broths were switched from a CO_2-rich environment in the bioreactor (10% CO_2 containing air is supplied continuously) to a CO_2-lean condition in the flasks. Even when the

pH was readjusted at the time of the transfers, the original culture broth pH could not be maintained.

In order to avoid this pH problem during the transfer experiments, another batch bioreactor experiment was carried out without the addition of the external CO_2 gas (Fig. 4). There was an initial period of much slower growth (Fig. 4 versus Fig. 3), before the faster exponential growth phase began. This might be expected from the serine pathway,[11] which requires one mole of CO_2 for the assimilation of two moles of formaldehyde. During the initial slow growth period of about 40 hrs, the whole-cell specific pMMO activity was also low, but it returned to a normal higher level during the faster exponential cell growth phase (Fig. 4, middle panel). The specific pMMO activity did not fall markedly again until about 70 hr in Figure 4, but this decrease nevertheless occurred at approximately the same cell density (A_{660}) as in Figure 3 (i.e., at 40-45 hr). In addition, the cell growth stopped abruptly at an absorbance of 6.5 in absence of external CO_2 (Fig. 4), accompanied by a rapid spike in the culture broth pH and heavy foaming. These data suggest that the cell lysis during prolonged nitrate depletion is related to the availability of CO_2. Control of the bioreactor culture broth pH between 6.9-7.1 did not prevent this cell lysis (data not shown).

Table 2. Summary of culture transfers from a batch bioreactor to side-arm shake-flasks[a]

Added fresh medium components(s)[b]	0 hr	8 hr			14 hr		
			pMMO activity[d]			pMMO activity[d]	
	A_{660}[c]	A_{660}[c]	+Formate	-Formate	A_{660}[c]	+Formate	-Formate
None (control)	0.215	0.280	56	14	0.320	69	12
Fe	0.225	0.286	56	12	0.321	64	12
Cu	0.214	0.231	22	5	0.232	22	4
Cu plus Fe	0.230	0.258	33	10	0.278	39	10
Other trace elements[e]	0.218	0.277	48	13	0.314	58	11
Nitrate	0.215	0.345	185	24	0.524	195	27
Complete medium	0.182	0.270	164	24	0.417	187	31

[a]Culture broth samples were removed at 78 hr. from a bioreactor run (Fig.4) in which no external CO_2 was supplied. They were diluted 10-fold with the supernatant liquid of the same culture broth and the pH was adjusted to 6.9 with 2N HCl. Each flask was then inoculated with 20 ml of the diluted, pH-adjusted bioreactor culture broth and incubated at 30°C and 300 rpm.

[b]Each component was added to give the same concentration as in freshly prepared 10 μmol Cu and 80 μmol Fe per L containing Higgin's medium.

[c]Direct readings of 300 ml shake-flasks equipped with 19 mm side-arms were taken the a Spectronic 21 instrument.

[d]The pMMO values given represent the nmols of propene oxide formed/mg dry cell wt-min.

[e]Mixture of trace metals other than Cu and Fe. See Ref. 16 for details.

Table 2 summarizes the results of transfer experiments from the batch bioreactor culture shown in Figure 4 into shake-flasks. The culture broth was taken from the bioreactor at 78 hr, just after the specific pMMO activity had decreased appreciably. Immediately prior to the transfers into flasks containing various medium components of interest, this broth was diluted 1fold with the supernatant of the same culture broth, aerated vigorously for 10 min to remove as much dissolved CO_2 as possible, and adjusted to pH 6.9. After both 8 hr and 14 hr of subsequent incubation, the shake-flask culture pHs ranged from 7.35 to 7.65, but no cell lysis was observed. Furthermore, there was no apparent relationship between these pH-s and either the measured growth (A_{660}) or the observed whole-cell specific pMMO activity. Table 2 clearly indicates that nitrate depletion, alone, is responsible for the precipitous decrease in the specific pMMO activity in Figure 4. The addition of iron and/or copper or other trace elements did not improve significantly either the cell growth or the pMMO activity compared to the control, after 8 hr and 14 hr. For the

copper and copper plus iron additions, the activity was even lower than that of the control.

Cultivation with concentrated medium

Since nitrate depletion appeared to be the major reason for the large decrease in the specific pMMO activity, a batch culture experiment with increased nitrate was conducted. When the standard initial medium concentration was raised 4-fold to 40 mM, nitrate was not depleted even after 80 hr of cultivation. However, this high nitrate concentration signiffcantly altered the overall characteristics of the cell growth profile, rather than merely preventing the exhaustion of nitrate. The maximal growth rate was lowered from 0.12 hr^{-1} to 0.08 hr^{-1}, and there was extensive cell lysis at the end of the exponential growth phase at 50-60 hr. As a result, a large decrease in the pMMO activity was measured again at around 50 hr when the cell density reached an A_{660} of only 2.3. Thus, a simple large increase in the initial nitrate concentration will not prevent the deterioration of whole-cell specific pMMO activity caused by the depletion of 10 mM nitrate from Higgin's standard medium.

Another batch bioreactor experiment was carried out with medium that was 4-fold concentrated with respect to each component except for the phosphate (20 mM, 2-fold), iron (80 μmol/L), and copper (10 μM). High phosphate (> 60 mM) seriously inhibits the activity of methanol dehydrogenase and subsequently the cell growth in both copper-containing and copper-deficient media (Ref. 16 and unpublished data). A copper concentration above 10 μM is also inhibitory as already shown in Figure 2. With this modified 4-fold concentrated medium, the maxiInal growth rate was reduced to about 0.075 hr^{-1} and the whole-cell specific pMMO activity began to decline as early as 40 hr. Cell lysis was not observed with the modified 4-fold concentrated medium, however, even after 80 hrs of cultivation.

Batch bioreactor culture with intermittent supplementation of nitrate

One way to avoid the decreased cell growth rate and subsequent cell lysis promoted by high nitrate-containing medium, and yet prevent its depletion in the batch mode, is to feed nitrate intermittently. Figure 5 shows a batch culture experiment conducted wi a 10 mM initial nitrate concentration, followed by intermittent nitrate additions. As seen in Figure 5 (bottom panel) the nitrate (10 mM) added to the initial culture medium was completely depleted at around 40 hr. A decrease in the specific pMMO activity occurred concomitantly. The addition of supplemental nitrate (28 mM) at 41 hr restored the whole cell specific pMMO acvity up to an A_{660} of 11 (3 g dry cell wt/L) at about 54 hr. This cell density is about 3.5 times higher compared to that in Figure 3 at 40 hr. The data in Figure 5 confirm the findings in Table 2, namely that nitrate depletion is primarily responsible for the decrease in the batch culture pMMO activity. However, a second addition of nitrate at 63 hr failed to boost

the pMMO activity again. Addition of Fe at 70 hr also did not help to regain the earlier high specific pMMO activity. This indicates that at higher cell densities (> 3 g/L), limiting medium components other than nitrate and iron contribute to the reduced pMMO activity.

Conclusions

In the present paper, we studied the obligatory methanotroph M. *trichosporium* OB3b in order to optimize the bioreactor batch culture conditions for the production of pMMO activity. Our major findings can be summarized as follows:

1. *M. trichosporium* OB3b displayed a much faster growth rate and a higher whole-cell specific MMO activity (exclusively pMMO) with 10 μM copper-containing medium than with copper-deficient medium in which the cells produce sMMO.
2. The addition of external CO_2 to copper-containing medium eliminated the initial slow or lag phase of cell growth, although the extent of the lag induced by omitting CO_2 was not nearly as prolonged as the one we observed previously[16] with copper-deficient medium.
3. The whole-cell specific pMMO activity that was produced in copper supplemented medium decreased markedly upon the depletion of nitrate.
4. Copper-supplemented medium containing either a fold increased nitrate concentration, alone, or 4-fold elevated levels of all medium components, as allowed, did not improve the bioreactor batch cultivation due to a high-nitrate growth-ratinhibition/cell fragility problem.
5. A supplemental addition of nitrate during batch cultivation provided relatively high specific pMMO activities at cell densities that were 3. 5 fold greater in comparison to the cell densities at which the pMMO could be maintained in Higgin's medium supplemented with 10 μmol Cu plus 80 μmol Fe per L, but initially containing only 10 mM nitrate.

References

1. Avakyan, Z. A. 1971. Comparative toxicity of free ions and complexes of copper and amino acids to Candida utilis. Miaobiology. **40**: 363 368.
2. Boutacoff, D. 1989. Methanol a fuel for the future? EPRI Journal. **Oct./Nov.**: 24-31.
3. Burrows, K.J., Cornish, A., Scott, D., Higgins, I.J. 1984. Substrate specificities of the soluble and particulate methane mono-oxygenases of *Methylosinus trichosporium* OB3b. J. Gen. Microbiol. **130**: 3327-3333.

4. Comish, A., MacDonald, J., Burrows, K.J., King, T.S., Scott, D., Higgins, I.J. 1985. Succinate as an in *vitro* electron donor for the particulate methane mono-oxygenase of *Methylosinus trichosporium* OB3b. Biotechnol. Lett. 7(5): 319-324.
5. Comish, A., Nicholls, K.M., Scott, D., Hunter, B.K., Aston, W.J., Higgins, I.J., Sanders, J.K.M. 1984. *In vivo* 13C-NMR investigations of methanol oxidation by the obligate methanotroph, *Methylosinus trichosporium* OB3b. J. Gen. Microbiol. **130**: 2565-2575.
6. Dalton, H., Leak, D.J. 1985. Methane oxidation by microorganisms. p. 173-200 In: RK. Poole and C.S. Dow (ed.), Microbial Gas Metabolism, Academic, New York.
7. Fogel, M.M., Taddeo, A.R., Fogel., S. 1986. Biodegradation of chlorinated ethenes by a methane-utilizing mixed culture. Appl. Environ. Microbiol. **51**: 720-724.
8. Habetsrutzen, A.Q.H., de Bont., J.A.M. 1985. Inactivation of aLkene oadadon by epodes in alkene- and alkangrown bacteria. Appl. Microbiol. Biotechnol. **22**: 428 433.
9. Harwood-Sears, V., Gorden, A. S. 1990. Copper-induced production of copper-binding supernatant proteins by the marine bacterium *Vibrio alginolyticus*. Appl. Environ. Microbiol. **56**: 1327-1332.
10. Higgins, I. J., Best, D. J., Hammond, R C., Scott, D. 1981. Methan oxidising microorganisms. Microbiol. Rev. **45**: 556-590.
11. Kell, D. 1987. Forces, fluxes and the control *of* microbial growth and metabolism. J. Gen. Microbiol. **133**: 1651-1665.
12. Lepkowski, W. 1991. Energy Policy. C&EN. **June 17**: 231.
13. Little, C.D., Palumbo, A.V., Herbes, S.E., Lidstrom, M.E., Tyndall, R.L., Gilmer, P.J. 1988. Trichloroethylene biodegradation by a methan oxidizing bacterium. Appl. Environ. Microbiol. **54**: 951-956.
14. Mehta, P.K., Mishra, S., Ghose, T.K. 1987. Methanol accumulation by resting cells of *Methylosinus trichosporium* (I). J. Gen. Appl. Microbiol. **33**: 221-229.
15. Oldenhuis, O., Vink, R.M.J.M., Jenssen, D.B., Witholt, B. 1989. Degradation of chlorinated aliphatic hydrocarbons by *Methylosinus trichosporium* OB3b expressing soluble methane monooxygenase. Appl. Environ. Microbiol. **55**: 2819-2826.
16. Park, S., Hanna, M.L., Taylor, R.T., Droege, M.W. 1991. Batch cultivation of *Methylosinus trichosporium* OB3b. I: Production of soluble methane monooxygenase. Biotechnol. Bioeng. **38**: 423 433 (Part I, this report).
17. Schreiber, D. R, Gordon, A. S., Millero, F. J. 1985. The toxicity of copper to the marine bacterium *Vibrio alginolyticus*. Can. J. Microbiol. **31**: 83-87
18. Stanley, S.H., Prior, S.D., Leak, D.J., Dalton, H. 1983. Copper stress underlies the fundamental change in intracellular location of methane mono-oxygenase in methane-oxidizing organisms: Studies in batch and continuous cultures. Biotechnol. Lett. 5(7): 487-492.

19. Taylor, RT., Hanna, M.L., Park, S., Droege, M.W. 1990. Chloroform oxidation by *Methylosinus trichosporium* OB3b- a specific catalytic activity of the soluble form of methane monooxygenase. Abstracts of the 90th Annual Meeting of the American Society for Microbiology, p. 221.
20. Tsien, H.., Brusseau, G.A., Hanson, RS., Wackett, L.P. 1989. Biodegradation of trichloroethylene by *Methylosinus trichosporium* OB3b. Appl. Environ. Microbiol. 55: 3153161.
21. Zevenhuizen, L.P.T.M., Dolfing, J., Eshuis, E.J., Scholten-Koerselman, I.J. 1979. Inhibitory effects of copper on bacteria related to the free ion concentration. Microbial Ecology. 5: 139-146.

Table 1. Effect of copper and nitrate on shake-flask cell growth and MMO activity.

Culture condition[a]	Specific growth rate, μ	MMO activity[c]	
		+ Formate	- Formate
+ Cu, + nitrate	0.12	220	21
+ Cu, - nitrate	0.024	90	14
- Cu, + nitrate	0.080	110	28
- Cu, - nitrate	0.012	87	10
Bioreactor[b]	0.070	120	30

[a]Cells adapted to 10 μM copper were employed as inocula. When added to the culture medium, the concentrations of $CuSO_4$ and $NaNO_3$ were 10 μM and 10 μM, respectively.

[b]Included for comparison are bioreactor batch culture data in the 40-60 hr time period (from Figure 3), when nitrate was no longer detectable.

[c]The whole-cell specific MMO activities were determined after 48 hr cultivations for the flasks containing nitrate and after 96 hr cultivations for the flasks lacking nitrate. The values listed are the nmols of propene oxide formed/mg dry cell wt-min, and are averages of at least three different experiments (standard deviation < 5%). They represent whole-cell pMMO activity when the culture medium contained added Cu and whole-cell sMMO catalysis when the medium lacked added Cu.

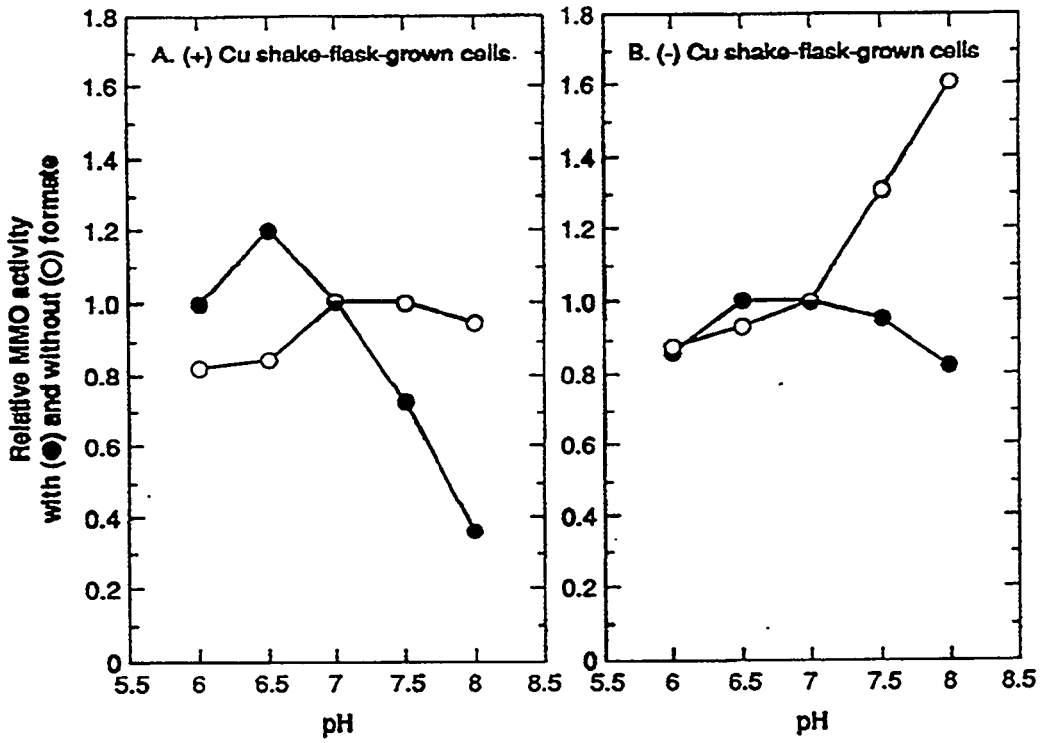

Figure 1. Effect of the assay mixture pH on the washed cell suspension MMO activities of shake-flask plus 10 μM $CuS0_4$-grown (A) and minus $CuSO_4$ grown (B) cells. Assays were performed in 25 mM MOPS plus 5 mM $MgCl_2$ buffer. At each pH, they were carried out both in the presence and in the absence of 20 mM formate. The absolute activities at pH 7.0 were 230 (with formate) and 35 (without formate) nmol of propene oxide formed/mg dry cell wt-min for the plus Cu-grown cells (A), and 110 (with formate) and 28 (without formate) nmol of propene oxide formed/mg dry cell wt-min for the minus Cu-grown cells (B), respectively.

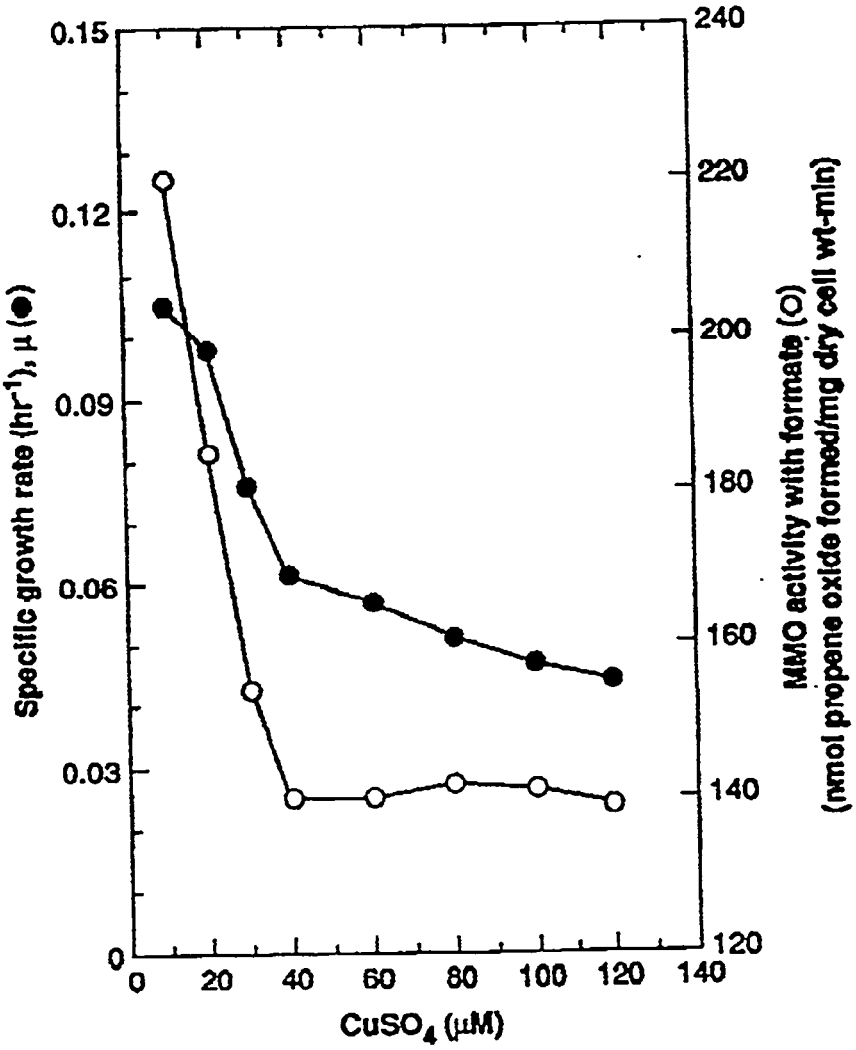

Figure 2. Effect of copper concentration on the specific growth rate and pMMO activity in shake-flask cultures. The MMO activities were measured when the cell cultures reached an absorbance of 0.4-0.9 (19 mm side-arm, Spectronic 21) after 496 hr of incubation at 30°C and 300 rpm.

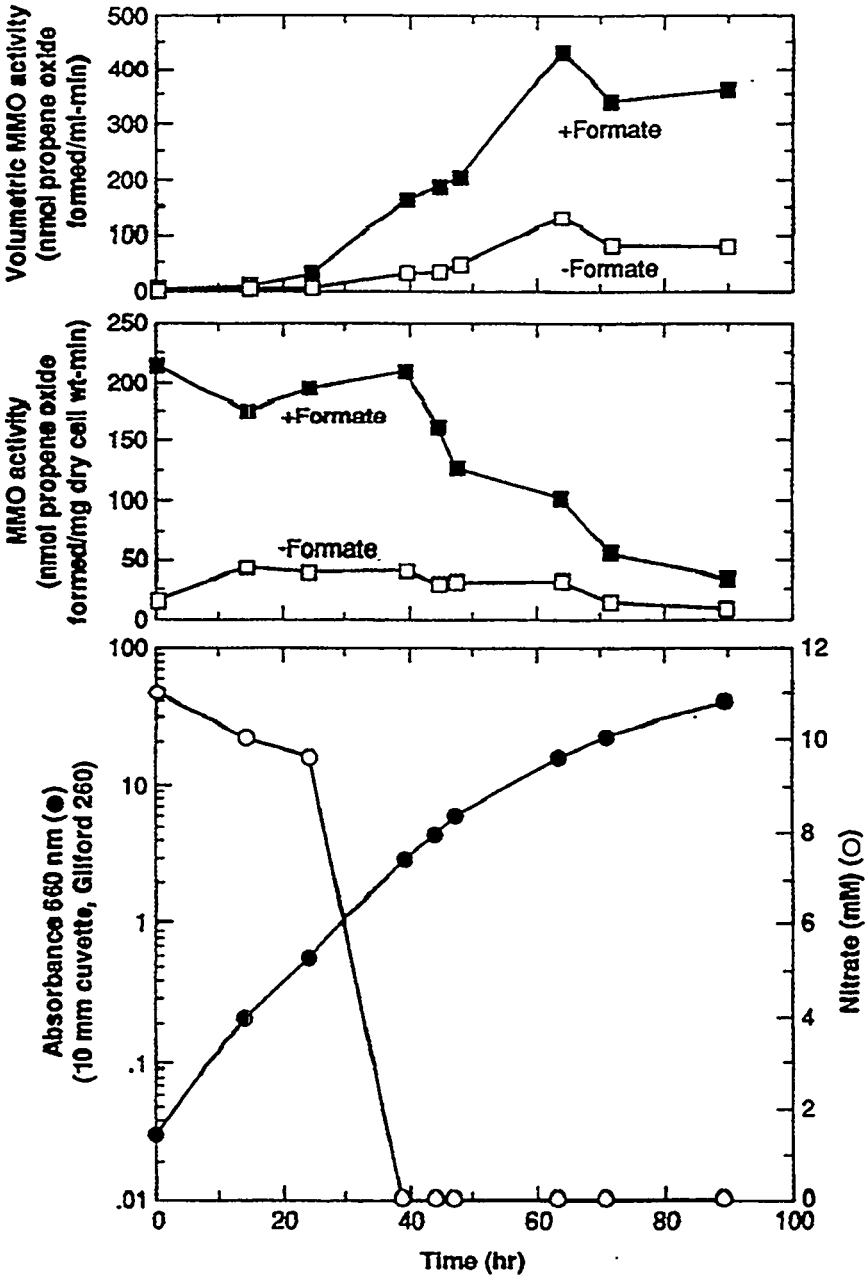

Figure 3. Bioreactor batch culture profiles of specific and volumetric pMMO activities, cell growth, and nitrate concentration. The cells were grown in Higgin's mediurn containing 10 µmol Cu, 80 µmol Fe, and 10 mmol nitrate per L with a continuous supply of methane and 9:1 (vol/vol) air/CO_2 gas mixtures. The agitation speed and gas flow rates were adjusted from time to time to maintain dissolved oxygen (DO) levels above 5%.

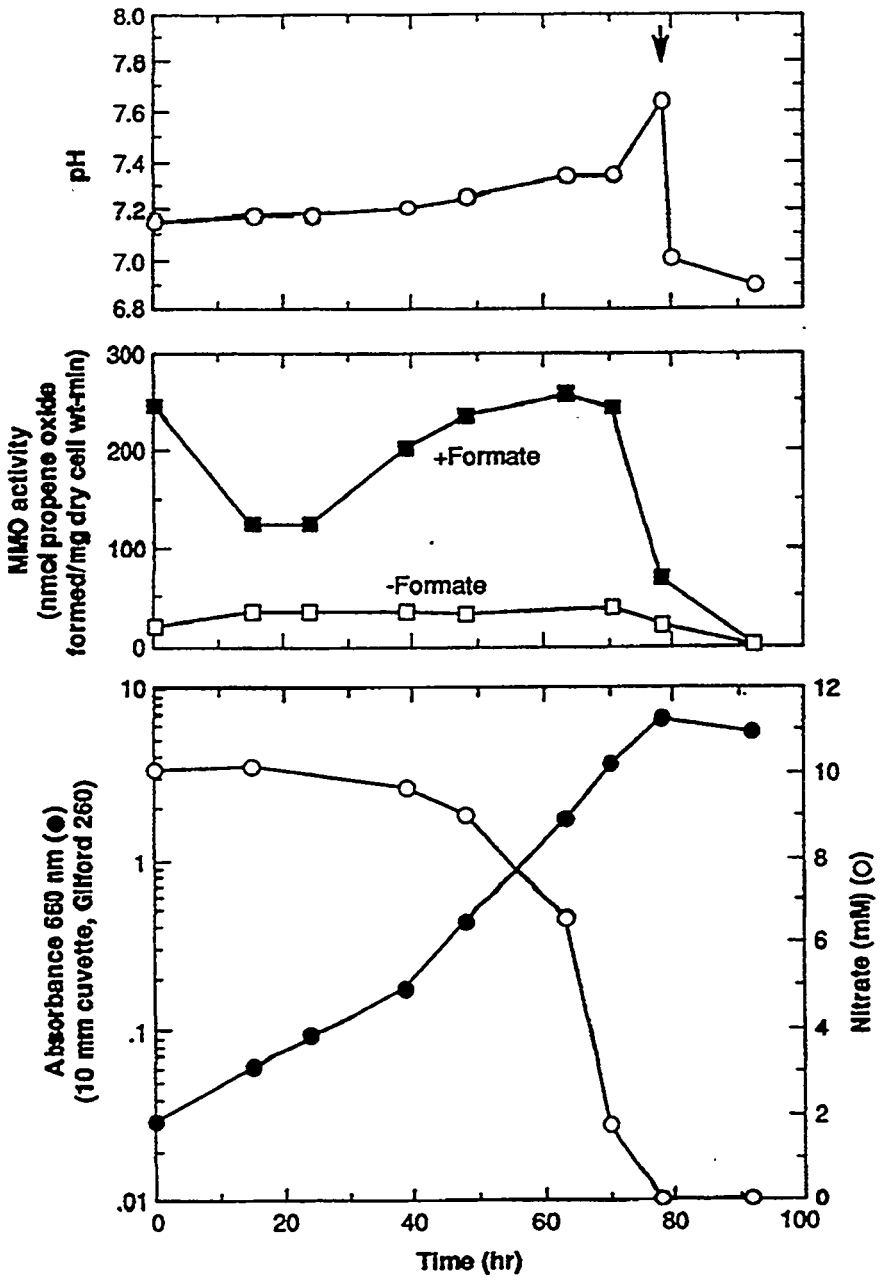

Figure 4. Bioreactor batch culture profiles without external CO_2 gassing. The bioreactor culture conditions were the same as for Figure 3, except for the omission of gaseous CO_2. Control of the culture broth pH with 2 N HCl was initiated at 78 hr, as indicated by an arrow in the top panel.

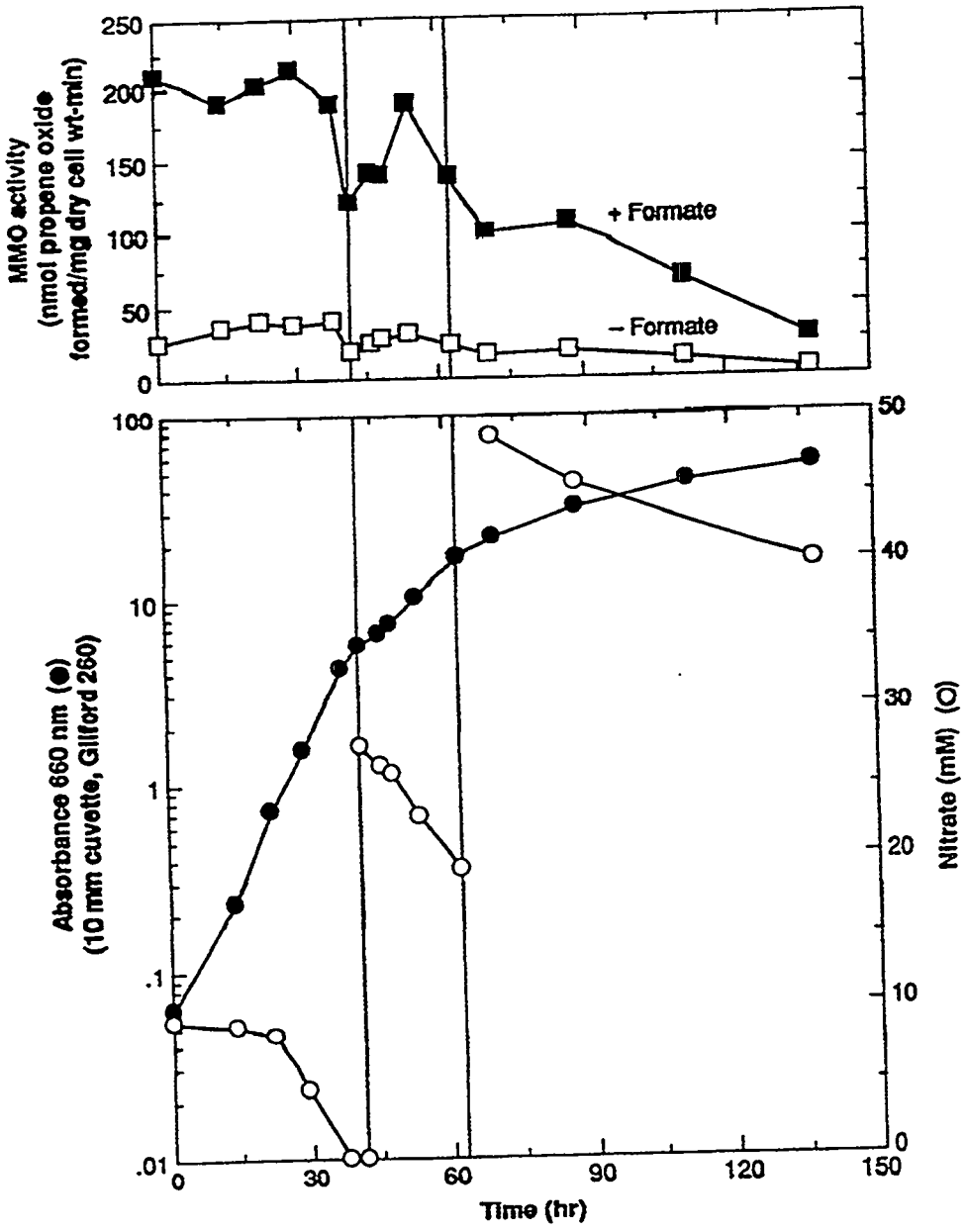

Figure 5. Bioreactor batch culture profiles with intermittent additions of nitrate. The bioreactor culture conditions were the same as for Figure 3, except for the addition of nitrate at 41 hr and 63 hr (vertical lines), respectively.

Part III: Production of Particulate Methane Monooxygenase in Continuous Culture

Introduction

Methanotrophs have promising applications in bioremediation[11,14,19,24] and the production of fuel-related chemicals[3,13,15,16] due to their methane monooxygenase (MMO) enzymes, and in the production of single-cell protein for animal feed supplementation 12 due to their growth on an inexpensive, readily available carbon source, methane gas. In some methanotrophs, such as *Methylosinus trichosporium* OB3b and *Methylococcus capsulatus* (bath), two distinct types of MMO, one soluble (sMMO) and the other particulate (pMMO), are synthesized depending on the copper availability in the culture medium. A membrane-bound pMMO is produced when copper is sufficient, while sMMO is formed when copper is scarce.[6,10,20,21,22] The sMMO oxidizes a wide range of hydrocarbons (e.g. n-alkanes, n-alkenes, aromatic and alicyclic compounds, and many chlorinated solvents) and uses exdusively NADH as an electron donor. The pMMO, on the other hand, has a much narrower substrate specificity, but functions with several electron donors (e.g. NADH, ethanol, and succinate).[61,22]

From a bioprocess standpoint, this copper effect needs to be more extensively investigated in a quantitative manner. It is the cell yield on copper ($Y_{X/Cu}$) or the amount of copper required to produce 100% pMM containing cells that enables one to determine the proper copper concentration in the initial batch culture medium or in the continuous culture feed mediurn when a given cell density is desired. Stanley *et al.* [22] reported that during the batch cultivation of M. *capsulatus* (Bath) with 0.2 mg/L $CuSO_4$-$5H_2O$ (0.8 μM Cu), sMMO became first detectable at a biomass concentration of 0.8 g dry cell wt/L. The ratio of soluble to particulate activity increased with biomass until at 1.6 g dry cell wt/L only sMMO could be detected. However, with a higher initial copper concentration of 1.0 mg/L $CuSO_4$-$5H_2O$ (4.0 μM Cu), the sMMO activity did not first appear until a biomass density of 1.4 g dry cell wt/L was reached. These results show that, qualitatively, the batch culture cell density at which sMMO activity first appears is dependent on the initial copper concentration,[8] but quantitatively, these cell-density-to-copper ratios between the high- and low-copper medium are not proportional.

We have been investigating bioreactor culture conditions for maximizing whole-cell sMMO and pMMO activity in M. *trichosporium* OB3b. From our previous batch culture experiments,[20,21] we concluded that copper redirects the overall metabolism of this microorganism in addition to switching the intracellular location and form of its MMO. During the exponential growth period, M. hichosporium OB3b exhibited a faster growth rate (μ) and a higher whole-cell specific MMO activity in 10 μM coppercontaining medium than in a copper-deficient medium. Also, the responses to nitrate depletion during the late growth period were much different:

with an initial 10 μM copper concentration, μ decreased slowly and the pMMO activity declined rapidly; but without added medium copper, 11 decreased drastically (about 10-fold) and the sMMO activity remained essentially constant until cell growth stopped.

These differences in the batch culture profiles of cell growth and whole-cell MMO activity[20,21] are most likely related to the appearance of nitrogenase and the subsequent utilization of gaseous nitrogen. Cells grown in copper-deficient medium displayed nitrogenase activity only after depletion of nitrate from the medium. Chen and Yoch have reported a similar observation for M. *trichosporium* OB3b grown in a different medium.[5] However, nitrogenase activity was observed even in the presence of 6 mM nitrate for cells grown in 10 μM Cu containing medium (unpublished data). It is the early expressed nitrogenase that may be needed to maintain a moderate growth rate upon nitrate depletion. This adaptation may divert the use of limited internal arnino acid pools from the production of pMMO into the synthesis of the enzynes necessary for the assimilation of gaseous nitrogen and lead to the precipitous decrease in the whole-cell specific pMMO activity that was observed upon depletion of the culture medium nitrate.[20]

In the present study, we have further examined the production of whole-cell pMMO activity in M. *trichosporium* OB3b for two reasons. The first was to determine the relationship between cell mass containing only pMMO activity and the amount of copper consumed under continuous culturing conditions with varying feed medium copper concentrations. The second was to optimize the culture conditions, especially for the continuous production of cells containing high pMMO activity. Whole-cell pMMO activity is the focus of this paper due to its sensitivity to both nitrate depletion and a high initial excess nitrate concentration of 40 mM in a batch culture mode.[20] Data are reported on the relationships between copper level, nitrate concentration, cell density, pMMO activity, and nitrogenase activity (or nitogen uptake rate), and the response of whole-cell pMMO activity to continuous culture operating parameters such as CO_2 gassing, impeller agitation speed, and dilution rate.

Materials and Methods

M. trichospoium OB3b was obtained from Professor R.S. Hanson (Gray Freshwater Biological Institute, University of Minnesota). The basal medium employed for the strain maintenance was Higgin's nitrate minimal salts medium.[7,21] For the various cell culturing experiments, the concentrations of several major components in the medium were modified as indicated in the text.

Fermentor-scale experiments were performed in a 5L bioreactor (Bioflo II, New Brunswick, NJ) at pH 6.7.2 and 30°C. Gaseous substrates, methane and air or

methane and 10% CO_2-containing air, were sparged continuously at a flow rate of 200 ml/min for methane and 600 ml/min for air or CO_2 containing air. The level of dissolved oxygen (DO) was maintained near zero throughout the continuous culture experiments. Bioreactor inocula were cultivated under a 1:1 (vol/vol) air/methane gas mixture in 2L shake-flasks with 200 mL of Higgin's medium containing 10 µM $CuSO_4$.[20] The bioreactor was run in a batch mode for about 50 hr after inoculation, after which it was switched to a continuous culture operation. An impeller speed of 500 rpm and a dilution rate of 0.06 hr^{-1} were used for the continuous culturing, unless stated otherwise. Fresh medium was prepared in 19L glass carboys using 0.22 m filter sterilization,[21] and was fed to the bioreactor by a peristaltic pump (Gilson, Model 312, Gilson Medical Electronics, Inc., Middleton, WI). Continuous magnetic stirring was used to keep the medium in the carboy in a well mixed state. The input medium flow rate was calibrated daily using a graduated pipet installed between the medium reservoir and the peristaltic pump. A steady-state growth rate was reached by maintaining the bioreactor under a desired set of culture conditions for more than three times the inverse of the dilution rate. A steady-state was assumed when two consecutive measurements of cell density and whole-cell MMO activity yielded approximately the sarne respective values.

Cell densities were determined by measuring the absorbance at 660 nm in a Gilford (Model 260, Gilford Instrument Lab., Inc., OH) or a Spectronic 21 (Milton-Roy Inc.) spectrophotometer as described earlier.[21] Nitrate concentration was determined with an ion-specific nitrate electrode (Orion, Model 93-07) and a double-junction reference electrode (Orion, Model 90-02) connected to a pH/ion meter (Model 701A, Orion Research Instruments, MA). Nitrogenase activity in the washed cells was measured by the reduction of acetylene to ethylene using sodium formate as an electron donor.[9] Nitrogenase assay incubations were carried out in 5 mL vials that were sealed with open-top-closure screw caps and PTFE-faced rubber septa. The reaction mixtures contained in a total liquid volume of 0.5 mL: 0.4 mg equivalents of dry cell mass; 12.5 lmol 3-(*N*- morpholino)- propanesulfonic acid (MOPS) buffer, pH 7.0; 2.5 µmol $MgCl_2$; and 5 µmol sodium formate. The headspaces were flushed with argon gas for one minute before injecting oxygen (4.46 µmol) and acetylene (17.84 µmol). Nitrogenase catalysis was initiated by transferring the vials from an ice bath at 0°C to a reciprocal water bath shaker (30°C, 180 rpm). Gas samples of 30 µ were analyzed at 10 min intervals over a period of 30-60 min with a gas chromatograph fitted with a flame ionization detector (Hach, Carle Chromatography Series 100, Hach Co.). A 6 ft HayeSep T stainless steel packed column (Hewlett-Packard) maintained at 85°C and helium as a carrier gas were used for analyzing both ethylene and acetylene. The copper contents of the washed freeze-dried cell samples were determined by inductively coupled plasma-atomic emission spectroscopy (ICP-AES) with the use of a Model JY38, Instrument S.A.. Sample preparation consisted of ashing 30 mg dry cell wts at 600°C for 2 hr, followed by dissolution of the ash in 10 ml of hot 0.5 N nitric acid. Total MMO activity (sMMO plus pMMO) of the intact cells was determined by measuring the epoxidation rate of

propene. For sMMO activity alone, the disappearance rate of chloroform was assayed, since the pMMO of M. *trichosporium* OB3b cannot degrade chloroform.[21,23] Additional information on the MMO assay procedures, and the shake-flask and previous batch bioreactor culture conditions can be found elsewhere.[20,21]

Results and Discussion

Effect of feed copper concentration and determination of cellular copper requirement

The first mediun component studied during the continuous culturing of M. *trichosporium* OB3b was copper. The feed medium nitrate concentration in standard Higgin's medium was raised from 10 to 20 mM to avoid nitrate limitation.[20,21] Figure 1 shows the effect of copper concentration on the steady-state cell density and the whole-cell total (assayed with propene), as well as the soluble (assayed with chloroform) MMO activities. The cell density increased sharply when 1 μM copper was added to medium containing no copper, and then increased gradually up to 10 μM before decreasing somewhat between 10 and 20 μM $CuSO_4$. Since the bioreactor operating conditions that affect the oxygen transfer rate (e.g. agitation speed, air flow rate, and DO level) were not changed, this trend suggsts a correlation between the cell yield on oxygen ($Y_{X/O}$) or oxygen utilization efficiency and copper availability at $CuSO_4$ concentrations below 10 μM. However, at $CuSO_4$ concentrations above 10 μM, we observed a small inhibitory effect of copper on both the cell density and the total MMO activity as found previously for batch cultivations.[20] In Figure 1 (upper panel), the whole-cell MMO activities measured with two separate substrates, propene and chloroform, show opposite profiles: the epoxidation activity increased, while the chloroform degradation activity became undetectable with increasing copper concentrations up to 7 μM. Since chloroform is a sMMO specific substrate,[23] these catalysis profiles indicate that, over the $CuSO_4$ range of 0 to 7 μM, the intracellular form of MMO switches from 100% soluble to 100% particulate. The copper-dependent rise in the whole-cell total MMO activity with propene (Figure 1, upper panel) is consistent with our past shake-flask and batch bioreactor experiments.[20,21,23] Batch cultures of the *M. trichosportum* OB3b that biosynthesize exclusively pMMO have an approamately 1.8-2.2 higher whole-cell activity with propene as a substrate in comparison to cells that produce exclusively sMMO.

The distribution of whole-cell MMO catalysis between its two intracellular forms during continuous culturing is demonstrated more clearly in the lower panel of Figure 1. Here, the percentage of pMMO activity relative to the total whole-cell epoxidation activity (pMMO plus sMMO) is plotted. Calculation of the percentage of whole-cell pMMO activity was based on the fact that the ratio of the whole-cell propene epoxidation rate to the chloroform degradaion rate is constant for the

soluble form of MMO. This ratio was obtained from the whole-cell propene and chloroform MMO activities in a copper-free medium, where only the soluble form is present. In this medium, the propene to chloroform substrate activity ratio was consistent.[3,4]

From the same continuous culture experiment in Figure 1, the corresponding copper contents in freeze dried cell masses were determined. They are plotted in Figure 2, along with the volumetric whole-cell pMMO activity as a function of the feed copper concentration. The volumetric pMMO activities were calculated from the ratios of the wholecell propene epoxidation and chloroform degradation activities as mentioned above. Figure 2 shows that both the volumetric pMMO and the copper content of the cell mass increased linearly with increasing feed copper concentration up to 10 μM. At higher copper concentrations, the volumetric pMMO gradually declined, while the cellular copper content began to deviate from a linear relationship.

In order to determine $Y_{X/Cu}$ or the quantitative amount of copper required to produce a certain cell mass containing 100% pMMO, one needs to know the copper consumption rate under copper-excess condition. In Figure 2, this condition seemed to be satisfied when the copper level in the feed medium exceeded 10 μM. An effort to measure the remaining residual copper concentrations in spent media, however, was not successful. Moreover, copper was not even detectable over the whole range that was tested in Figures 1 and 2. The modified Higgin's nitrate salts medium that we used in this study had an iron content of 80 μmoles/L.[20,21] During culturing, some of this ferrous iron is oxidized to insoluble ferric iron which can coprecipitate copper. Consequently, copper is removed from the culture broth during centrifugation, and, therefore, can not be accurately determined as an unused spent medium component. Another factor interfering with the measurement of spent medium copper is the non-growth related, nonspecific adsorption of copper onto the cell surface. Cells which had been pregrown on 10 μM $CuSO_4$, repeatedly washed, and then resuspended at 1 g dry weight equivalent/L could lower the copper concentration by more than 50% within 30 min when incubated in distilled water containing 10 μM copper.

Since it was impossible to determine $Y_{X/Cu}$ under copper-excess continuous culturing conditions, an alternative approach was undertaken. In the range of 0 to 10 μM copper, a straight line can be fit through the volumetric pMMO activity data (Figure 2, upper panel). It has a slope of 52.5 μmol of propene oxide formed/1mol Cu-min-ml. If it is assumed that. (a) the added copper is consumed completely over this $CuSO_4$ range, and (b) the whole-cell pMMO activity is 210 μmol of propene oxide formed/mg dry cell wt-min when 100% pMMO is formed under the given operating conditions, then the foregoing slope term can be rearranged to give 3.9×10^3 g dry cell wt/g Cu ($Y_{X/Cu}$) or 2.6×10^{-4} g Cu/g dry cell wt (copper requirement or copper content). This latter value is in excellent agreement with the ICP-AES

copper analyses of the freeze-dried cells. Cells, for example, taken from the bioreactor operated with 10 μM copper in the feed medium (Figure 1), contained 253 ppm or 2.6×10^{-4} g Cu/g dry cell wt (Figure 2, lower panel).

In addition to the cell density and the MMO activity, the feed copper level also had a significant effect on the source of nitrogen utilized as shown in Figure 3. The lower panel indicates that, although the feed medium nitrate concentration ($[NO3^-]f$) was held constant at 20 mM, the residual culture broth concentrations at the various copper steady-states ($[NO3^-]s$) ranged from 0.3 to 5 mM. Since the cell yield on nitrogn ($Y_{X/N}$) is constant at 7.14 g dry cell wt/g N (or 0.1 g dry cell wt/mmol NO-3),[1-20] this varying [NO3-]5 implies that M. *Trichosporium* OB3b assimilates differing amounts of X_{N2} as a function of the input copper concentration. Cell density derived from gaseous nitrogen, X_{N2}, was therefore calculated for each copper level from Eq. (1) below

$$X_{N2} = X_T - \{[NO_3^-]_f - [NO_3^-]_s)\}/Y_{X/N} \qquad (1)$$

Figure 3 (lower panel) reveals that X_{N2} increases as the feed medium copper concentration is raised from 2 to 15 μM and strongly suggests that the assimilation of N_2 is dependent on copper availability in the culture medium.

Nitrogenase activity and the specific N_2 assimilation rate (q_N) are also plotted in Figure 3 (upper panel). No nitrogenase activity was detected at low copper concentrations up to 2 μM, where an appreciable amount of the steady-state MMO was still present in the soluble form (Figure 1). The nitrogenase activity then inaeased abruptly between 2 and 4 μM copper and gradually reached a maximum at 15 μM. This nitrogenase activity pattern is in close agreement with the N_2 assimilation rate (Figure 3, upper panel) that was derived from the residual steady-state $[NO_3^-]_S$ measurements in the lower panel of Figure 3. It is interesting that the nitrogenase activity dropped sharply when the copper concentration was raised from 15 to 20 μM, whereas the pMMO activity decreased only slightly when the medium copper was elevated to 20 μM (compare Figures 1 and 3). Clearly, the feed medium copper has separable effects on these two enzymes.

Effect of Feed Nitrate Concentration

The second medium component studied in continuous culture was nitrate. Effects of the feed nitrate concentration on the steady-state cell densities (total as well as nitrogen fixation derived), and the whole-cell activities of the pMMO and nitrogenase enzymes are plotted in Figure 4. The feed medium copper concentration was held at 10 μM to produce exdusively pMMO. It can be seen that both the steady-state total cell density and the pMMO activity increased when the feed nitrate level

was raised from 5 to 40 mM. However, when the nitrate concentration was raised further to 50 mM, the cell density increased marginally, but the pMMO activity decreased sharply by 30% (Figure 4, upper panel). At feed nitrate concentrations from 5 to 20 mM, most of the available medium nitrate was consumed (90-100%) and gaseous nitrogen assimilation declined over this feed nitrate concentration range (Figure 4, lower panel). In contrast, when the incoming nitrate concentration was raised above 20 mM, it was only partially utilized (35% at 40 mM and 15% at 50 mM) and more nitrogen was again derived by fixing gaseous N_2. These data establish that feed nitrate concentrations up to 40 mM have no adverse effects on either the whole-cell pMMO activity or biomass production. It is surprising that the nitrogenase activity did not follow the pattern of the N_2-derived cell density when the feed nitrate concentration was raised above 20 mM. In the higher nitrate concentration range of 20 to 50 mM, the whole-cell specific nitrogenase activity remained almost constant while the N_2-derived cell density more than doubled.

Although no specific reference could be found on the mode of medium nitrate conversion to ammonia by methanotrophs, it presumably takes place through a two step process known as assimilatory nitrate reduction.[4] The first step is the reduction of nitrate to nitrite by the enzyme nitrate reductase. The second step involves the reduction of nitrite to ammonia by nitrite reductase. Ammonia is then incorporated into the cell mass. Consistent with this assumption are our observations (data not shown) that M. *trichosporium* OB3b grows at similar logarithmic rates during the first 60 hr (30°C) of shakeflask culturing when the 10 mM nitrate is replaced by either 1 mM $NaNO_2$ (Higgin's basal medium lacking copper) or by 0.5 mM $NaNO_2$ (same mediun supplemented with 10 μM $CuSO_4$). Higher concentrations of $NaNO_2$ were inhibitory for growth, with or without added copper in the medium. On the other hand, when methanotrophs fix gaseous nitrogen, the conversion of this nitrogen to ammonia is carried out by the nitrogenase system.[18] This reduction which is catalyzed by nitrogenase requires both reducing power and energy in the form of ATP, and the enzyme system is repressed by the fixed nitrogen sources.[17,18] Hence, it is interesting that in the present work, M. *trichosporium* OB3b not only exhibited an active nitrogenase system in the presence of nitrate, but also derived cellular nikogen from both available sources of nitrogen.

Effect of Feed Medium Concentration

After the optimal concentration ranges of copper and nitrate had been established, the combined effects of most of the other medium components were examined under continuous culturing conditions. The feed medium concentration was varied from 1-fold (1X) to 4-fold (4X), except for the phosphate, copper, nitrate, and iron. The nitrate and iron were held constant at 40 mM and 80 μM, respectively. From the results in Table 1, the steadystate cell densities for all three experiments with 10 μM Cu averaged 2.1 g/L. The cell densities were somewhat higher when copper was increased from 10 to 20 μM in richer media. Whole-cell specific pMMO activity was

essentially constant around 210 in all experiments, except when CO_2 was omitted from the gas stream. Thcse data suggest that Higgin's minimal medium fortified with 40 mM nitrate, 10 μM copper and 80 μM iron (will be referred to as Higgin's "modified lX medium", hereafter) is sufficient to support a high pMMO activity up to a cell density of 2.2 g/L.

We have reported previously that CO_2 gassing is very important to abolish an initial long lag period of more than 150 hr during the batch bioreactor cultivations with copper-deficient medium.[21] However, the effect of external CO_2 was negligible on both the cell growth and whole-cell specific sMMO activity when the cell density reached 0.1 g/L. In the case of bakh 10 M copper-containing medium, the initial lag was reduced to about 40 hr without CO_2 addition and the proRles of cell growth and pMMO activity after the lag period were essentially the same as those with CO_2 addition.[20]

Therefore, it was somewhat surprising to observe a decrease in MMO activity when CO_2 was omitted from the gas phase during continuous culturing (Table 1, experiment 5). Chloroform activity was also measured for each experiment in Table 1 to verify that the reduced whole-cell specific activity with propene was not due to a shift in the expressed catalysis to the sMMO form. No activity with chloroform as a substrate was detected under any of these conditions. Hence, it is essential to add CO_2 to the incoming gas mixture for maximal pMMO activity during the continuous mode of bioreactor operation.

Effect of Agitation Speed

Figure 5 shows the effect of agitation speed on the cell density, residual nitrate concentration, whole-cell specific pMMO activity, and overall pMMO productivity when Higgin's "modified lX medium" and a dilution rate of 0.064 hr^{-1} were used. Overall pMMO productivity is defined as the amount of pMMO activity produced per unit time and unit bioreactor volume. When the agitation speed was varied in a range of 300 to 700 rpm, the steady-state cell densities, total as well as those derived from the gaseous nitrogen, increased continuously due to the increased oxygen transfer rate. Nitrate utilization, however, showed a different trend. Maximal nitrate was consumed (8.5 mM) at 500 rpm, and either a higher or a lower agitation speed resulted in a reduced nitrate consumption (Figure 5, lower panel). In contrast, the whole-cell specific pMMO activity was maximal at 400 rpm. It decreased rapidly with increasing agitation speeds between 400 and 600 rpm, and rather slowly thereafter (Figure 5, upper panel). This trend clearly indicates that the whole-cell pMMO activity is very sensitive to mechanical shear at high agitation speeds. Overall pMMO productivity exhibited a maximum at 500 rpm. This maximum is a result of the combined influence of the cell density and specific pMMO activity. At lower agitation speeds, the low cell densities offset the high pMMO activities, while

at higher speeds, the low pMMO activities offset the high cell densities. Thus, one should select the agitation speed of the bioreactor depending on the application. A higher agitation speed should be used for single cell protein production, but a lower speed would be preferred for optimal wholcell specific pMMO activity.

Effect of Dilution Rate

The last continuous culture operating parameter that we studied was the dilution rate (D). Its effects on biomass production and whole-cell catalytic activity are shown in Figure 6. Higgin's "modified lX medium" was used and the agitation speed was fixed at 500 rpm (optimal for overall pMMO productivity). With increasing dilution rate, the steady-state cell density decreased sharply in the range of 0.02 to 0.04 hr^{-1} and rather gradually thereafter. Nitrate consumption was essentially constant at low dilution rates, but it decreased gradually with increasing dilution rates above 0.04 hr-1. Whole-cell specific pMMO activity, on the other hand, increased with the dilution rate up to 0.06 hr^{-1}, and it remained constant upon further increases of the dilution rate to 0.10 hr^{-1}. The overall pMMO productivity exhibited a maximum at a dilution rate of 0.08 hr^{-1}. This maximum is also the result of the concerted effects of both the cell density and the whole-cell specific pMMO activity. At a lower dilution rate, low pMMO activity offsets the high cell density, and at a higher dilution rate, a low cell density offsets the high pMMO activity. The variation of overall productivity over the entire range of dilution rates studied is relatively small compared to those cornInonly found in literature.[2] Apparently, this is due to the continuously decreasing steady-state cell densities associated with the increasing dilution rates.

When the concentration of nitrate was reduced to 10 mM in the feed medium, the steady-state patterns observed were similar to those in Figure 6, but with minor differences. The nitrate consumption was higher and the whole-cell specific pMMO activity was lower at each dilution rate than the values plotted in Figure 6 (data not shown). Thus, the effects of the dilution rate observed here are independent of the feed medium nitrate concentration.

Conclusion

In the present paper, we studied the obligatory methanotroph *M.trichosporim* OB3b in order to optimize the bioreactor continuous culture conditions for generating biomass and producing whole-cell pMMO activity. Our major findings are summarized below:

1. Under standard operating conditions (500 rpm agitation speed, and 0.06 hr^{-1} dilution rate), both the soluble and the particulate forms of MMO were produced at copper concentrations up to 7 μM. A maximal cell density and whole-cell specific pMMO activity were observed with 10 μM copper in the

feed medium. Also, the cell yield on Cu was 3.9 X 103g dry cell wt/g Cu for the exclusive production of pMMO.

2. The bacteria assimilated nitrogen from both the medium nitrate and the gaseous nitrogen, when the copper concentration was greater than 2 μM in Higgin's feed medium containing 20 mM nitrate and 80 μM iron.
3. Bacterial growth under standard operating conditions in Higgin's medium containing 10 μM copper and 80 μM iron was associated with a complete consumption of the feed nitrate up to an input level of 20 mM. Higher feed medium nitrate concentrations resulted in only a partial utilization of the available nitrate, but caused no adverse effect on the cell density. A maximal wholcell specific pMMO activity was measured with a feed nitrate concentration of 40 mM.
4. Optimal overall pMMO productivity was observed in Higgin's "modified lX medium" at a dilution rate of 0.064 hr^{-1}, an agitation speed of 500 rpm, and gaseous substrate flow rates of 200 ml/min for methane and 600 ml/min for an air/ CO_2 (9:1) mixture. The whole-cell specific pMMO activity, however, was maximal when the agitation speed was reduced to 400 rpm. Also, the pMMO activity repeatedly decreased by 30% when CO_2 was omitted from the incoming gas mixture.

References

1. Anthony, C. 1982. Chap. 9. The biochemistry of Methylotrophs. Academic, New York.
2. Bailey, J.E., Ollis, D.F. 1986. Chap. 7. Biochemical engineering fundamentals. 2nd edition. McGraw-Hill, New York.
3. Boutacoff, D. 1989. Methanol a fuel for the future? EPRI Journal. **Oct./Nov.**: 24-31.
4. Brock, T.D., Smith, D.W., Madigan, M.T. 1984. Chap. 5. Biology of microorganisms. 4th edition. Prentice-Hall, New Jersey.
5. Chen, Y.-P., Yoch, D.C. 1988. Reconstitution of the electron transport system that couples formate oxidation to nitrogenase in *Methylosinus trichosporium* OB3b. J. Gen. Microbiol. **134**: 3123128.
6. Cornish, A., MacDonald, J., Burrows, K.J., King, T.S., Scott, D., Higgins, I.J. 1985. Succinate as an in itro electron donor for the particulate methane mono-oxygenase of *Methylosinus trichosporium* OB3b. Biotech. Lett. 7(5): 319-324.
7. Cornish, A., Nicholls, K.M., Scott, D., Hunter, B.K., Aston, W.J., Higgins, I.J., Sanders, J.K.M. 1984. *In vio* 13C-NMR investigations of methanol oxidation by the obligate methanotroph, *Methylosinus tr*hosporium* OB3b. J. Gen. Microbiol. **130**: 2565-2575.
8. Dalton, H., Prior, S.D., Leak, D.J., Stanley, S.H. 1984. Regulation and control of methane monooxygenase. p. 782 In: R.L. Crawford and R.S. Hanson

(ed.), Microbial growth on C1 compounds, American Society for Microbiology, Washington, D.C.

9. Dalton, H., Whittenbury, R 1976. The acetylene reduction technique as an assay for nitrogenase activity in the methane oxidizing bacterium *Methylococcus* capsulatus strain bath. Arch. Microbiol. **109**: 147-151.
10. Das, K., Cornish, A., Higgins, I.J. 1987. Regulation of the intracellular location of methane mono-oxygenase during growth of *Methylosinus trichosporium* OB3b on methanol.J. Gen. Microbiol. **133**: 291-297.
11. methane-utilizing mixed culture. Appl. Environ. Microbiol. **51**: 72724.
12. Higgins, I.J., Best, D.J., Hammond, R.C., Scott, D. 1981. Methaneoxidizing microorganisms. Microbiol. Rev. **45**: 556-590.
13. Lepkowski, W. 1991. Energy Policy. C&EN. **June 17:** 20-31.
14. Little, C.D., Palumbo, A.V., Herbes, S.E., Lidstrom, M.E., Tyndall, R.L., Gilmer, P.J. 1988. Trichloroethylene biodegradation by a methaneoxidizing bacterium. Appl. Environ. Microbiol. **54**: 951-956.
15. Mehta, P.K., Mishra, S., Ghose, T.K. 1987. Methanol accumulation by resting cells of *Methylosinus trichosporium (I). J.* Gen. Appl. Microbiol. **33**: 221-229.
16. Mountfort, D.O., Pybus, V., Wilson, R. 1990. Metal ion-mediated accumulation of alcohols during alkane oxidation by whole cells of *Methylosinus trfchosporium*. Enzyme Microb. Technol. **12**: 343-348.
17. Murrell, J.C. 1988. The rapid switch-off of nitrogenase activity in obligate methane-oxidizing bacteria. Arch. Microbiol. **150**: 48995.
18. Murrell, J.C., Dalton, H. 1983. Nitrogen fixation in obligate methanotrophs. J. Gen. Microbiol. **129**: 3481-3486.
19. Oldenhuis, O., Vink, R.M.J.M., Jenssen, D.B., Witholt, B. 1989. Degradation of chlorinated aliphatic hydrocarbons by *Methylosinus trichosporfum* OB3b expressing soluble methane monooxygenase. Appl. Environ. Microbiol. **55**: 2819-2826.
20. Park, S., Shah, N.N., Taylor, R.T., Droege, M.W. 1991. Batch cultivation of *Methylosinus trichosporium* OB3b: II. Production of particulate methane monooxygenase. Biotechnol. Bioeng. in press.
21. Park, S., Hanna, M.L., Taylor, R.T., Droege, M.W. 1991. Batch cultivation of *Methylosinus trichosporium* OB3b. I: Production of soluble methane monooxygenase. Biotechnol. Bioeng. **38**: 42333.
22. Stanley, S.H., Prior, S.D., Leak, D.J., Dalton, H. 1983. Copper stress underlies the fundamental change in intracellular location of methane mono-oxygenase in methane-oxidizing organisms: Studies in batch and continuous cultures. Biotechnol. Lett. **5**(7): 48792.
23. Taylor, R.T., Hanna, M.L., Park, S., Droege, M.W. 1990. Chloroform oxidation by *Methylosinus trichosporium* OB3b- a specific catalytic activity of the soluble form of methane monooxygenase. Abstracts of the 90th Annual Meeting of the American Society for Microbiology, p. 221.

24. Tsien, H.-C., Brusseau, G.A., Hanson, R.S., Wackett, L.P. 1989. Biodegradation of trichloroethylene by *Methylosinus trichosporium* OB3b. Appl. Environ. Microbiol. **55**: 3155-3161.

Table 1. Effect of the medium concentration on the steady-state cell density and whole-cell pMMO activity[a]

Bioreactor experiment	Continuous culture medium composition[b]			Steady-state cell density (g/L)	pMMOC
	Phosphate (mM)	Copper sulfate (μM)	All other medium components		
1	20	10	4X	2.02	212
2	20	20	4X	2.60	213
3	20	20	2X	2.80	219
4	10	10	1X	2.22	211
5	10	10	1X, but no CO_2 gassing	2.16	148

[a]Continuous culture conditions were: a dilution rate of 0.064 h^{-1}, an agitation speed of 500 rpm, and gas flow rates of 200 ml/min for methane and 600 ml/min for 10% CO_2-containing air (except for experiment 5). Under these conditions, the pH remained at 6.7-7.2 and the dissolved oxygen stayed at 2-5% of saturation.

[b]With the exception of phosphate, copper, nitrate, and iron, the basal medium was Higgin's nitrate salts medium (see Refs. 7,21). Nitrate and iron were fixed at 40 mM and 80 μM, respectively, in all of these experiments.

[c]The whole-cell specific pMMO activity values given represent the nmols of propene oxide formed/mg dry cell wt-min.

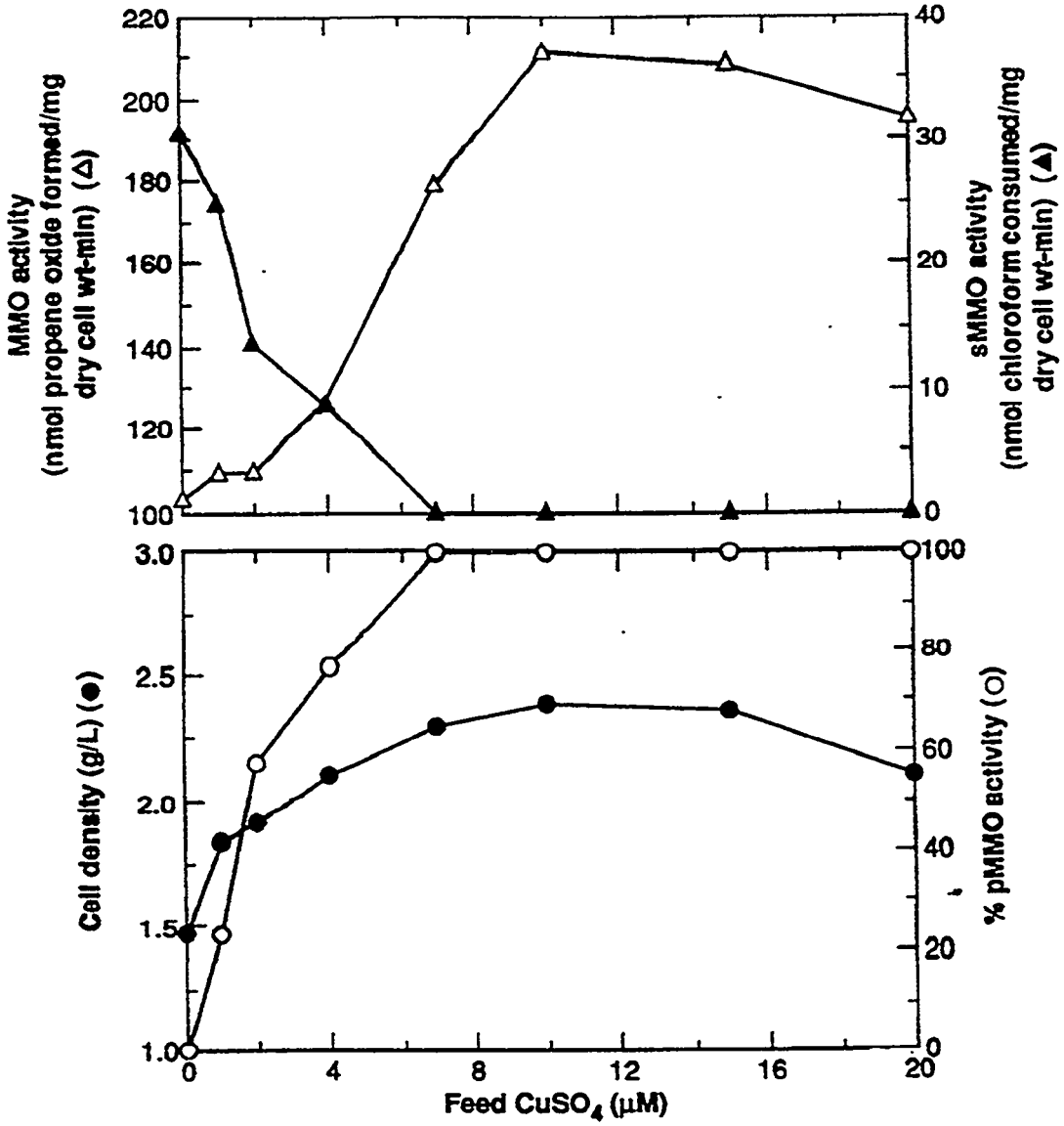

Figure 1. Effect of feed medium copper concentration on whole-cell specific MMO activity, cell density, and percentage of the total MMO activity due to the particulate form in a 5L bioreactor during oxygen limited continuous culture conditions. Cells were grown in Higgin's medium containing 80 μM Fe and 20 mM nitrate with a continuous supply of methane (200 mL/min) and a 9:1 (vol/vol) air/CO_2 gas mixture (600 mL/min). The agitation speed was 500 rpm and the dilution rate was 0.06 hr^{-1}.

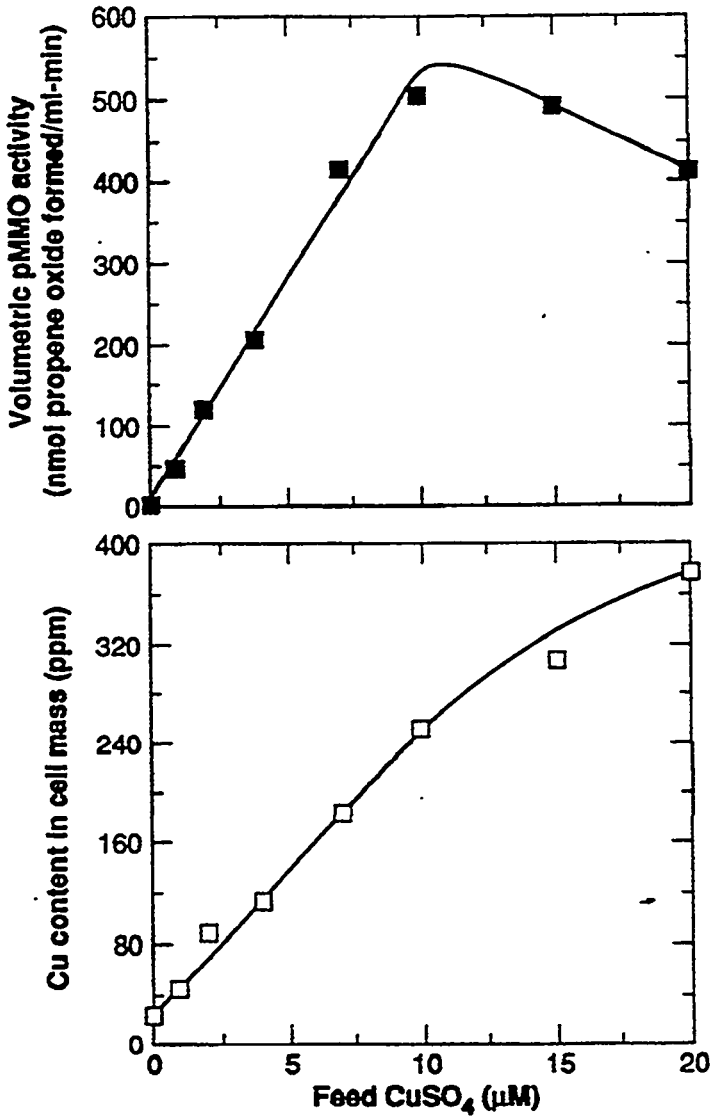

Figure 2. Effect of feed medium copper concentration on volumetric pMMO activity and copper content of the biomass during the continuous culturing experiment in Figure 1. Input medium and operating parameters were, therefore, the same as in Figure 1. The copper content of the cells was determined by ICP-AES.

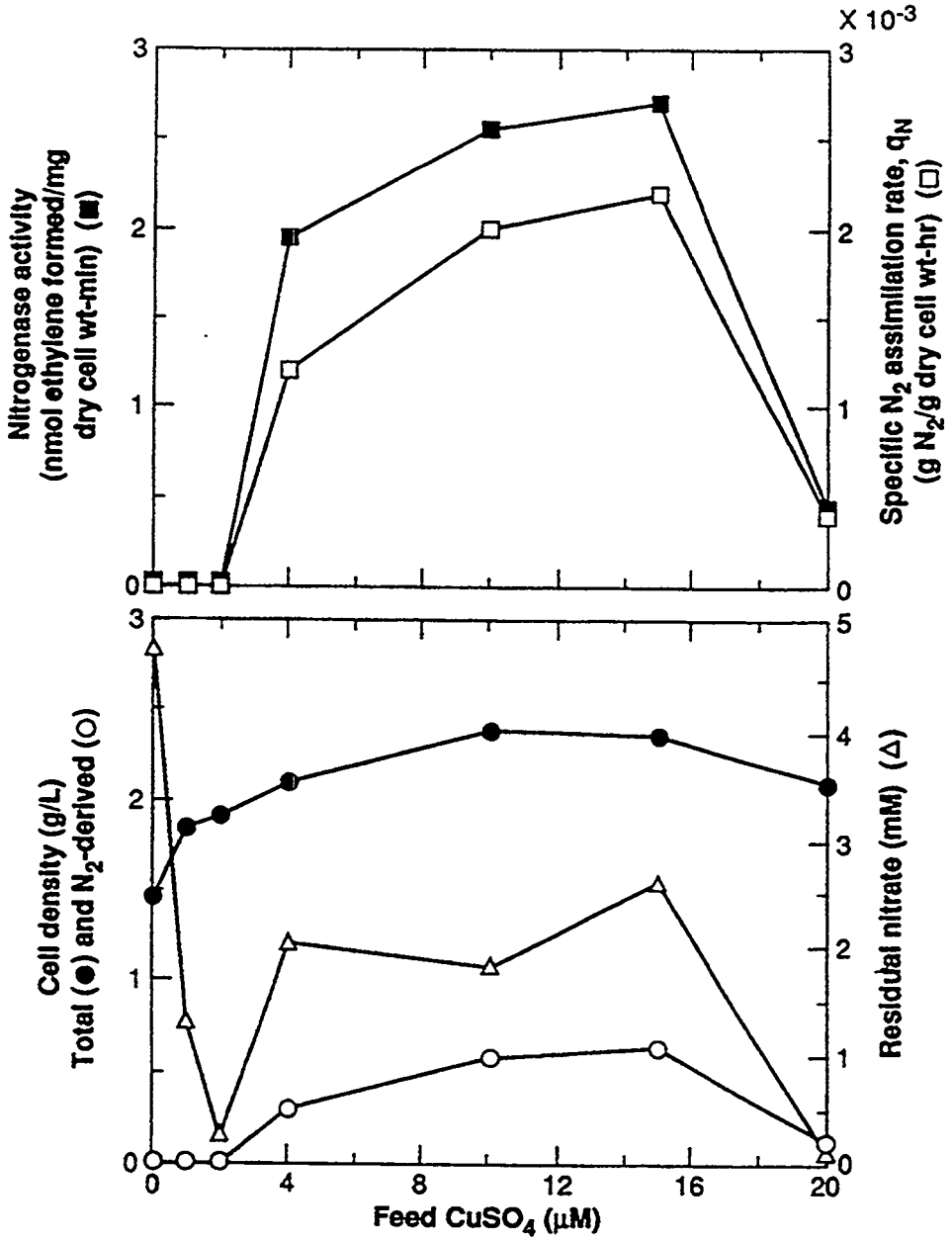

Figure 3. Whole-cell nitrogenase activity, specific N_2 assimilation rate, total cell density, cell density derived from gaseous N_2, and nitrate consumption as function of the feed medium copper concentration for the same continuous culture experiment described in Figure 1. Nitrate concentrations shown are the residual nitrate in the medium at each steady state. Nitrogen derived cell density was calculated from the total cell density, nitrate utilized, and cell yield on nitrogen (see text for details).

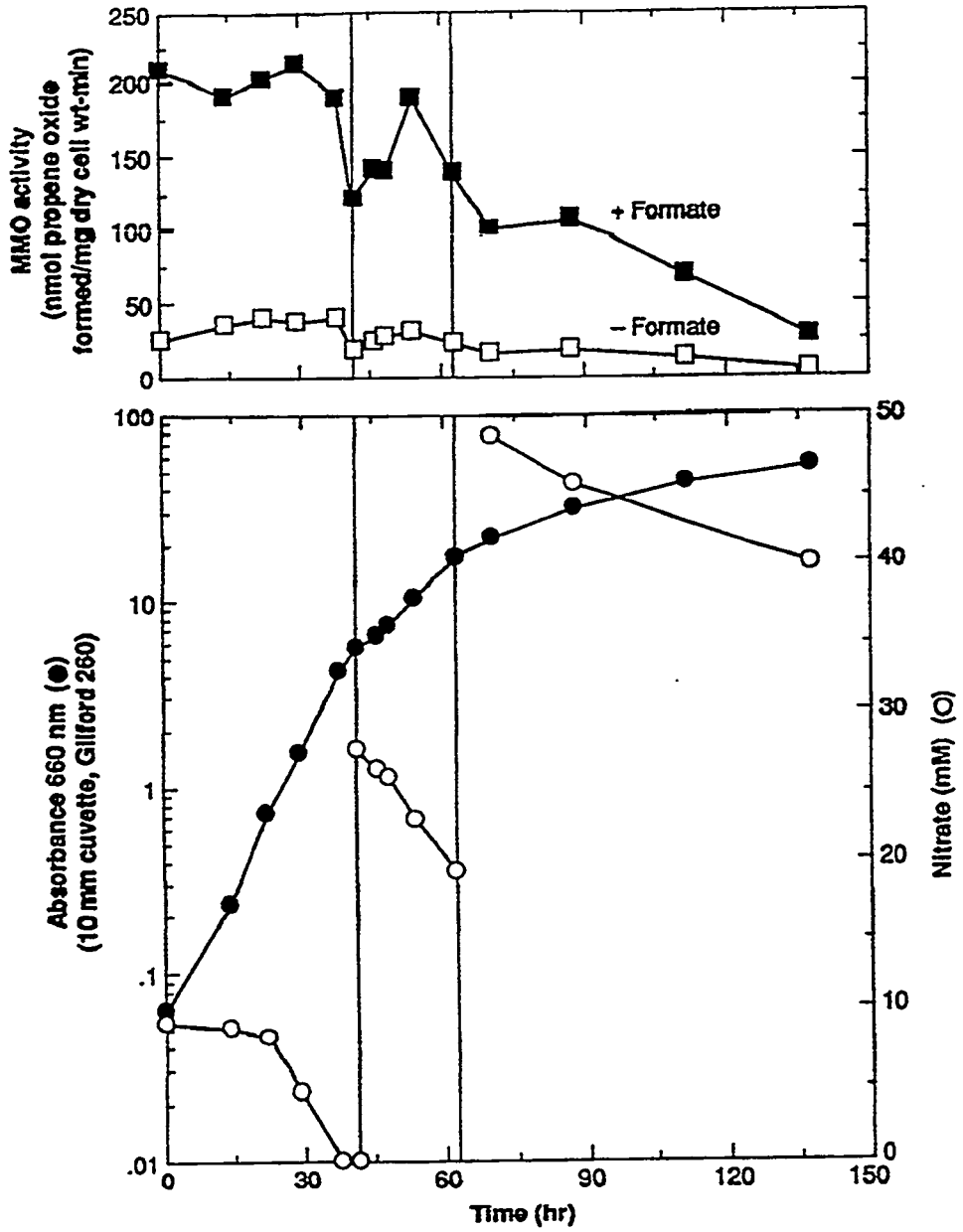

Figure 4. Effect of feed medium nitrate concentration on the whole-cell speciffc pMMO and nitrogenase activities, total and gaseous nitrogen derived cell densities, and residual steady-state nitrate. Cells were grown in Higgin's medium containing 80 μM Fe and 10 μM Cu at an agitation speed of 500 rpm and a dilution rate of 0.06 h^{-1}. The bioreactor was sparged with a continuous flow of methane and a 9:1 (vol/vol) air/CO_2 gas mixture as in Figure 1.

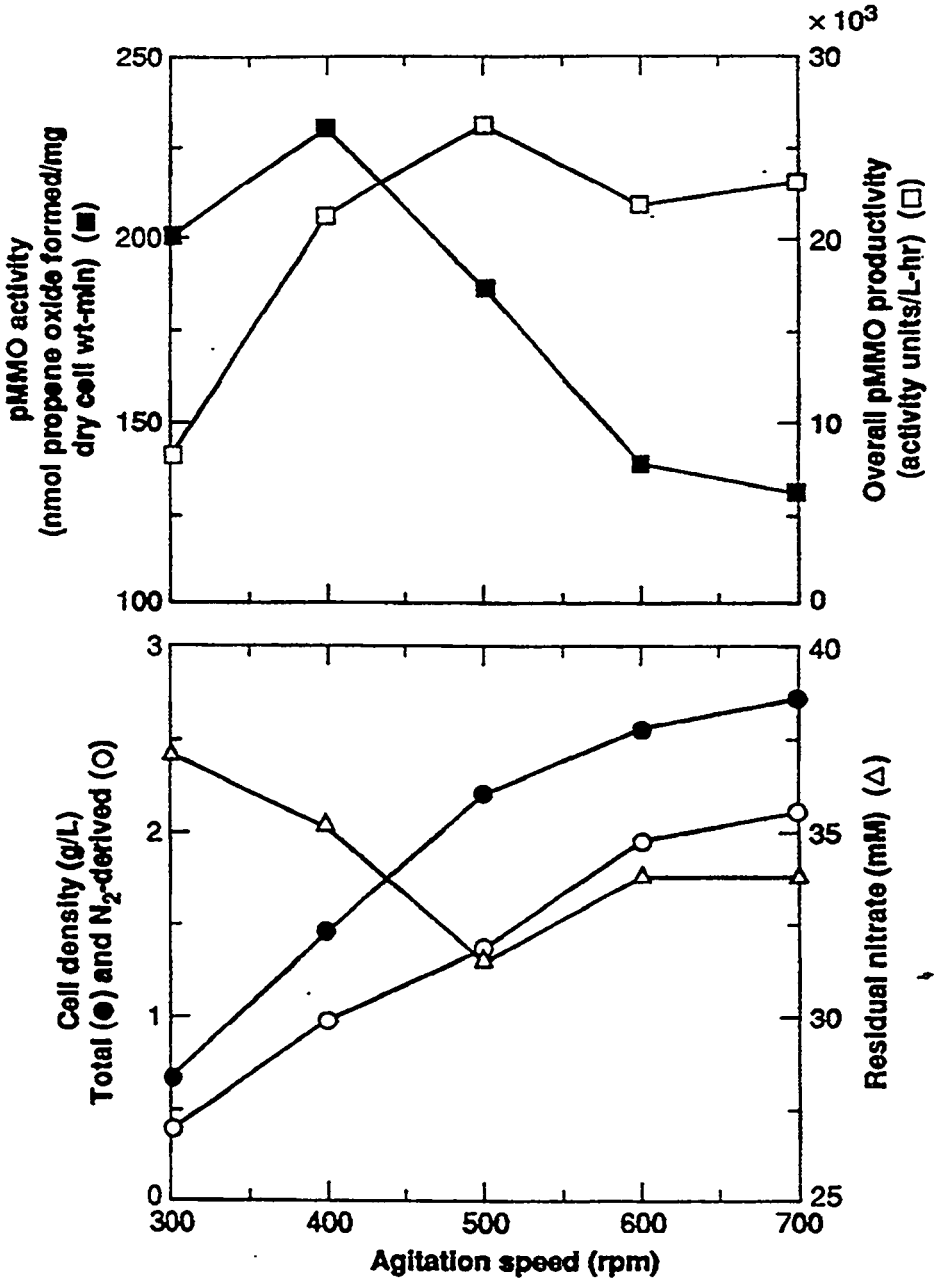

Figure 5. Effect of agitation speed on whole-cell specific pMMO activity, overall pMMO productivity, total and gaseous nitrogen derived cell densities, and residual steady-state nitrate. The cells were grown in Higgin's "modified lX medium" that is defined in the text. Gas sparging conditions were the same as in Figure 1 and the dilution rate was 0.064 hr^{-1}.

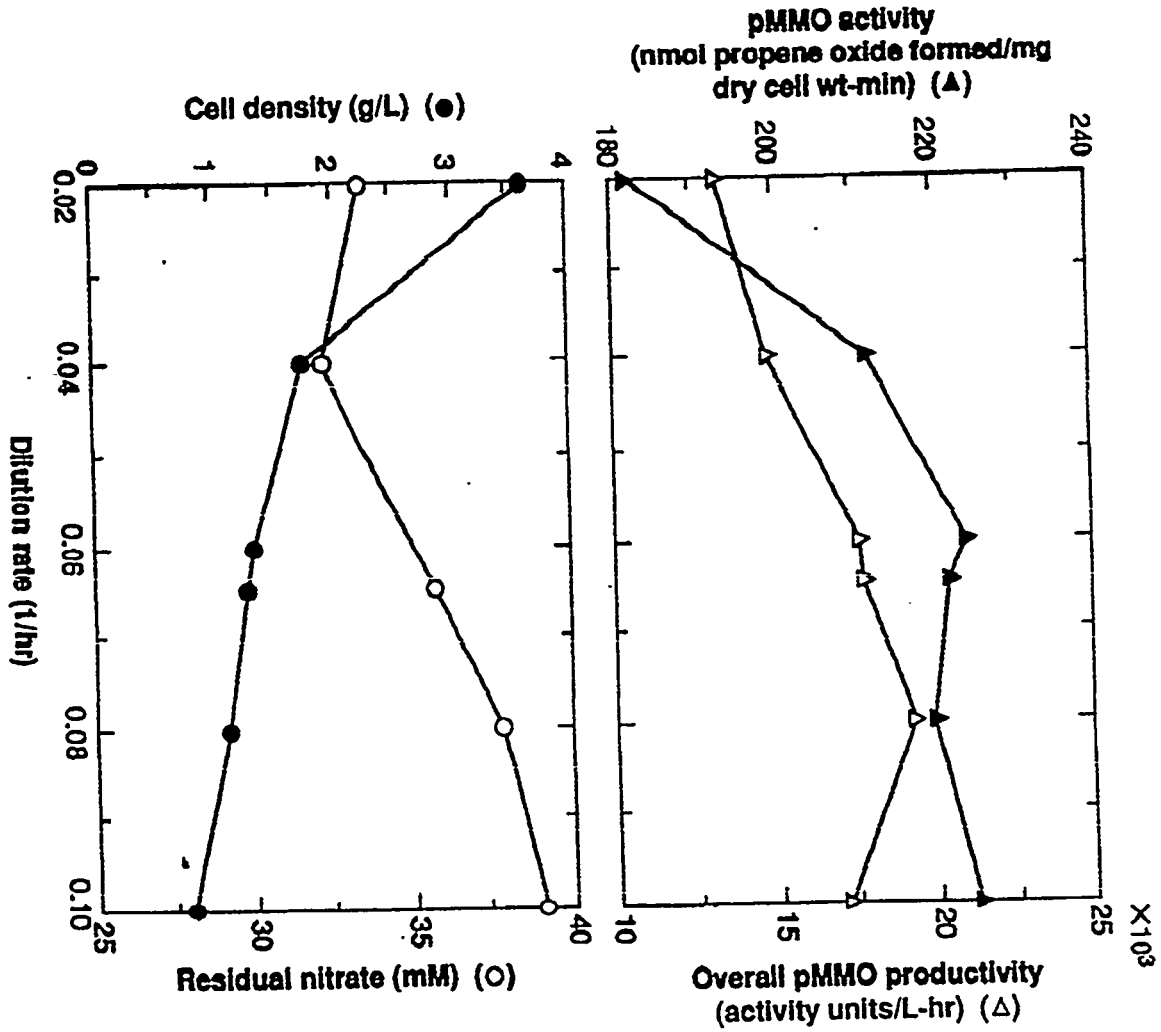

Figure 6. Effect of dilution rate on specific pMMO activity, overall pMMO productivity, total cell density, and residual steady-state nitrate in Higgin's "modified 1X medium". Agitation speed was 400 rpm, and the gas sparging conditions were the same as in Figure 1.

Part IV: Subunit Resolution for Active Site Identification of *Methylosinus trichosporium* OB3b Soluble Methane Monooxygenase

Introduction

Information concerning the selective transformation of methane to methanol, which occurs in a special group of microorganisms, would be of great value for several reasons. First, economic factors motivate the production of methanol from methane. Second, the ability to produce methanol selectively from methane is unique from a chemical perspective, as little selectivity for the alcohol is observed in the known oxidation reactions of methane. One way to design and synthesize catalysts that produce methanol on an industrial scale is to carefully study enzyme systems that can convert methane to methanol. Identification of unique chemical features in these systems should facilitate a more rational approach to the synthesis of biomimetic industrial catalysts. We have therefore chosen to examine the active site structure of the cytoplasmic methane-oxidizing enzyme produced by the bacterium *Methylosinus Trichosporium* OB3b.

Within this bacterium, methane monooxygenase (MMO) is the specific enzyme complex that converts methane to methanol. Under ambient conditions, the soluble form of MMO (sMMO) produces methanol at the rate of approximately four molecules per molecule of enzyme per second*; the cell then uses methanol as a source of carbon for biomass generation and for energy storage.[1] The production of methanol (CH_3OH) by sMMO requires stoichiometric amounts of methane (CH_4), molecular oxygen (O_2), and a source of intracellular electrons that are supplied by reduced nicotinamide adenine dinucleotide (NADH):

$$CH_4 + O_2 + NADH + H^+ \rightarrow CH_3OH + H_2O + NAD^+$$

Three proteins (A, B, and C) facilitate this complex interaction, which results in a controlled partial oxidation of methane. Figure 1 shows these three proteins that comprise the soluble enzyme system. According to current understanding, methane oxidation occurs at a hydroxo-bridged dinuclear iron center in protein A, while proteins B and C participate in the transfer of electrons from NADH to the iron center in protein A.

Our investigation focuses on protein A because it appears to have the key features necessary for CH_4 activation. It is an oligomeric protein, composed of three distinct subunits in an $\alpha 2\ \beta 2\ \gamma 2$ configuration, with a molecular weight of 245,000 daltons. Currently, the location of the iron center in protein A is not known. It is also not

---

* Both a soluble form and a particulate form of this enzyme are known for *Methylosinus trichosporium* OB3b. We discuss only the soluble form (sMMO) here.

known whether this cofactor links with the amino-acid side chains of only one type of subunit, or whether it bridges an interface between two unlike polypeptide subunits. Our project aims to identify portions of the amino-acid sequence within protein A that surround the iron center. To do this, it was necessary to first determine conditions for separating and resolving the α β and γ subunits of protein A. This will allow us to define more accurately the location of the enzyme's active site, to understand the subunit interactions and their impact on CH_4 activation, and to simplify the purification of polypeptide fragments derived from the active site.

Experimental Methods

We obtained purified protein A by modifying published procedures.[2,3] Initially, we guided enzyme purification at each step by correlating the enzymatic activity with the ultraviolet (UV) absorption profile (280 nm) and determined purity by sodium dodecyl sulfate polyacrylamide gel electrophoresis (SDS-PAGE). Later purifications relied solely on the UV profile and the protein subunit composition indicated by gel electrophoresis.

We grew *M. Trichosporium* OB3b according to the method of Park et al.[4] A typical purification used 12 to 16 g of dry cell weight equivalent, which was suspended in 25 m*M* 3-(*N*-morpholino) propanesulfonic acid (MOPS), 5 m*M* $MgCl_2$, and 5 m*M* dithiothreitol (DTT). Two passages through a Manton-Gaulin homogenizer ruptured the cells, which we then stirred at 4°C with DNase. Centrifugation at 40,000 ¥ gravity for 1 h produced the cell-breakage supernatant fluid. We then transferred this cytoplasmic material into an Amicon ultrafiltration cell under nitrogen (this and all subsequent steps were carried out at 4°C). Passage across an XM 300 membrane concentrated the supernatant fluid and provided a bulk discrimination between the high- and low-molecular-weight protein components. Next, we loaded the high-molecular-weight XM 300 retentate onto a diethylaminoethyl (DEAE) Sepharose Fast Flow anion-exchange column, equilibrated with 25 m*M* MOPS and 5 m*M* DTT, and eluted with a linear salt gradient from 0 to 0.25 *M* NaCl. We pooled and concentrated the peak that eluted at approximately 0.14 *M* NaCl and took it onto a second anion-exchange column. Gel filtration chromatography in the same buffer completed the final purification of protein A. We obtained approximately 240 to 480 mg of protein, which we judged to be ~95% pure using SDS-PAGE.

To generate subunits, we denatured protein A by incubating the protein in buffered urea solutions for 1 h at 21°C. Gel filtration chromatography was carried out at room temperature in an attempt to improve the flow rate and resolution by this technique. Later, we obtained subunit separations more successfully by denaturing anion-exchange chromatography at pH 8 in tris(hydroxymethyl)aminomethane buffer (Tris), which was performed at 4°C.

Results and Discussion

SDS-PAGE of purified protein A showed three distinct bands, indicating the expected subunit composition and molecular weights: a (54,000), b (43,000), g (23,000). Other than the electrophoretic separation of microgram quantities of the subunits achieved in the polyacrylamide gel matrix, the individual properties of the subunits have not been reported or explored. To carry out studies such as these, milligram quantities of each subunit are required.

To dissociate protein A in an aqueous solution, we attempted a number of denaturing conditions. The chemical denaturants included sodium dodecyl sulfate, guanidine hydrochloride, and urea, coupled with variations in the salt concentration, temperature, and pH. For an oligomeric protein in a denaturing medium, dissociation followed by subunit unfolding is thought to occur in a stepwise manner. One of the most difficult problems was to define conditions that maintained the solubility of the dissociated subunits. This problem is common in protein unfolding because the hydrophobic interactions that stabilized the globular protein now drive the interchain association of the unfolded strands and result in aggregation and precipitation.[5] Using a combination of the factors listed above, we obtained the only satisfactory results were with the reversible denaturant urea. We treated the protein with urea in the presence of DTT, which prevented disulfide formation. Initially, we tried gel filtration chromatography to resolve the individual subunits and to provide information regarding the extent of dissociation.

A precipitate formed on our first effort to dissociate protein A in urea (pH 7). Analysis of the supernatant indicated that most of the γ subunit remained in solution. We were able to dissolve the precipitated protein under alkaline conditions, and we subsequently subjected the solution to gel filtration chromatography. The elution profile (see Fig. 2) showed three major peaks, which we analyzed using SDS-PAGE. The earliest eluting peak, corresponding to material with the highest molecular weight, was identified as a complex containing both α and β. This indicated that the subunits of protein A had not been completely dissociated. The second peak corresponded to the sequential elution of α and β—α eluting on the front half and β eluting on the back half—and the last peak contained only the γ fraction. Observation of the γ subunit in solution following precipitation of the α and β subunits, coupled with the partial retention of an ($\alpha\beta$) complex under alkaline conditions, indicates that the a and b subunits have higher affinities for each other than for γ.

To determine the effect on dissociation of the subunits and their chromatographic separation, we then probed other factors. We examined the salt concentration by

adding 0.3 *M* sodium chloride to a 6 *M* urea solution at pH 7. Analysis of the solution by gel filtration chromatography, followed by electrophoresis, again indicated that incomplete dissociation had occurred, as the ($\alpha\beta$) complex remained the major component in solution. Protein unfolding and denaturation is known to be a very sensitive function of temperature,[6] and we determined that protein A was very easily heat-denatured with precipitation, even at 40°C. Consequently, temperatures above 21°C cannot be used to enhance subunit dissociation. Finally, we found that adjusting the pH to 8 or above would optimize the dissociation of the subunits, presumably because of electrostatic repulsion between the negatively charged side chains. In addition, we raised the urea concentration to 7 *M* to maintain the solubility of the polypeptides. Gel filtration chromatography of protein A in glycine buffer at pH 9.3 (see Fig. 3) showed that very little of the ($\alpha\beta$) complex was present. However, as the profile indicates, very little resolution of the dissociated subunits was achieved with this chromatographic technique.

Anion exchange chromatography provided much higher resolution of the dissociated subunits under the window of conditions discussed here. Chromatography of denatured protein A on DEAE Sepharose CL-6B resulted in three distinct peaks, corresponding to each of the subunits (see Fig. 4). Because ion exchange chromatography does not discriminate on the basis of size, but rather on charge, the elution profile provides some measure of the subunit net-charge properties. The g subunit is not bound by the anion exchange resin under these conditions, which suggests that it is positively charged at pH 8. The α and β subunits bind to the column, indicating that they both possess a negative charge at this pH. We again detected a small amount of the ($\alpha\beta$) complex in this mixture and found it to elute as a shoulder on the trailing edge of the a subunit. SDS-PAGE of the peak fractions (see Fig. 5) clearly indicates a high degree of subunit resolution.

Conclusions

We have defined conditions that allow us to dissociate the sMMO protein A into its constituent subunits. Given the high mutual affinity of the α and β subunits, these subunits could be dissociated only under slightly alkaline conditions in 7 *M* urea. We achieved the resolution of these three subunits—for the first time on a preparative (milligram) scale—by anion exchange chromatography.

References

1. C. Anthony, "Bacterial Oxidation of Methane and Methanol," *Adv. Microbial Physiol.* 27, 113 (1986).

2. H. Dalton, S. J. Pilkington, "Soluble Methane Monooxygenase from *Methylococcus capsulatus* Bath," in *Methods in Enzymology* 188, M. E. Lidstrom, Ed. (Academic Press, San Diego, CA, 1990), p. 181.
3. B. G. Fox, W. A. Froland, D. R. Jollie, J. D. Lipscomb, "Methane Monooxygenase from *Methylosinus trichosporium* OB3b," in *Methods in Enzymology* 188, M. E. Lidstrom, Ed. (Academic Press, San Diego, CA, 1990), p. 191.
4. S. Park, M. L. Hanna, R. T. Taylor, M. W. Droege, "Batch Cultivation of *Methylosinus trichosporium* OB3b. I: Production of Soluble Methane Monooxygenase," *Biotechnol. Bioeng.* 38, 423 (1991) (Part I, this publication).
5. R. Jaenicke, R. Rudolph, "Refolding and Association of Oligomeric Proteins," in *Methods in Enzymology* 131, C. H. W. Hirs and S. N. Timasheff, Eds. (Academic Press, Orlando, FL, 1986), p. 228.
6. K. A. Dill, "Dominant Forces in Protein Folding," *Biochem.* 29, 7133 (1990).

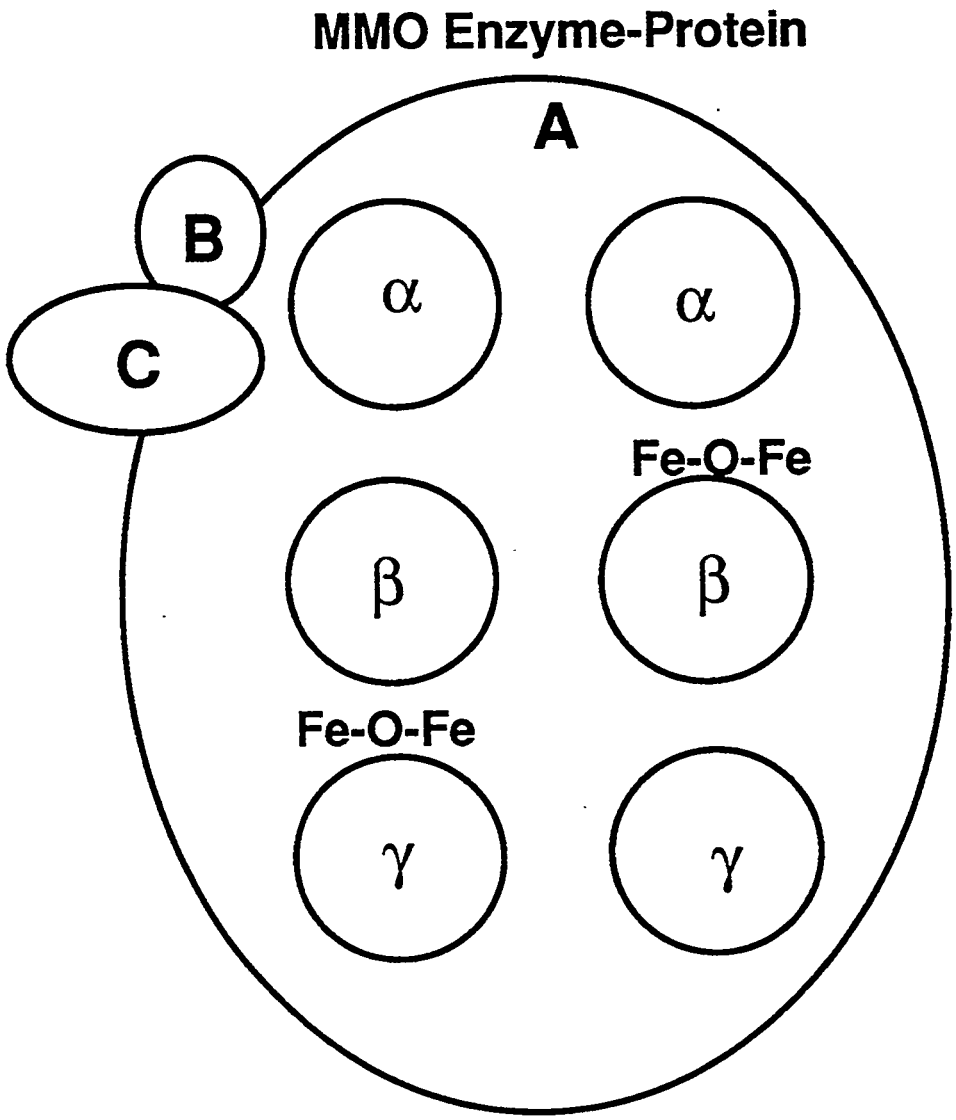

Figure 1. Protein components of the soluble methane monooxygenase system.

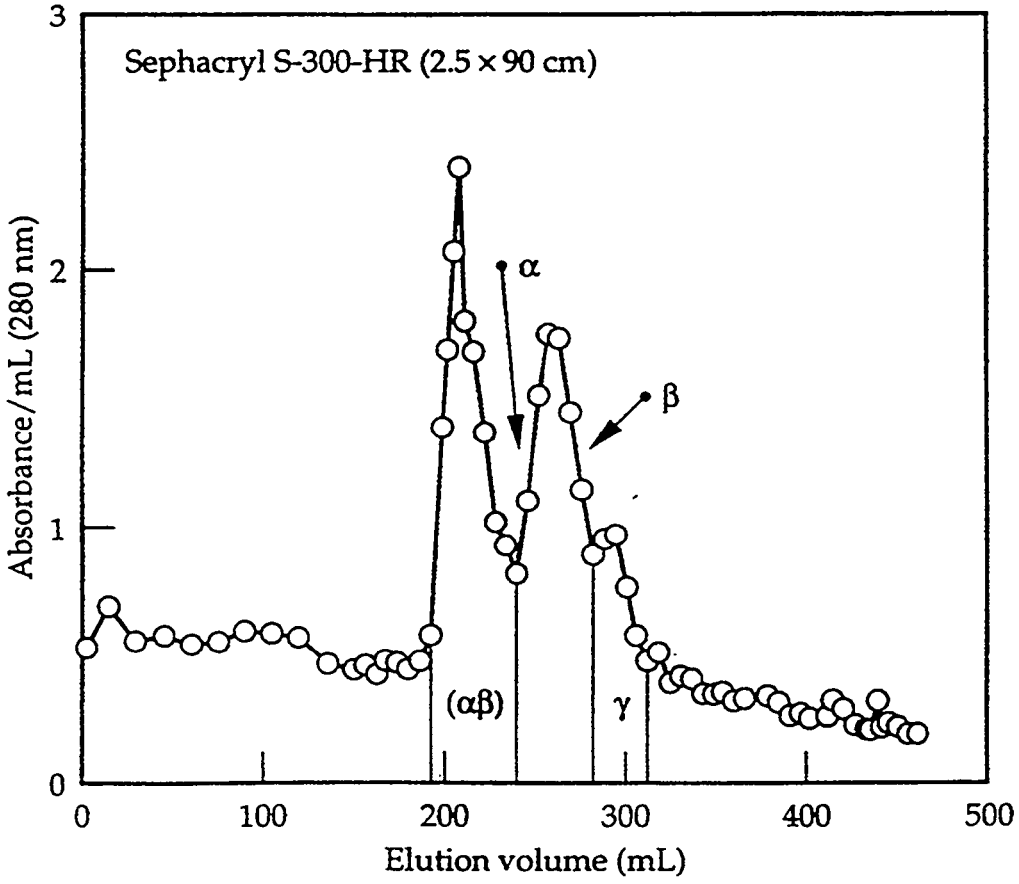

Figure 2. Gel filtration profile in 50 m*M* MOPS (pH 7), 6 *M* urea, 5 m*M* DTT, following a 1-h incubation at 21°C in the same buffer.

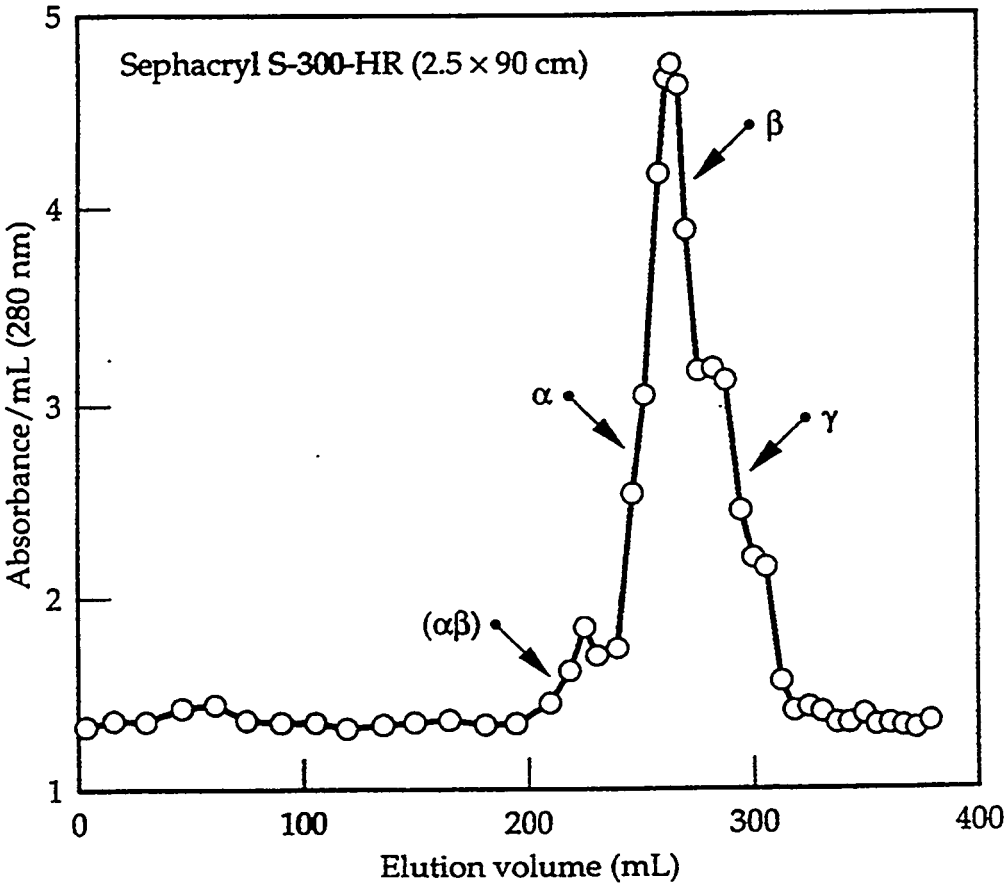

Figure 3. Gel filtration profile in 50 m*M* glycine (pH 9.3), 7 *M* urea, 5 m*M* DTT, following a 1-h incubation at 21°C in the same buffer.

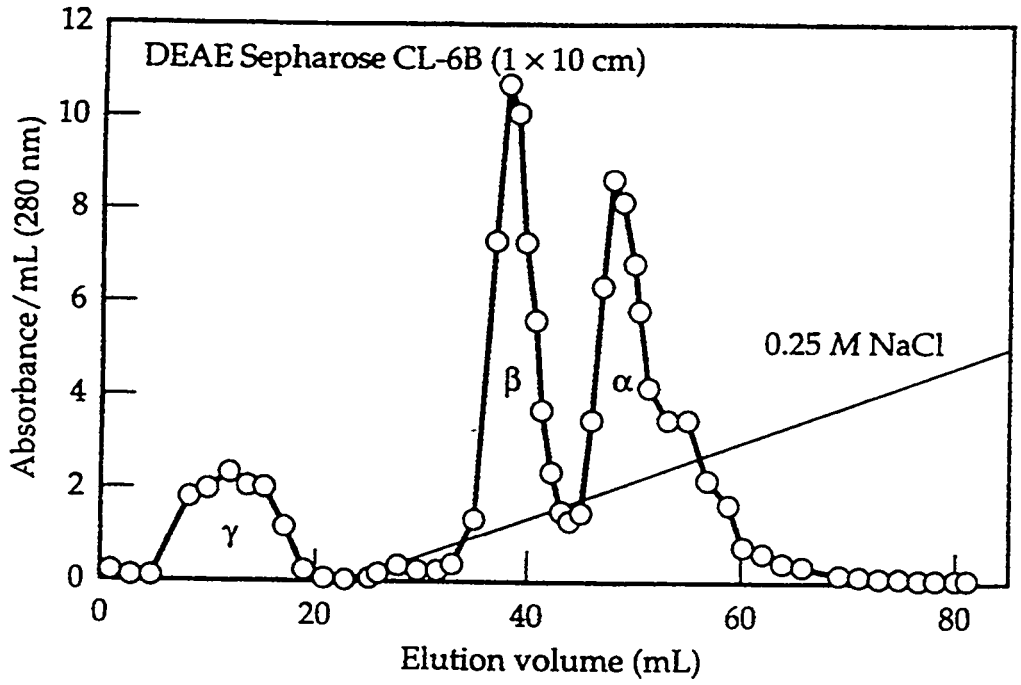

Figure 4. Anion exchange profile in 25 m*M* Tris (pH 8), 7 *M* urea, 5 m*M* DTT, following a 1-h incubation at 21°C in the same buffer.

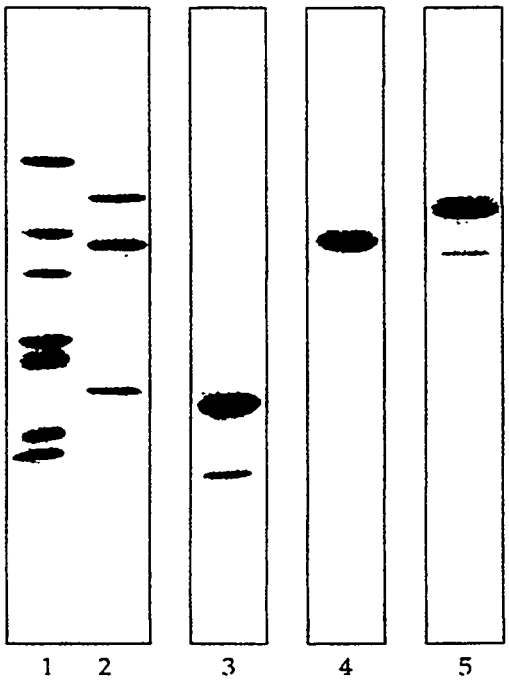

LANES:

1. **Molecular-weight standards**
2. **Column load**
3. **Fraction 12**
4. **Fraction 38**
5. **Fraction 48**

Figure 5. SDS-PAGE of the individual subunits obtained by denaturing anion exchange chromatography (fraction number corresponds to elution volume in Fig. 4).

Part V: The Synthesis and Characterization of New Copper Coordination Complexes Containing an Asymmetric Coordinating Chelate Ligand: Application to Enzyme Active Site Modeling

Introduction

The catalytic oxidation of light hydrocarbons, especially methane derived from natural gas, is an important research area attracting considerable attention. The potential for natural gas (methane) processing will depend on the development of catalyzed routes directly converting methane to higher valued products (heavier hydrocarbons, olefins, and alcohols). However, methane is chemically quite inert and has not proved easy to convert to liquid hydrocarbons. As a result, no technologies are currently available to process methane economically. It is well-known that a select group of aerobic soil/water bacteria called methanotrophs can efficiently and selectively utilize methane as the sole source of their energy and carbon for cellular growth.[1] The first reaction in this metabolic pathway is catalyzed by the enzyme methane monooxygenase (MMO) forming methanol:

$$CH_4 + O_2 + NADH + H^+ \xrightarrow[MMO]{25\text{-}50^\circ C} CH_3OH + H_2O + NAD^+$$

Methanol is a technologically important product from this partial oxidation of methane since it can be easily converted to liquid hydrocarbon transportation fuels, used directly as a liquid fuel itself, or serve as a feedstock for fine chemicals production.

Microorganisms can produce MMO in two distinct forms: a membrane-bound particulate form or a discrete soluble form. The soluble form consist of three main proteins: A, B, and C. Protein A is an iron-containing oxygenase that reacts with methane, producing methanol,[2] and is therefore the focus of our work. Spectroscopic and thermodynamic studies have postulated that the metals in Protein A occur in a binuclear iron center and function as the active site for methane oxidation.[3,4,5] Although some of the details vary, the general description of the iron site in Protein A is a binuclear cluster containing some type of μ-oxo ligand between the iron atoms. The remaining ligands (derived from adjacent amino acid residues) coordinate to the metals through nitrogen or oxygen and the Fe-Fe distance is between 3.0-3.5 Å. Compared to the soluble form of MMO the particulate form is poorly characterized and is thought to contain copper ions at the active site. This form is also active in methane oxidation in the biological system.[6]

Our work centers on the synthesis and characterization of inorganic/organic chemical models of the active site of MMO (both particulate and soluble). We have focused on the synthesis of an unsymmetrical, binuclear chelating ligand possessing an alkoxo group that can serve as a bridging μ-oxo ligand. The advantage of such a ligand system is twofold: (a) metal complexes of an asymmetric binucleating ligand will provide coordinative unsaturation at only one metal resulting in focused substrate reactivity at that site and (b) a single ligand with binuclear coordination provides a more robust environment for metal oxidation state changes and accompanying chemical reactivity.

We report here the synthesis of a prototype asymmetrical binuclear chelating ligand, its reactivity with copper ion, and characterization of two new copper chelate complexes. This work provides the first proof-of-concept for the formation of a binuclear complex with different coordination at each metal ion. Such complexes are relevant to the development of model systems for the active site of MMO.

Experimental

The synthesis of the chelating ligand HMeL obtained by a five step procedure in ~35% overall yield is outlined in scheme[1].

N-methyl-1,3-diamino-2-propanol . 47.54g (0.326 mole) of 1-amino-3-chloro-2-propanol hydrochloride was dissolved in 150 ml water. To this solution 280 ml of 40% aqueous methylamine (101 g, 3.26 mole) was added slowly and the solution was stirred at room temperature overnight. NaOH (26.08g, 0.652 mole) was added and the solution was evaporated by aspiration at 70-80°C to a resulting salt/oil mixture. The mixture was taken up in a minimum volume of 2-propanol and filtered on a glass frit to remove NaCl. The alcohol solution was evaporated to a viscous oil at 80°C, dissolved in chloroform, shaken with sodium sulfate, and again aspirated to a viscous slightly yellow oil. The dried oil was distilled through a short path distillation apparatus at 0.3 torr and the water white fraction between 83 and 90°C was collected. (25.30g, 74.6% yield). Anal. Calcd. for $C_4H_{12}N_2O$: C, 46.13; H, 11.61; N, 26.90. Found: C, 46.12; H, 11.67; N, 27.06. (lit.9 bp 95-100°C, 3 torr).

N-methyl-1,3-diamino-2-propanol-N,N,N'triacetic acid. 10.4g (0.1 mole) of N-methyl-1,3-diamino-2-propanol was dissolved in 25 ml of water. To this solution was added 50 ml of an aqueous NaCN solution containing 17.15g (0.35 mole) of NaCN and one gram NaOH. The mixture was placed in a 250 ml three neck flask equipped with a reflux condenser, an addition funnel, and a gas dispersion tube connected to a N2 purge. The solution was heated to 80°C with stirring and 29.6 ml (0.37 mole) of 36.9% aqueous formaldehyde was added dropwise over a period of not less than 8 hrs. The mixture was maintained at 80oC and purged until the evolution of ammonia could no longer be detected above the condenser by pH

paper. The total reaction time varied from 20 to 30 hrs depending on the purge rate. The cooled reaction mixture was acidified to pH<1.2 with conc HCl refluxed for 3 hrs to remove unreacted NaCN and then used directly in the next step.

N,N,N'-tris ((N-methyl)-2-benzoimidazolylmethyl)-N'-methyl-1,3-diamino-2-propanol [HMeL]. The HCl treated mixture of N-methyl-1,3-diamino-2-propanol-N,N,N'triacetic acid containing 0.1 moles of the triacid was concentrated by rotary evaporation to an oil salt mixture and then dissolved in 150 ml 5N HCl to undergo the condensation reaction in the manner of Stephan.11 To this solution was added 56.1g (0.285 mole) of N-methyl-phenylenediamine dihydrochloride. The mixture was refluxed for 24-48 hrs during which time to solution color changed from pink to dark green. The mixture was cooled to 0° C and conc NH_4OH was added slowly to pH>9 while maintaining the temperature below 15° C. At ~pH 7 a white flocculant began to develop which turned to a green-brown oil on further addition of NH_4OH. The supernatent was decanted from the oil, fresh water was added, and the oil was worked with a glass rod with slight warming (~40° C) until a tan powder resulted. The powder was filtered on a glass frit washed twice with water and vacuum dried to yield 33.9 g (63.2%) of crude ligand. The crude product was dissolved in acetonitrile at which time a light tan granular precipitate formed in solution as the crude material dissolved: 1H NMR (300 MHz, $CDCl_3$), d 2.23 (m, 1H), 2.28 (s, 3H), 2.49 (m, 1H), 2.76 (m, 2H), 3.49 (s, 6H), 3.69 (s, 3H), 3.76 (s, 3H), 4.02 (s, 4H), 7.2 (m, 9H), 7.7 (m, 3H); 13C NMR (75.4 MHz, $CDCl_3$) d 151.6, 151.5, 141.8, 141.6, 135.9, 135.7, 122.4, 122.3, 121.8, 119.3, 119.1, 109.0, 67.1, 61.4, 59.7, 55.1, 51.8, 43.6, 29.7, 29.4. Anal. Calcd for $C_{31}H_{38}N_8O_2$: C, 67.13, H, 6.91, N, 20.20. Found: C, 67.61; H, 6.77; N, 20.35.

(N,N,N'-tris-((N-methyl)-2-benzoimidazolylmethyl)-N'-methyl-1,3-diamino-2-proprionato) copper(II) perchlorate [CuHMeL]$(ClO_4)_2 \cdot CH_3CN$ **(1)**. A solution of 1.00g (1.86 mmol) of HMeL in 15 mL methanol was treated with a solution of 0.688g $Cu(ClO_4)_2 \cdot xH_2O$ (17.2% Cu, 1.86 mmol Cu^{2+}) in 15 mL methanol with stirring. A blue precipitate forms immediately on addition of copper solution and the mixture was allowed to stir at room temperature for 10 minutes. The resulting mixture was cooled at -20° C for ~1 hr, the blue solid collected on a glass frit (pale green filtrate), washed with 10-15 ml cold methanol and dried under vacuum at 25° C. Crude yield was 1.3256g of blue-green solid. The dried solid was dissolved in 75 mL hot acetonitrile, filtered hot, and cooled. X-ray quality crystals were obtained by vapor diffusion of ether into this solution. The blue-green crystals were collected on a frit and vacuum dried (83% yield). Anal. Calcd. for $C_{33}H_{39}Cl_2CuN_9O_9$: C, 47.18; H, 4.68; N, 15.00. Found: C, 47.07; H, 4.85; N, 14.73.

(m-O,O'-acetato)(N,N,N'-tris ((N-methyl)-2-benzoimidazolylmethyl)-N'-methyl-1,3-diamino-2-proprionato)dicopper(II,II) bisperchlorate $[Cu_2MeL(OAc)](ClO_4)_2.2H_2O$ **(1).** A solution of 1.00g of HMeL (1.86 mmol) and 0.507g sodium acetate trihydrate (3.72 mmol) in 15 mL of methanol was treated with 1.377g $Cu(ClO_4)2{\cdot}xH_2O$ (17.2% Cu, 3.72 mmol Cu^{2+}) in 15 mL methanol with stirring. A light blue precipitate forms initially and is quickly replaced (~30 sec) by a deep blue solid. The mixture was stirred for 30 min. at room temperature and then cooled at -20° C overnight. The solid was collected on a glass frit, washed with 10mL of cold methanol, and air dried to yield 1.703g of sky-blue powder. Further purification was achieved by vapor diffusion of ether into 50 mL of an acetonitrile solution of this solid to yield dark blue crystals (90.3% yield). Anal. Calcd. for $C_{33}H_{42}Cl_2Cu_2N_8O_{13}$: C, 41.43; H, 4.64; N, 11.71. Found: C, 41.34; H, 4.64; N, 11.13. (b) A 0.1036g (0.125 mmol) sample of **(2)** was placed in 10 mL of methanol to produce a pale blue-green solution and solid. To this suspension 0.046g of $CuClO_4{\cdot}xH_2O$ (0.125 mmol) followed by 0.034g sodium acetate trihydrate (0.25 mmol) were added sequentially as solids. The mixture was warmed to 50° C and stirred for 30 minutes. The solid was collected and washed with cold methanol, and recrystallized by vapor diffusion of ether in acetonitrile to yield dark blue crystals of

Results and Discussion

Scheme 1 shows the synthetic route for the prototype binuclear chelating ligand, HMeL. Elemental analysis and NMR studies confirm the composition and structure of the ligand. It possesses a hydroxy functionality that could serve as a bridging alkoxo group and aliphatic and aromatic nitrogen coordination groups (benzimidazole). Using the C-OH bond as a bisecting line in this molecule, it is clear that the ligand has the potential to coordinate two metal ions in different environments. One half of the ligand provides three coordination sites (2 nitrogens and 1 bridging oxygen) while the other half provides four coordination sites (3 nitrogens and 1 bridging oxygen).

Reactions with copper ion demonstrate that the ligand is a potent chelating agent. Blue or blue-green colored complexes are formed rapidly in the presence of copper(II). The complexes are synthesized by stoichiometric reactions in methanol using hydrated metal salts. Characterization by elemental analysis and single crystal x-ray crystallography show that either mononuclear or binuclear complexes are obtained. For a metal-to-ligand ratio of 1:1 a mononuclear complex is obtained (Figure 1). The structure of the complex shows a distorted, trigonal bipyramidal coordination environment around Cu with five Cu-N bonds (average Cu-N distance ~ 2 Å). In this case, the hydroxo functionality does not coordinate to the metal and in the structure is located remote from the metal. On the other hand,

with a metal-to-ligand ratio of 2:1 and in the presence of 2 equivalents of sodium acetate, a binuclear complex is formed (Figure 2). The structure shows that the ligand has chelated two copper ions, that the copper ions share the alkoxo oxygen (bridging μ-oxo), and that a coordinated acetate ion bridges the two metals. As a result, one Cu ion is coordinatively saturated (5-coordinate distorted trigonal pyramidal) while the other Cu is only four coordinate (distorted square pyramid). The mixed oxygen, nitrogen ligation have average Cu-N(O) distances of ~2 Å typical of Cu(II) coordination complexes. The role of acetate in this reaction is both to serve as a coordinating bridge between the two copper sites and as a general base that assists in deprotonation of the organic hydroxo group forming the charged alkoxo bridging species. Interestingly, the crystal structure shows that in the solid-state an oxygen from one of the ClO_4^- counterions is weakly bound to the 4-coordinate Cu ion (about 2.6 Å away) suggesting that this Cu is coordinatively unsaturated and that there is a potential 5th site for binding. Initial attempts to demonstrate this binding site have been successful and an azido bridged binuclear Cu complex has been prepared and isolated.[7] It appears that complexes of this type can show selective reactivity at one metal site. Such behavior is a key requirement for bioinorganic mimics of the MMO active site.

These complexes were evaluated for their ability to oxidize cyclohexane and to disproportionate hydrogen peroxide and compared to unchelated Cu(II) under the same conditions. The results are presented in Table 1. Neither the unchelated Cu(II) or the mononuclear complex is capable of either disproportionating hydrogen peroxide or oxidizing cyclohexane. However, the binuclear Cu(II) complex is capable of oxidizing cyclohexane to a mixture of cyclohexanol and cyclohexanone, as well as disproportionating hydrogen peroxide. It is not clear if only the vacant binding (peroxide binding) site in sufficient for peroxide activation or if the coupled copper ions possess unique redox properties. These data show the proof-of-principal that these coordinately asymmetric complexes will function as biomimetic catalysts and that they have the ability to oxidize hydrocarbons.

Table 1. Oxidation of Cyclohexane

Complex	% H_2O_2 Converted	Products	Turnover
$Cu(BF_4)_2 \cdot 6\ H_2O$	0 (24 hrs)	--	--
$[CuMEL][ClO_4]_2$	0 (48 hrs)	--	--
$[Cu_2MELOAc][ClO_4]_2$	40 (48 hrs)	cyclohexanol cyclohexanone	3

Conclusions

A binuclear, unsymmetric coordinating ligand that is an effective metal chelator has been designed and prepared. The new ligand has been shown to react rapidly with copper(II) forming a variety of copper coordination complexes. The binuclear complex is of significant interest since it represents proof-of-principle for the development of coordinatively asymmetric, binuclear metal chelate complexes. Although this structural type of chelator now appears to be common in biological systems, it has not been previously described for inorganic coordination chemistry. It is expected that this ligand and derivatives of it will play an important role in the development of bioinorganic complexes that aim to mimic enzyme active sites that function by substrate interaction at only one metal site of a multimetal active site.

Our catalyst development effort has gone one full cycle in the design, synthesis and evaluation of a binuclear, coordinately-asymmetric coordination complex. Unchelated and a mononuclear copper complex do not show catalytic properties to activate hydrogen peroxide or to oxidize cyclohexane. However, the binuclear copper complex tested was capable of activation hydrogen peroxide and the presumed oxo-copper intermediate was able to oxidize cyclohexane.

References

1. Dalton, H. *Adv. Appl. Microbiol.* **1980**, *26*, 71-87.
2. (a) Woodland, M.P.; Dalton, H. *J. Biol. Chem.* **1984**, *259*, 53-59. (b) Green, J.; Dalton, H. *J. Biol. Chem.* **1985**, *260*, 15795-15801. (c) Fox, B.G.; Froland, W.A.; Dege, J.E.; Lipscomb, J.D. *J. Biol. Chem.* **1989**, *264*, 10023-10033.
3. (a) Woodland, M.P.; Patil, D.S.; Cammack, R.; Dalton, H. *Biochim. Biophys. Acta* **1986**, *873*, 237-242. (b) Fox, B.G.; Surerus, K.K.; Munck, E.; Lipscomb, J.D. *J. Biol. Chem.* **1988**, *263*, 10553-10556.

4. Prince, R.C.; George, G.N.; Savas, J.C.; Cramer, S.P.; Patel, R.N. *Biochim. Biophys. Acta* **1988**, *952*, 220-229.
5. Ericson, A.; Hedman, B.; Hodgson, K.O.; Green, J.; Dalton, H.; Bentsen, J.G.; Beer, R.H.; Lippard, S.J. *J. Am. Chem. Soc.* **1988**, *110*, 2330-2332.
6. (a) Stanley, S.H.; Prior, S.D.; Leak, D.J.; Dalton, J. *Biotechnol. Lett.* **1983**, *5*, 487. (b) Park, S., Hanna, M.L., Taylor, R.T., Droege, M.W. *Biotechnology and Bioengineering* **1991**, *38*, 423-433.
7. Droege, M.W.; Satcher, J.H., Jr.; Weakley, T.J.R. Unpublished results.

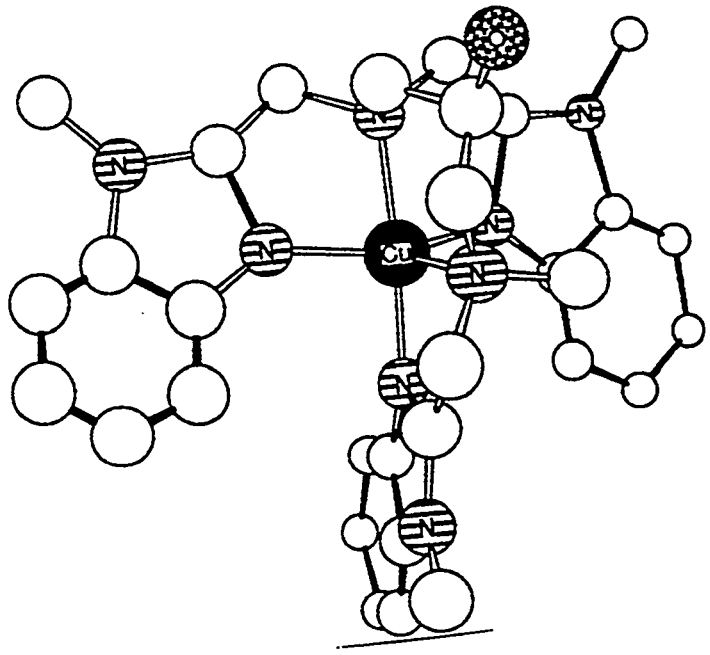

Figure 1. Structure of momomuclear Cu(II) complex (1). Open circles represent carbon atoms. Hydrogen atoms not shown for clarity.

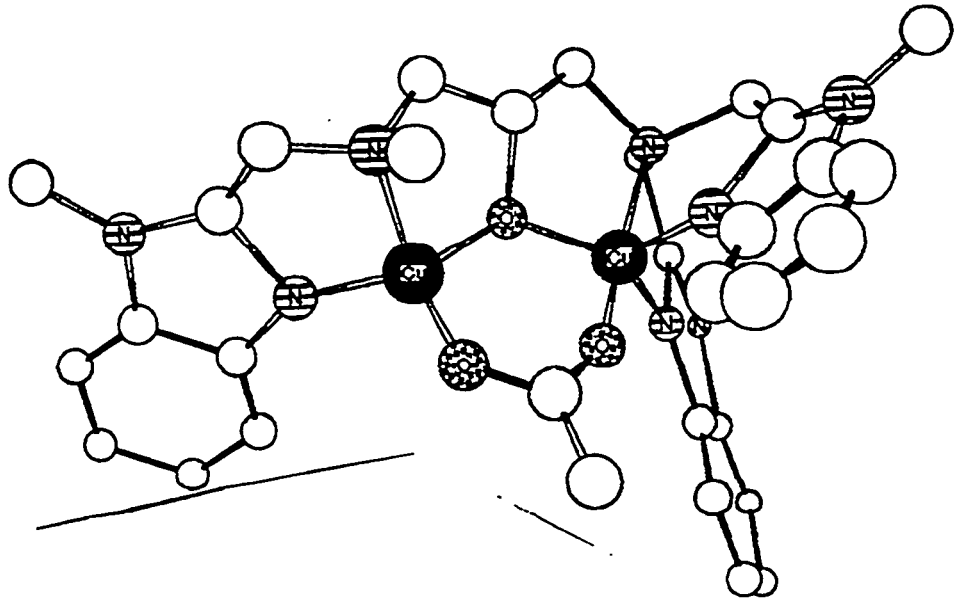

Figure 2. Structure of binuclear Cu(II) complex (2). Open circles represent carbon atoms. Hydrogen atoms not shown for clarity.

Part VI: The Synthesis and Characterization of New Iron Coordination Complexes Utilizing an Asymmetric Coordinating Chelate Ligand

Introduction

Microorganisms can produce MMO in two distinct forms: a membrane-bound particulate form or a discrete soluble form. The soluble form contains an oxygenase subunit, whose active site includes a binuclear iron center.[3,4,5]. The complete details of the structure of the active site are not known, however, the general description of the iron site in the soluble form is a binuclear cluster containing some type of μ-oxo ligand between the iron atoms. The remaining ligands are derived from adjacent amino acid residues and the Fe-Fe distance is 3.4 Å. The best description of the amino acids coordinating the binuclear iron center is surmised by the close amino acid sequence homology between MMO and ribonucleotide reductase[6], an enzyme containing a binuclear iron center whose X-ray crystal structure has been determined[7]. Recent Mossbauer and EPR studies on soluble MMO[8] have demonstrated that coordination number asymmetry occurs about the two metal centers similar to that found in the related binuclear iron oxygen transport enzyme, hemerythrin. X-ray crystallography has clearly shown a 5,6 coordination sphere about the iron atoms in hemerythrin and reaction studies reveal that oxygen binding occurs at the five coordinate iron.[9] A X-ray crystal structure of soluble MMO has recently been determined.[1]

It is speculated that the active site of particulate form of the enzyme is similar to the soluble form, except that the coordinated metal is copper. We have previously reported on the synthesis of asymmetrically coordinated copper complexes and their ability to catalyze the oxidation of cyclohexane to a mixture of cyclohexanol and cyclohexanone[10].

Project Description

Our work centers on the synthesis and characterization of inorganic/organic chemical models of the active site of MMO. We have focused on the synthesis of an asymmetrical, binuclear chelating ligand possessing an alkoxo group that can serve as a bridging μ-oxo ligand. The advantage of such a ligand system is twofold: (a) metal complexes of an asymmetric binucleating ligand will provide coordinative unsaturation at only one metal resulting in focused substrate reactivity at that site and (b) a single ligand with binuclear coordination provides a more robust environment for metal oxidation state changes and accompanying chemical reactivity.

We report here the synthesis of new prototype asymmetric iron complexes, and characterization of oxidized chelate compounds. This work provides the first proof-

of-concept for the formation of binuclear iron complexes with different coordination at each metal ion. Such complexes are relevant to the development of model systems for the active site of MMO.

Results

Synthesis of the chelating ligand HMeL obtained by a five step procedure has been described previously.[11, Part IV] When HMeL was allowed to react with two equivalents of iron(III) nitrate and excess sodium acetate in acetone/water (1:1), red crystals of (**1**) were deposited in 70% yield. The structure consists of a 5 coordinate (distorted square pyramidal) iron atom bridged to a 6 coordinate (distorted octahedral) iron atom through an alkoxide bridge supplied by the ligand (Figure 1). The metal-metal separation for this intra-ligand pair of iron atoms is 3.530Å which is similar to reported alkoxo bridged complexes.[12] The reported tetranuclear complex is further bound to an identical binuclear unit through an inversion center in which the 5 coordinate iron atom is bridged to the 6 coordinate iron through an oxo and a bidentate carboxylato bridge, the metal-metal separation for this inter-ligand pair being 3.224Å. This compound represents a proof-of-concept for the generation coordination asymmetry about two metals of a binuclear system.

Complex (**2**) results from the reaction of methanolic iron(II)tetrafluroborate, sodium benzoate and HMeL under anaerobic conditions (65% yield). Under these conditions a discrete binuclear complex is generated as the tetrafluoroborate salt (Figure 2). In the crystal structure one iron is five coordinate (distorted trigonal bipyramidal) utilizing three nitrogen donor atoms and an alkoxy oxygen atom from the chelate and an oxygen atom from a bridging benzoate group. The other iron atom is six coordinate (distorted octahedral) with nitrogen and oxygen donation from chelate and benzoate moieties and an additional donation from two methanol solvent molecules making a 5,6 coordinate pair. The ease of solvent removal (confirmed by elemental analysis) indicates that the molecule may be more appropriately considered 5,4 coordinate system. Initial attempts to exploit the coordinative unsaturation have led to two additional compounds: the bis-thiocyanato complex (**3**) and a bis-phosphato complex (**4**) shown in Figures 3 and 4 respectively. Complex (**3**), prepared by the addition of two equivalents of ammonium thiocyanate to an acetonitrile solution of (**2**), still retains coordination number asymmetry by binding both anions to the formerly four coordinate iron. This yields a neutral 6,5 coordinate molecule still bridged by an exogenous benzoate with the nitrogen atoms of two thiocyanate anions replacing the solvent groups. Complex (**4**) is formed when two equivalents of $(n\text{-}Bu_3N)_2HPO_4$ are added to a methanol/acetonitrile solution of (**2**). In this case one equivalent replaces the bridging benzoate in a bidentate binding mode and the second binds in a monodendate "end-on" fashion to a single iron atom. This leaves a 5,5 coordinate system in which coordination asymmetry is not preserved, yet coordinate unsaturation still exists. The reaction of both compounds (**3**) and (**4**) with molecular oxygen is currently being explored.

The oxidation of complex (**2**) with molecular oxygen in acetonitrile was found to conform to a 1:1 stoichiometry. When an acetonitrile solution of (**2**) is exposed to air and subsequently layered with ether a crystalline material (**5**) is formed (Figure 5). The structure reveals a tetrameric iron(III) unit supported by an alkoxo oxygen (intra-molecular) and two oxo (inter-molecular) bridges, the bridging benzoate moiety has been eliminated. In addition there is a terminal hydroxy anion bound to two of the iron centers making all iron atoms six coordinate. It has not been determined at this point if the oxygen bridges are formed from molecular oxygen. The lack of a benzoate bridge in this structure led to the investigation of the oxidation behavior in the presence of excess sodium benzoate. When an acetonitrile solution of (**2**) and five equivalents of sodium benzoate is exposed to air single crystals of (**6**) were formed (Figure 6). In this case the binuclear system remains intact supported by an endogenous alkoxo and two exogenous bidentate benzoate bridges. There is also a monodentate benzoate bound to one iron atom again making a 6,6 coordinate pair of metals. The crystal structure difference map shows only one tetrafluoroborate anion in the unit cell leading to Fe(II)/Fe(III) oxidation state assignment for charge balance. In both of the above oxidation structures the central core of the ligand remains intact and the metal:ligand ratio remains constant. Finally, if the oxidation reaction is carried out in a large excess of tetrabutylammonium perchlorate in acetonitrile, crystals of (**7**) are formed (Figure 7) in which the metal:ligand ratio has been increased to 3:1.

Conclusions

A binuclear, unsymmetric coordinating ligand that is an effective metal chelator has been designed and synthesized. The new ligand has been shown to react readily with iron(II)/(III) forming a variety of coordination complexes. The binuclear complexes are of significant interest since they represents proof-of-principle for the development of coordinatively asymmetric, binuclear metal chelate compounds. Although this structural type of chelator now appears to be common in biological systems, it has not been previously described for inorganic coordination chemistry. The isolation of oxidation products will be helpful in establishing reaction mechanism(s) of these complexes with molecular oxygen. It is expected that this ligand and derivatives of it will play an important role in the development of bioinorganic complexes that aim to mimic enzyme active sites that function by substrate interaction at only one metal site of a multimetal active site.

References

1. Rosenzweig, A.C. *et al., Nature* 1993, *366*, 537-543.
2. Dalton, H. *Adv. Appl. Microbiol.* 1980, *26*, 71-87.
3. (a) Woodland, M.P.; Dalton, H. *J. Biol. Chem.* 1984, *259*, 53-59. (b) Green, J.; Dalton, H. *J. Biol. Chem.* 1985, *260*, 15795-15801. (c) Fox, B.G.; Froland, W.A.; Dege, J.E.; Lipscomb, J.D. *J. Biol. Chem.* 1989, *264*, 10023-10033.
4. (a) Woodland, M.P.; Patil, D.S.; Cammack, R.; Dalton, H. *Biochim. Biophys. Acta* 1986, *873*, 237-242. (b) Fox, B.G.; Surerus, K.K.; Munck, E.; Lipscomb, J.D. *J. Biol. Chem.* 1988, *263*, 10553-10556.
5. Prince, R.C.; George, G.N.; Savas, J.C.; Cramer, S.P.; Patel, R.N. *Biochim. Biophys. Acta* 1988, *952*, 220-229.
6. Ericson, A.; Hedman, B.; Hodgson, K.O.; Green, J.; Dalton, H.; Bentsen, J.G.; Beer, R.H.; Lippard, S.J. *J. Am. Chem. Soc.* 1988, *110*, 2330-2332.
7. Pilkington, S.J.; Salmond, G.P.C.; Murrell; Dalton, H. FEMS Microbology Letters 1990, *72*, 345-348.
8. Nordlund, P.; Sjöberg, B.-M.; Eklund, H. Nature 1990, 345, 593-598.
9. (a) Stenkamp, R.E.; Sieker, L.C.; Jensen, L.H. *Proc Natl Acad Sci. U.S.A* 1976, *73*, 349. (b) Stenkamp, R.E.; Sieker, L.C.; Jensen, L.H. *J. Mol. Bio.* 1978, *126* , 457.
10. B.E.Watkins, M.W. Droege, R.T. Taylor, and J.H. Satcher Biommimetic methane oxidation, Preprint, IGRC meeting, Orlando, FL, November 16-19, 1992.
11. Droege, M.W.; Satcher, J.H.; Reibold, R.A.; Weaklely, T.J.R. Preprint, ACS National Meeting, April 6-10, 1992, San Francisco, CA. (Part V, this publication)
12. Fox, B.G,; Hendrich, M.P.; Surerus K.K.; Andersson K.K.; *J Am Chem Soc* 1993 , *115*, 3688-3701.

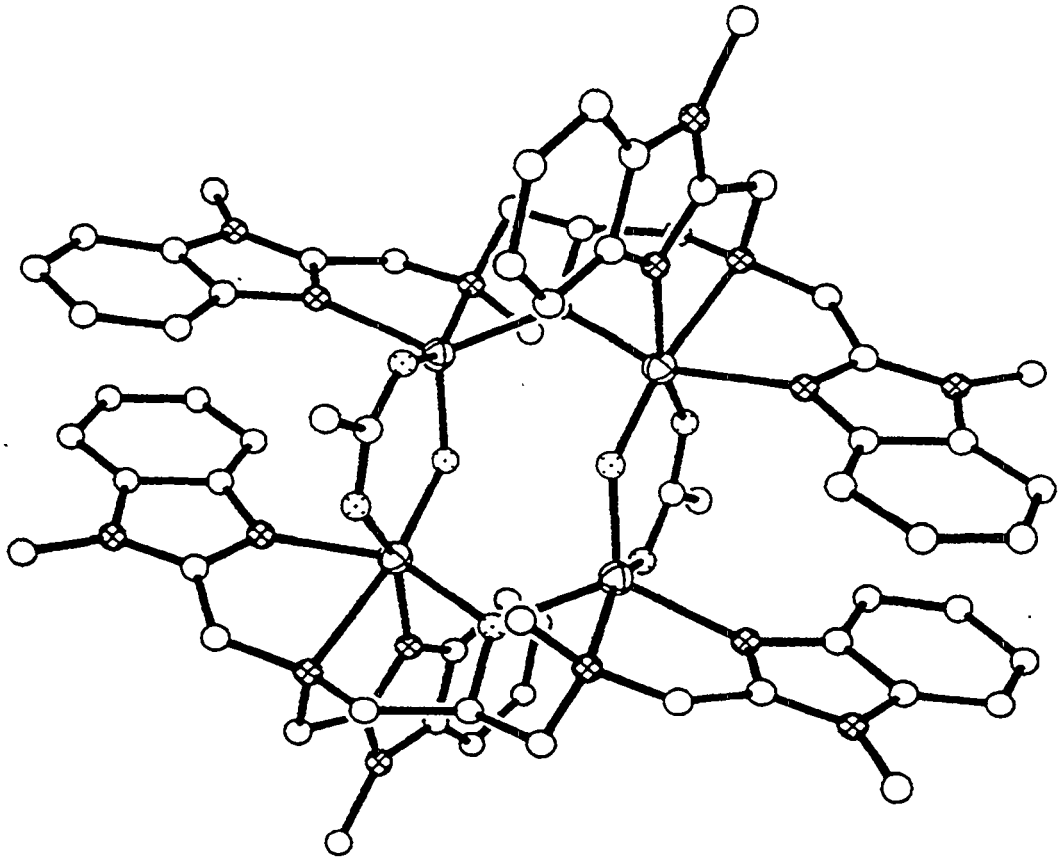

Figure 1. Cation of $(Fe_4(MeL)_2(OAc)_2(O)_2]\ (NO_3)_4$ Hydrogen atoms omitted for clarity
50% thermal elipsoids: Fe / open circles: C / cross-hatched circles: N / dotted circles: O

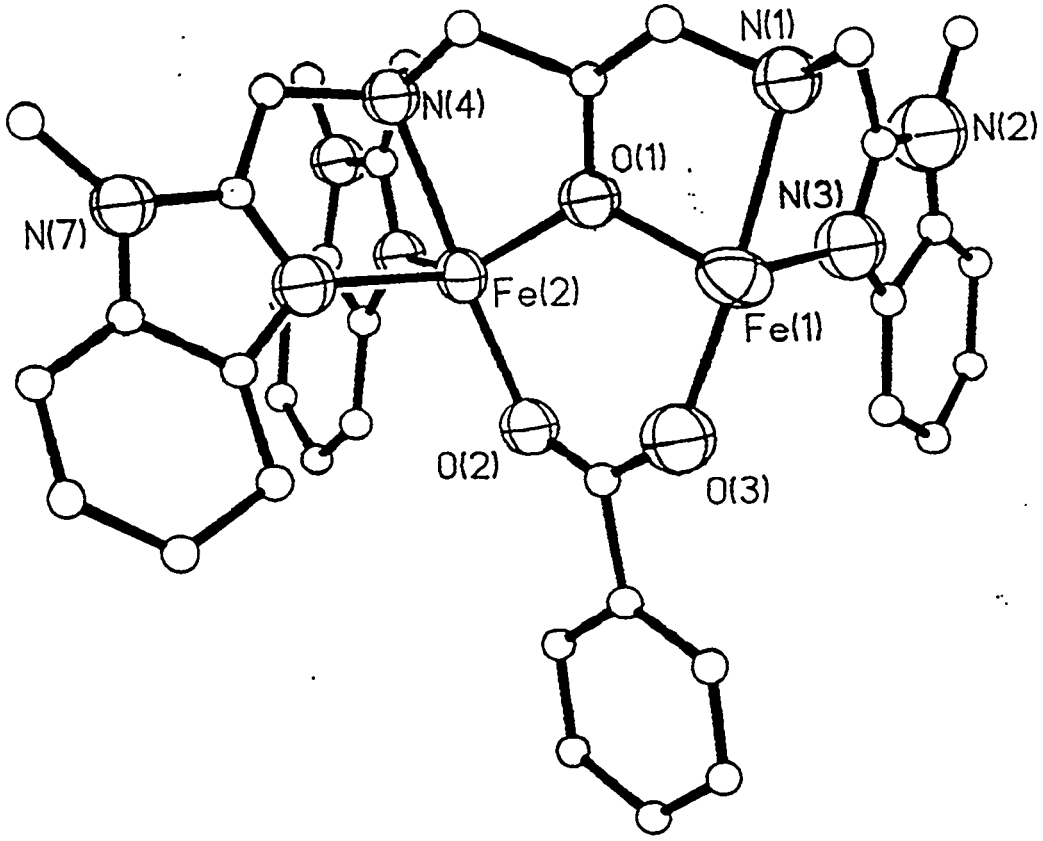

Figure 2. Cation of $[Fe_2(MeL)(O_2CPhl][BF_4]_2$ Bound solvent and hydrogen atoms omitted for clarity

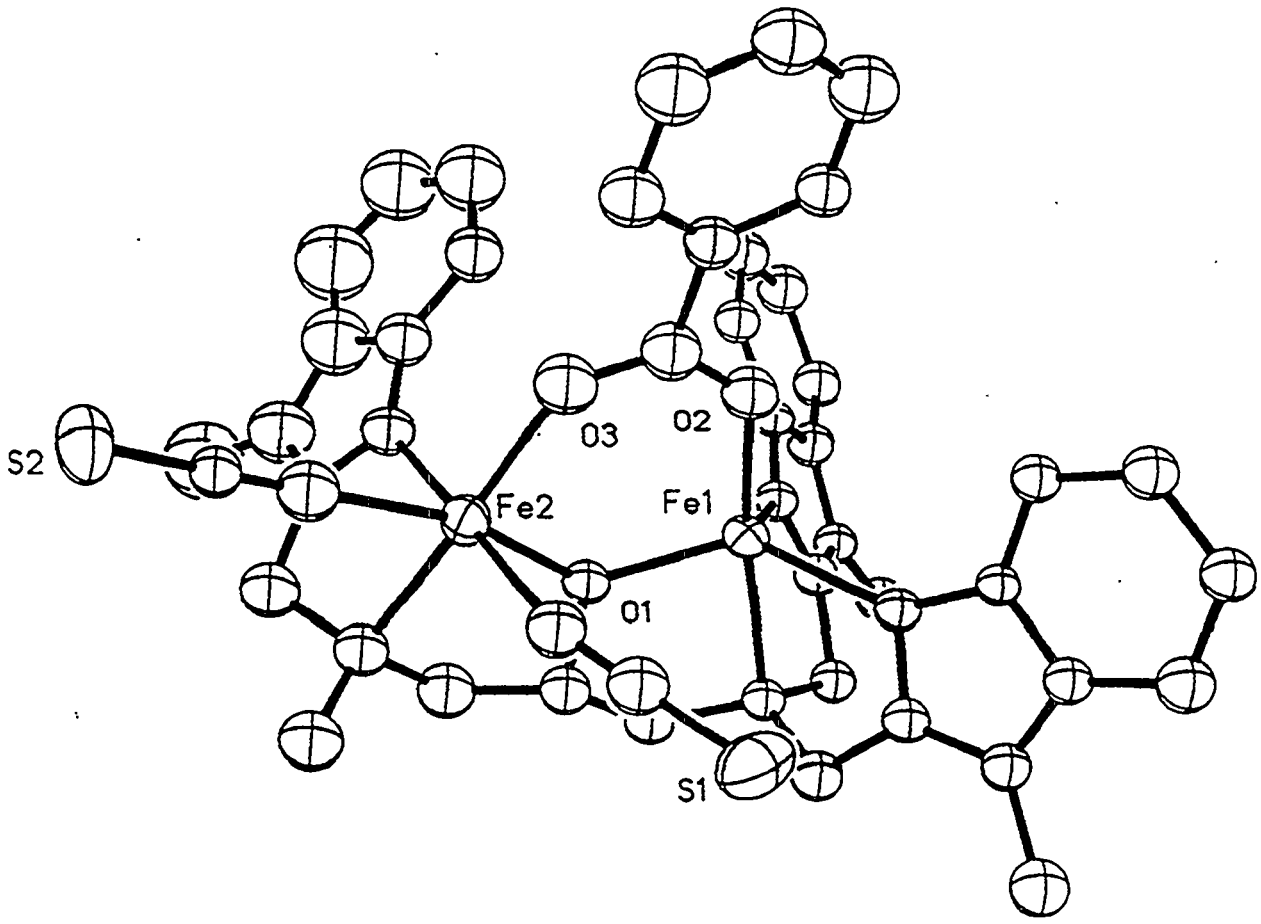

Figure 3. $[Fe_2(MeL)(O_2CPh)(SCN)_2]$ Hydrogen atoms omitted for clarity

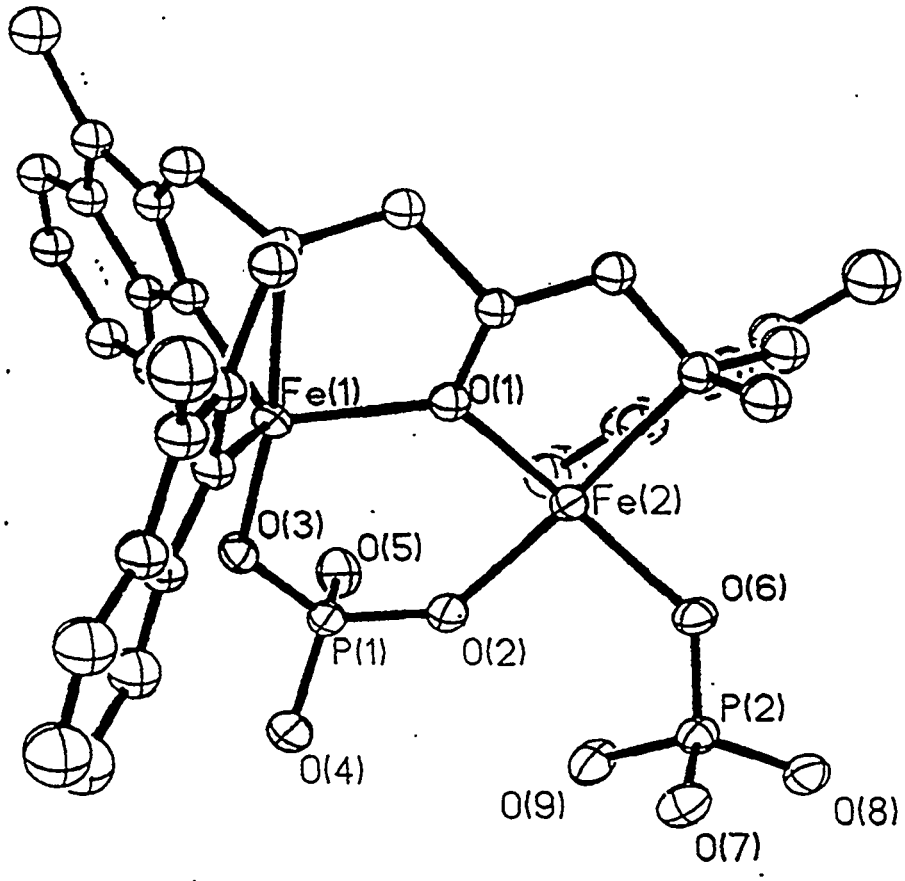

Figure 4. $[Fe_2(MeL)(H_2PO_4)(HPO_4)]$ **Hydrogen atoms omitted for clarity**

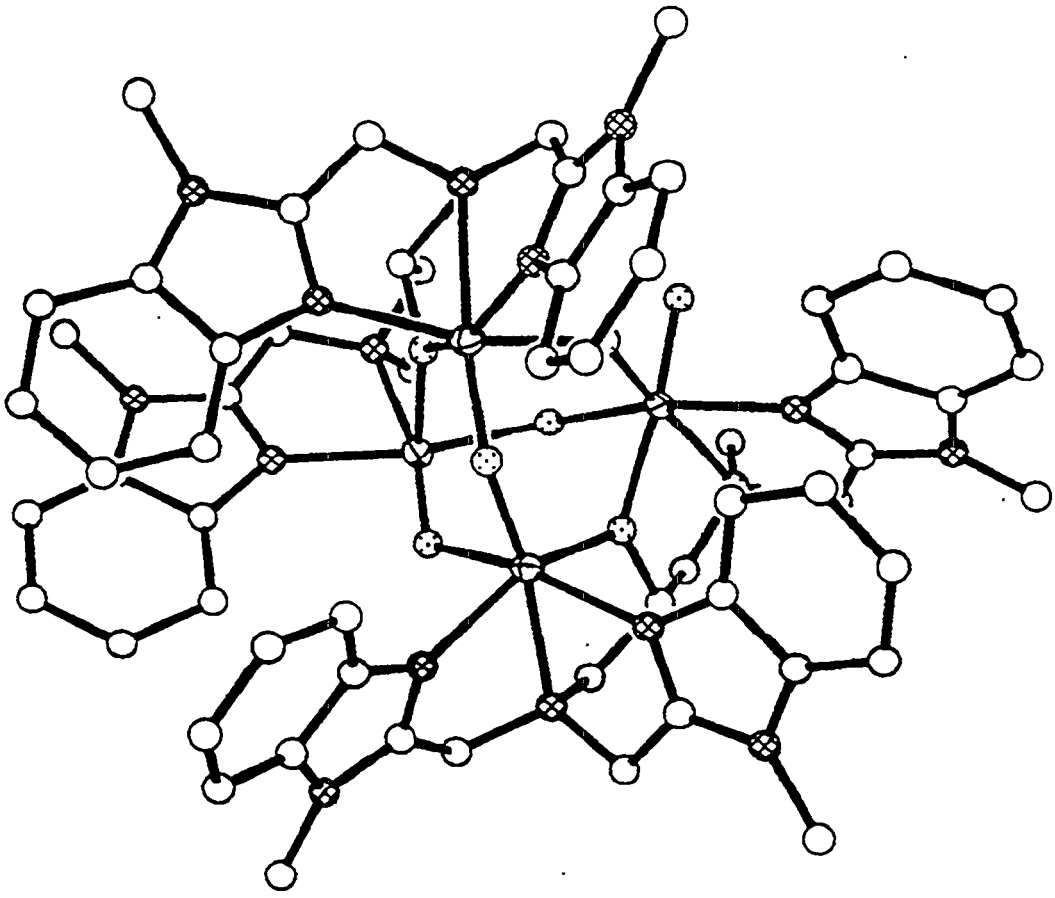

Figure 5. Cation of $[Fe_4(McL)_2(O)(OH)_5]\,[BF_4]_3$ Hydrogen atoms omitted for clarity
50% thermal elipsoids: Fe / open circles: C / cross-hatched circles: N / dotted circles

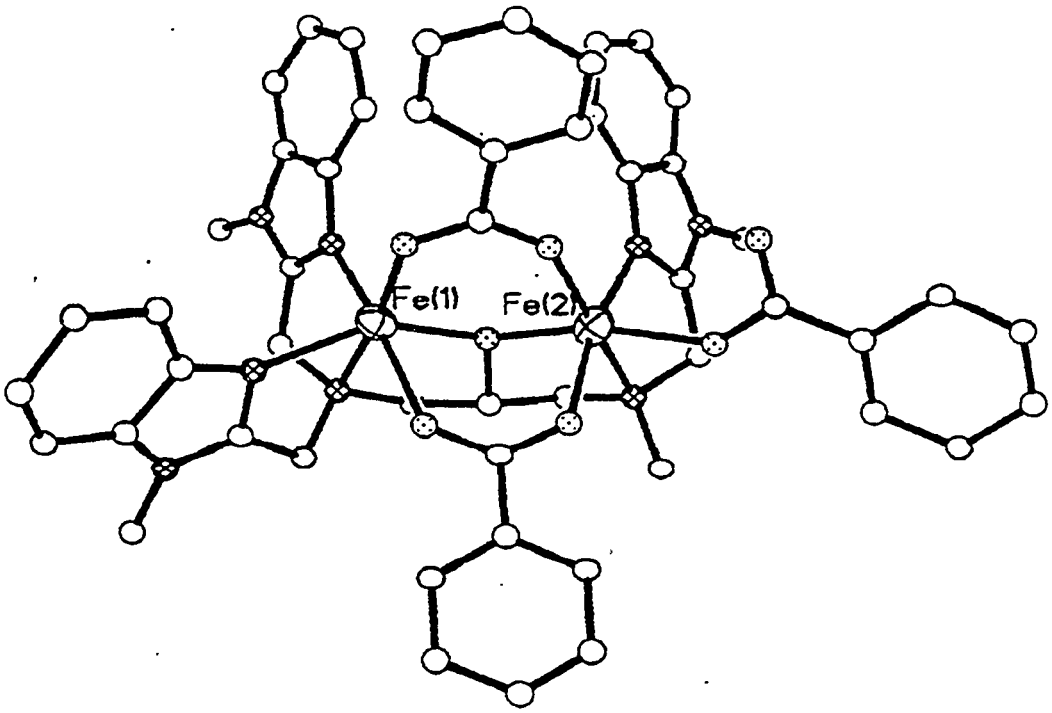

Figure 6. Cation of $[Fe_2(MeL)(O_2CPh)_3][BF_4]$ Hydrogen atoms omitted for clarity 50% thermal ellipsoids: Fe / open circles: C / cross-hatched circles: N / dotted circles: O

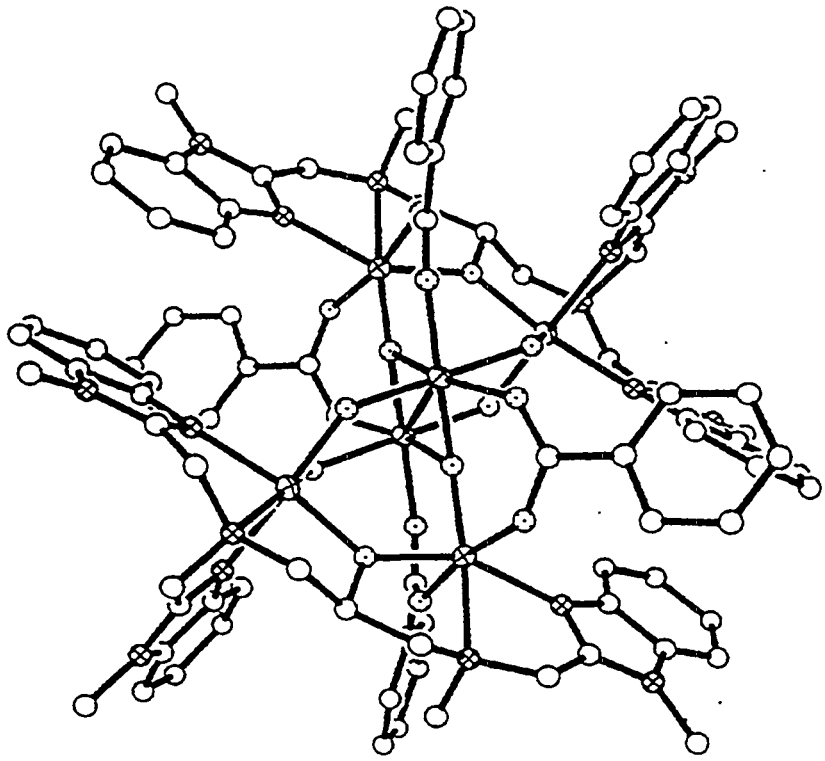

Figure 7. Cation of $[Fe_6(MeL)_2(O_2CPh)_4(O)_2(OH)_4]\ [ClO_4]_4$ Hydrogen atoms omitted for clarity 50% thermal ellipsoids: Fe / open circles: C / cross-hatched circles: N / dotted circles: O